SOLAR MODULATION OF GALACTIC COSMIC RADIATION

U. R. RAO

Physical Research Laboratory, Ahmedabad-9, India

(Received 21 May, 1971)

Abstract. In this review an attempt is made to present an integrated view of the solar modulation process that cause time variation of cosmic ray particles. After briefly surveying the relevant large and small scale properties of the interplanetary magnetic fields and plasma, the motion of cosmic ray particles in the disordered interplanetary magnetic fields is discussed. The experimentally observed long term variations of different species of cosmic ray particles are summarised and compared with the theoretical predictions from the diffusion-convection model. The effect of the energy losses due to decelaration in the expanding solar wind are clearly brought out. The radial density gradient, the modulation parameter and their long term variation are discussed to understand the dynamics of the modulating region. The cosmic ray anisotropy measurements at different energies are summarised. At high energies ($E \gtrsim 1$ GeV), the average diurnal anisotropy is shown to be energy independent and along the 18.00 h direction consistent with their undergoing partial corotation with the sun. The average semi-diurnal anisotropy seems to vary with energy as E^{+1} and incident from a direction perpendicular to the interplanetary field line, consistent with the semi-diurnal component being produced by latitudinal gradients. Both the diurnal and semi-diurnal components are shown to be practically time invariant. On a day to day basis, however, the anisotropy characteristics such as the exponent of variation, the amplitude and the phase show very high variability which are interpreted in terms of convection and variable field aligned diffusion due to the redistribution of the galactic cosmic ray density following transient changes in the interplanetary medium. The anisotropy observation at low energies ($E \lesssim 100$ MeV) are, however, not explained by the theory.

The rigidity dependence and the anisotropies during short term variations such as Forbush decreases are discussed in terms of the proposed field models for the interplanetary field structure and are compared with the observed rigidity dependence of long term variations. The data pertaining to the 27 day corotating Forbush decreases and their association with enhanced diurnal variation are also presented. The relationship between the energetic storm particle events which are caused by the acceleration of particles in the shock fronts and the Forbush decreases which are caused by the exclusion of galactic particles by the enhanced field structure in the same fronts are clearly brought out. Thus the recurrent increases at low energies and recurrent decreases at high energies may both be caused by the field structure in the shock front. In conclusion, the properties of the very short period fluctuations (18–25 cph) are summarised.

1. Introduction

It is generally accepted that the galactic cosmic radiation is largely isotropic. The Sun and the interplanetary medium, however, exert a profound influence on the cosmic radiation upto helio-centric distances of 10–50 AU causing them to undergo deviation from isotropy and change of energy spectrum and intensity. Just as seismic waves have been used to study the interior structure of the Earth and whistlers to study the ionized portion of the Earth's outer atmosphere, intensive study of cosmic ray variations have been used as an effective probe for investigating the interplanetary 'meteorological' conditions.

Most of the time variation studies in the past 30 yr have been conducted using ground based cosmic ray observations. From a knowledge of the geomagnetic

Space Science Reviews **12** (1972) 719–809.

effects and atmospheric transition effects, it has been possible to infer the primary cosmic ray secondaries at ground (Rao *et al.*, 1963). In the recent past, however, our knowledge of both the interplanetary conditions and of cosmic ray time variations has greatly increased with the availability of direct measurements obtained from instrumentation on board satellites and deep space probes. In this review, we summarize the experimental observations relevant to the understanding of the solar modulation of galactic cosmic radiation and discuss them in the light of the important theoretical models that have been proposed.

The galactic cosmic ray time variations include both essentially isotropic time variations such as 11 yr solar cycle variation, Forbush decreases and 27 day variations of intensity and anisotropic (spatial) variations such as the solar diurnal and semi-diurnal variations. Besides, at times, the Sun has been known to emit energetic particles, often upto energies $\sim 10^{10}$ eV which cause noticeable enhancements of particle radiation at Earth. Since solar flare cosmic ray enhancements have been reviewed very recently (McCracken and Rao, 1970), we shall only deal with the solar modulation of galactic cosmic radiation in this review.

As most of the data on cosmic ray time variations are still derived from ground based observations, a comprehensive knowledge of the interaction of particles in the atmosphere and their behaviour in the geomagnetic field is essential to relate the observed variations of secondary particles with the primary cosmic ray variations occurring in the interplanetary space. The atmospheric transition effects of cosmic ray particles include a knowledge of (a) the cascade processes responsible for the production of secondary cosmic ray particles at different levels in the atmosphere due to primary particles impinging on the top of the atmosphere, and (b) the effects of the variation of meteorological conditions such as pressure and temperature throughout the atmosphere on the intensity fluctuations observed at different levels. Various theoretical treatments of the complex cascade processes in the atmosphere are available in literature. However, in actual practice, quantitative evaluation of the 'specific yield functions' through the experimentally observed primary cosmic ray spectrum and the latitude effect of secondaries has been found to be simple and satisfactory. The 'specific yield function' at any ground based detector for each incident primary particle of a given rigidity, has been derived by a number of workers (Webber and Quenby, 1959; Webber, 1962; Dorman, 1963).

The cosmic ray variations due to changing meteorological conditions have been studied extensively both theoretically and by employing correlation techniques using the observed cosmic ray intensity variations and meteorological data as input parameters. A comprehensive review of the atmospheric effects has been recently given by Bercovitch (1967). An important conclusion of considerable interest to our basic interpretation of ground based data is that whereas both neutron and meson monitor observations are affected by atmospheric pressure variations, it is only the meson monitors which are sensitive to atmospheric temperature variations. Since the accurate estimation of temperature correction, which is of the same order of magnitude as the cosmic ray variations of interest ($\sim 0.5\%$), is rendered difficult due to the non-

availability of temperature measurements at different levels and during different times (meteorological observations are seldom made more than twice a day which is insufficient to derive diurnal temperature variation), the interpretation of neutron monitor observations is considerably easier and more unambiguous.

The effect of the geomagnetic field, likewise, has been very well studied both theoretically (See Rossi and Olbert, 1970) and by model experiments (Brunberg and Dattner, 1953). Asymptotic directions of approach for particles of different rigidities incident from different azimuths on the top of the atmosphere have been calculated using realistic simulations of the geomagnetic field (McCracken *et al.*, 1962, 1965). Utilising the trajectory data, it is possible (Rao *et al.*, 1963) to calculate the 'asymptotic cone of acceptance' of any ground detector, i. e. the solid angle in space containing all the asymptotic directions of approach that significantly contribute to the counting rate of the detector. Knowing the specific yield functions and the asymptotic cones of acceptance of the detectors, it is possible to calculate, with perfect generality, the time variations due to any primary cosmic ray anisotropy.

2. Known Features of Interplanetary Medium

2.1. Introduction

It is now well realised that the entire problem of galactic cosmic ray modulation basically reduces to a clear understanding of the motion of cosmic ray particles in the disordered interplanetary magnetic fields. These magnetic irregularities which act as effective scatterers are carried away from the sun by the solar plasma moving radially outward with a velocity of 300–1000 km/s. Both observationally (Ness *et al.*, 1964; McCracken, 1962) and theoretically (Parker, 1958), it is now well established that the frozen in magnetic fields carried away from the Sun by the radially blowing solar wind are stretched in the form of Archimedes spiral, the angle θ which the average spiral field line makes with the radius vector at a distance r from the Sun being given by $\tan\theta = \Omega r/V$ where V is the solar wind velocity and Ω is the angular velocity of solar rotation. The cosmic ray particles essentially random walk through the magnetic field. An exact treatment of the statistical motion of the particles in the interplanetary medium can be realised, in practice, only if the diffusion coefficient is well known. Since the diffusion coefficient is dependent on the power spectrum of the magnetic field irregularities moving with the solar wind, a realistic knowledge of the structure of the interplanetary magnetic fields and the properties of the interplanetary plasma are essential to understand the cosmic ray modulation phenomena.

2.2. Interplanetary field

Large number of direct observations of the interplanetary plasma and the magnetic field near the orbit of the Earth are now available through various satellite observations. Based on these near-Earth measurements, extrapolation to other portions of the solar system can be made. The experimental observations of the interplanetary plasma and magnetic fields will thus form the boundary conditions which will be used to test the

specific theoretical models invoked to explain the cosmic ray modulation processes. Two major properties of the interplanetary magnetic field are of particular relevance to our present discussion.

(i) The average large scale structure of the field (Ness *et al.*, 1964) is in good agreement with the concept of the field lines being stretched in the form of Archimedes spiral. In addition to the average garden hose spiral direction, a well defined sector

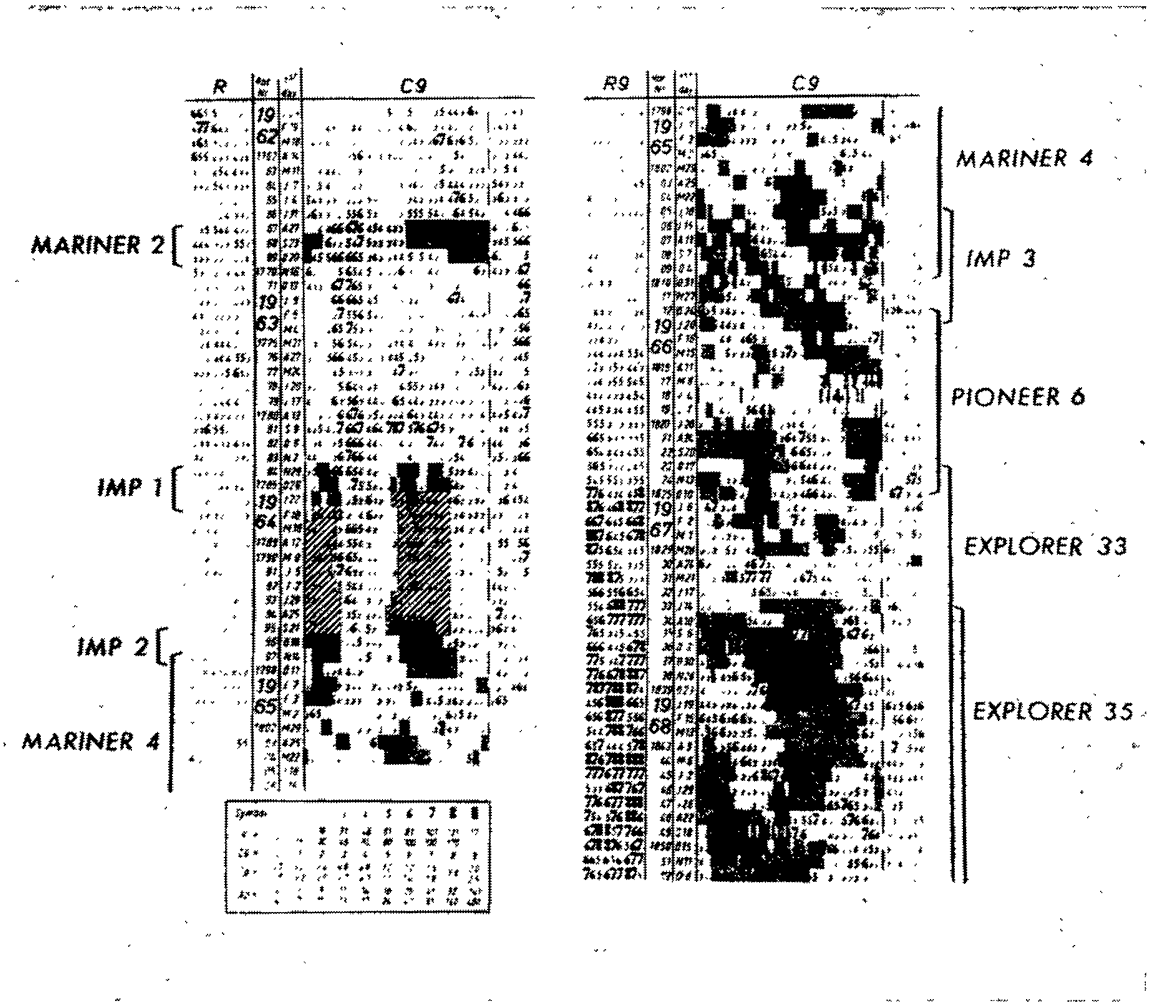

Fig. 1. Observed sector structure of the interplanetary magnetic field during 1962–1968 and the geomagnetic character index C_9 as prepared by the Geophysikalisches Institut in Göttingen. Sectors with field directed predominantly away from the Sun are indicated by light shade and sectors with field towards the Sun by dark shade. The sector structure in 1964 shown by diagnal cross line shading has been obtained through interpolation (after Wilcox and Colburn, 1970).

structure of the field exists according to which the field is divided into 'sectors' in which the field direction is alternatively towards and away from the Sun. Such a quasi-stationary sector structure of the field which was first observed by Wilcox and Ness (1965) has now been confirmed by many authors (Coleman *et al.*, 1966; Wilcox and Colburn, 1969; 1970) over the entire period 1962–1968. The observations indicate that even during the period of maximum solar activity, when a large number of high

velocity plasma streams are emitted from active regions, the sector structure remains well established. Figure 1 shows the observed sector structure during the entire period 1962–1968, the light shading indicating the time when the field direction was away from the Sun and the dark shading indicating when it was predominantly towards the Sun. Except during 1963–1964 when there existed four sectors, during the rest of the period two prominent quasi-stationary sectors with a mean rotation period of 27.0 ± 0.1 days were observed. From the close correlation, between the direction of the interplanetary field observed near Earth and the polarity of the mean solar photospheric field (Ness and Wilcox, 1966; Wilcox and Ness, 1967) with a lag of about 4.5 days corresponding to the transit time of solar wind from the Sun to the Earth, the solar origin (Severny *et al.*, 1971) of the interplanetary field has been established. Since the sector structure plays an important role in determining the azimuthal gradients in the solar cosmic ray flux, and in establishing the conditions that are responsible for recurrent cosmic ray phenomena such as 27 day variations of intensity and corotating Forbush decreases, a knowledge of the sector structure of the interplanetary field is considered essential to our understanding of the cosmic ray phenomena.

(ii) Superimposed on this large scale structure exists a continuous distribution of small scale magnetic field irregularities or 'Kinks' which are essentially frozen into the solar wind and hence corotate with it.

Michel (1967) and Jokipii and Parker (1968a, 1969) have attributed the origin of the small scale irregularities to the motion of prominent photospheric features such as granulations ($\sim 10^3$ km diam) and supergranulations ($\sim 2 \times 10^4$ km diam). Since the magnetic lines of force are tied to the ambient solar plasma, which is turbulent, the field lines will eventually be generally stochastic, even if they were to be highly symmetrical to start with. In other words, the field lines will execute a random walk. A large part of the random walk is probably due to the horizontal displacement of the feet of the lines of force resulting from the motion of granules and supergranules. A granularity with a nominal size of 5×10^3 km on the solar surface, when projected on the Earth's orbit, corresponds to a size of $\sim 10^6$ km, which is in agreement with the typical scale sizes of filamentary inhomogeneities observed by McCracken and Ness (1966) and Bartley *et al.* (1966) during solar flare events and the correlation length D derived from magnetic field observations (Jokipii and Coleman, 1968). Thus the flux tubes in the 'wet spaghetti' model of interplanetary field suggested by Bartley *et al.* (1966) and McCracken *et al.* (1967) can be considered as a direct proof for the existence of random walk of field lines. Figure 2 shows the artistic sketch of the interplanetary field after Jokipii and Parker (1969).

A consequence of major importance that arises due to the random walk of field lines is to increase the value of $K_\perp$, the diffusion coefficient perpendicular to the lines of force. At energies below ~ 1 MeV, the ratio $K_\perp / K_\parallel$ i.e. the ratio between the diffusion coefficient perpendicular to the field lines to that parallel to the field lines may approach unity, suggesting that low energy particles can, under these circumstances move across the field lines as freely as they move along the field lines.

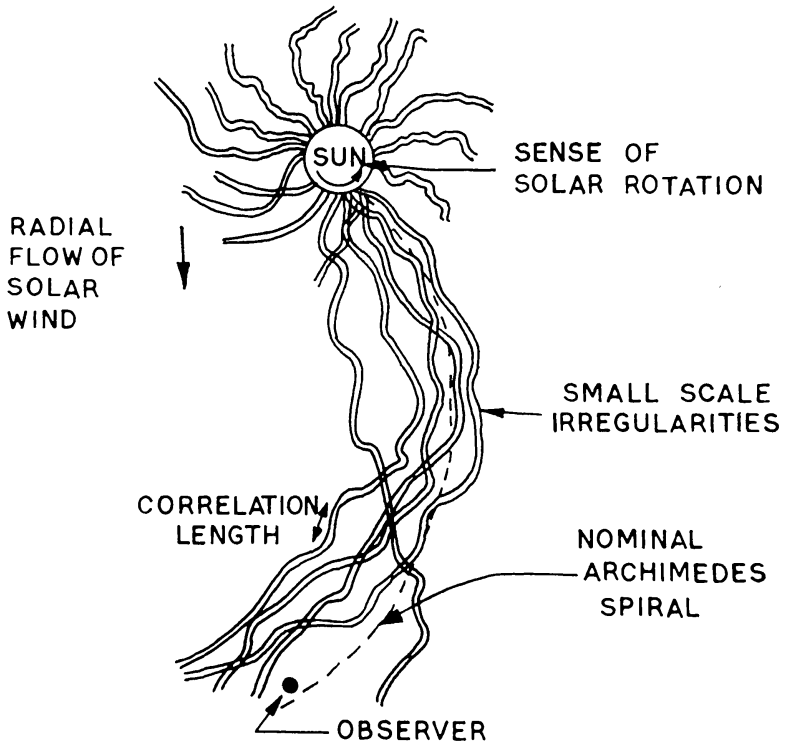

Fig. 2. Interplanetary magnetic field configuration illustrating the random walk of field lines as a result of large scale inhomogeneities in the solar wind. The perfect Archimedes field line due to uniform radial expansion of solar wind is represented by the dotted line (after Jokipii and Parker, 1969).

2.3. Power Spectrum of the Interplanetary Field

In a uniform field, the pitch-angle of a charged particle will not undergo any change and the particles will be strongly collimated. The introduction of random small scale irregularities into such a field will cause random changes in the pitch-angles of the particles as they move along the lines of force. The integrated effect of a large number of scattering irregularities in the field is essentially to produce a three-dimension random walk in the motion of particles. The scattering due to the irregularities is maximum for particles whose cyclotron radius is of the same order as the scale size of the irregularities i.e. the scattering for particles of rigidity R GV depends mainly on the power in the transverse component of the field in the vicinity of the 'resonant frequency' given by

$$f(R) = 10^{-4} R^{-1} \text{ Hz}. \tag{2.1}$$

Figure 3 shows the representative power spectra (which is simply the Fourier transform of the auto co-variance function) of the interplanetary magnetic field during 1962–1966 obtained by several authors (Coleman, 1966; Holzer *et al.*, 1966; Jokipii and Coleman, 1968; Siscoe *et al.*, 1968; Sari and Ness, 1969). On the basis of such power spectra, we shall attempt to derive a few relationships that will aid us in understanding the cosmic ray modulation phenomena. We can approximate the power in the transverse component of the field to a power law in frequency i.e. $P_{xx}(f) \propto f^{-\alpha}$. Under such an approximation, we can derive useful relationships for the estimation of the parallel

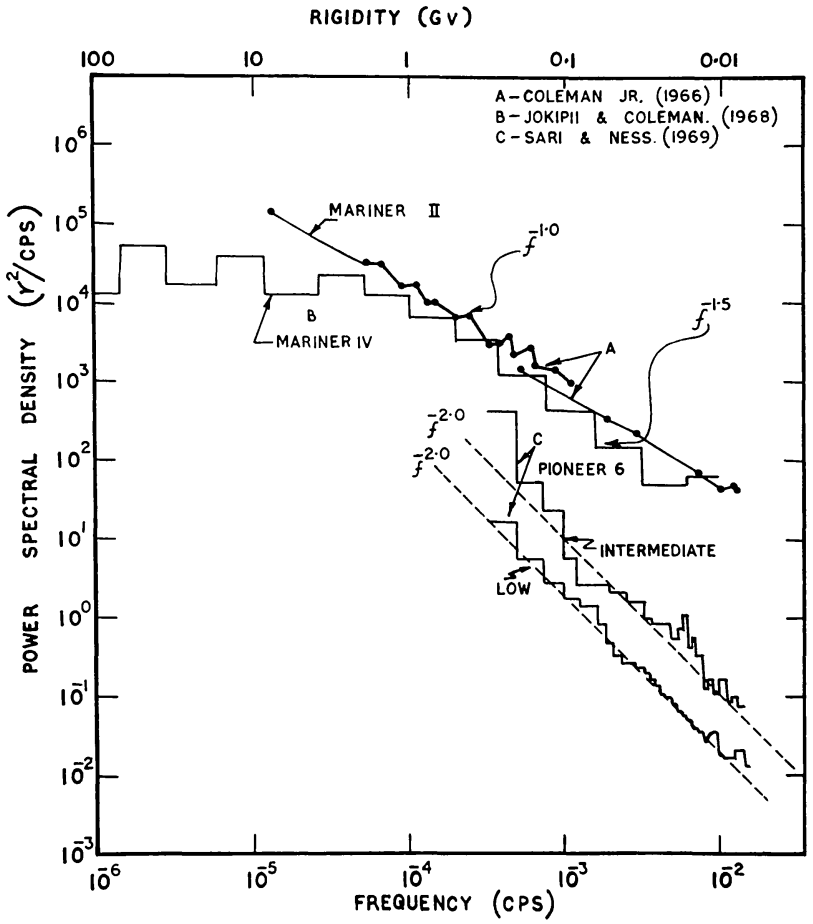

Fig. 3. The representative power spectra of the colatitudinal component of the interplanetary magnetic field obtaining during selected periods in 1962–1963 (Mariner 2), 1964 (Mariner 4) and in early 1966 (Pioneer 6). The two curves for Pioneer 6 correspond to periods of low and intemediate geomagnetic activity (adopted from McCracken and Rao, 1970).

diffusion coefficient, following the mathematical treatment developed by Jokipii (1966, 1967, 1968), Roeloff (1965). Dolginov and Toptygin (1966) and Jokipii and Parker (1968a).

$$K_{\parallel} = \begin{cases} A\beta R^{2-\alpha} & \text{for} \quad R_u > R > R_l \\ \frac{1}{3}cD\beta & \text{for} \quad R < R_l \end{cases} \tag{2.2}$$

where A is a constant, R_u is the rigidity at which the cyclotron radius of the particle becomes approximately equal to the scattering mean free path given by $\lambda = 3\,K_{\parallel}/c\beta$ and R_l is the particle rigidity for which the mean free path λ becomes smaller and approaches D the correlation length of the interplanetary magnetic field, which is typically 2×10^{11} cm. Figure 4 shows the plot of the parallel diffusion coefficient derived from the power spectral density observed on Mariner 4 (Jokipii and Coleman, 1968) as a function of rigidity. The rigidity of about 2 GV which corresponds to the transition point where the slope changes, is to be identified with the particles of rigidity R_l whose cyclotron radius approaches the correlation length D of the magnetic field.

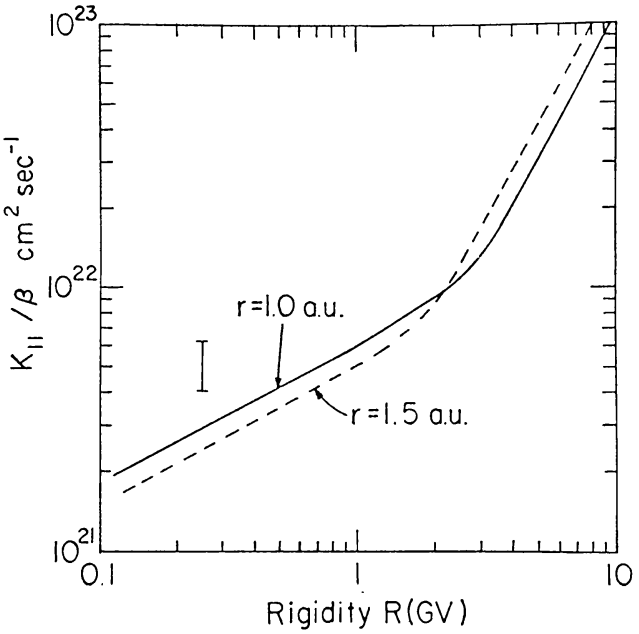

Fig. 4. Parallel diffusion coefficient derived from the power spectral density of magnetic field observed on Mariner 4 spacecraft plotted as a function of rigidity. The change of slope at 2 GV corresponds to particles whose cyclotron radius approaches the correlation length of the magnetic field (after Jokipii and Coleman, 1968).

The perpendicular diffusion coefficient $K_\perp$ due to the power at the 'resonant' frequency is given by

$$K_\perp = K_\perp^m + \left(\frac{r_c^2}{\lambda^2}\right) K_\parallel \tag{2.3}$$

where r_c is the cyclotron radius of the particle. We immediately note that $K_\perp$ is composed of two parts, the first term $K_\perp^m$ on the right-hand side of Equation (2.3) representing the contribution due to the random walk of field lines and the second term due to the resonant scattering by field fluctuations. If diffusion across the field lines were to be principally due to scattering by field fluctuations, then the ratio $K_\perp/K_\parallel$ would be very small, of the order of $0(\lesssim 10^{-2})$ for protons of energy ~ 10 MeV. Jokipii and Coleman (1968) find that during 1968, the contribution from the 'meandering' origin of the interplanetary field lines, to the diffusion coefficient at these energies dominates over the second term in Equation (2.3) making $K_\perp^m \simeq K_\parallel$ for 10 MeV protons. The physical implications of $K_\perp/K_\parallel \approx 1$ would be that at the corresponding particle energies, isotropic diffusion will dominate and probably cause a complete cancellation of corotation effects.

From an examination of Figure 3, it is clear that (1) The small scale irregularities affect all charged particles of rigidity lower than about ~ 5 GV corresponding to resonant frequencies greater than $\sim 5 \times 10^{-4}$ Hz. In terms of scale sizes, the scattering irregularities correspond to dimensions $< 5 \times 10^{-2}$ AU. The power spectral density for particles of higher rigidities ($R \gtrsim 5$ GV), however, seems to be independent of frequency. (2) The power spectral density of the interplanetary magnetic field shows a

large variation from day to day, the spectral density on a disturbed day often showing an increase by as much as a factor 10 compared to the density on a quiet day, with the spectral shape, however, remaining practically unaltered. (3) Even though the power spectral density in 1962 (Mariner 2) and 1965 (Mariner 4) were comparable to each other within a factor of two, the power density in 1966 as observed on Pioneer 6 (Sari and Ness, 1969) shows, surprisingly, a much lower (> factor of 10) spectral density. Re-examination (Belcher *et al.*, 1971) of the latter data, however, has cast some doubt on the absolute level of power spectral density derived by Sari and Ness (1969) and therefore with the presently available evidence, it is not possible to draw definitive conclusions regarding the long term variation of power spectral density of the interplanetary magnetic field.

For particles in the rigidity range 10 MV $< R <$ 5 GV, the spectral exponent α of the power density in Figure 3 shows significantly different values at different epochs indicating different rigidity dependencies for $K_{\|}$. Table I summarizes the rigidity

TABLE I

Summarizing the rigidity dependence of the diffusion coefficient at different epochs during 1962–1966 derived from the power spectral observations of the interplanetary magnetic field. A correlation length D of 2×10^6 km has been assumed for calculating R_l (after McCracken and Rao, 1970).

Epoch	Spacecraft	α	R_l(GV)	$K_{\|}(R, \beta)$[a]	$\lambda(R, \beta)$[a]	Author
1962	Mariner 2	1.0	0.4	$AR\beta$	$\lambda_0 R$	Coleman, 1966
Nov./Dec. 1964	Mariner 4	1.5	0.16	$AR^{1/2}\beta$	$\lambda_0 R^{1/2}$	Jokipii and Coleman, 1968
Dec. 1965/Jan. 1966	Pioneer 6	2.0	–	$A\beta$	Const.	Sari and Ness, 1969

A and λ_0 are constants.
[a] The values are for $R_u > R > R_l$

dependence of $K_{\|}$ and of λ, the mean free path during different epochs derived from the power spectral observations shown in Figure 3. The table reveals that (a) the mean free paths may vary as R, $R^{1/2}$ and R^0 depending on the power spectra at each epoch, and (b) the lower limit of rigidity R_l below which the mean free path is constant can vary as

$$0 < R < 0.4 \text{ GV} \quad \text{or} \quad 0 < E_p < 80 \text{ MeV}.$$

In spite of the reasonably satisfactory theoretical treatment leading to the derivation of quantities characterising the cosmic ray particle motion from the observed magnetic field data, it should be pointed out that many difficulties are still present before the magnetic data can be explicitly employed.

(1) Recent studies of correlated field and plasma measurements have shown that the power spectral densities computed from the magnetic data also include the contribution from tangential plasma-magnetic microstructures of scale lengths in the order of 0.01 AU. These microstructures have been interpreted by Burlaga (1968,

1969) and Burlaga and Ness (1968) as due to sharp directional discontinuities whereas Belcher and Davis (1971) and Belcher *et al.* (1971) conclude that the microscale fluctuations are dominated by Alfvén waves. Even though considerable doubt exists as to the true nature of these microstructures, nevertheless, the detailed studies (Sari and Ness, 1969) have shown that such structures contribute a substantial power with a f^{-2} frequency dependence, particularly at $f \gtrsim 5 \times 10^{-4}$ Hz. These microstructures which are more in the nature of characteristics between adjacent tubes of force are not likely to have significant effect on cosmic rays. If due allowance is made to account for their contribution to the general power spectral density, the estimates of the effective parallel diffusion coefficients will be increased by roughly a factor of 2 at rigidities $R < R_u$, besides distorting the effective power spectra of the magnetic field. It is, therefore, obvious that a more precise knowledge of the microstructures is essential for applying the magnetic data to cosmic ray phenomena.

(2) Since all the ground based neutron monitor studies, which have yielded the maximum information on the modulation of galactic cosmic radiation, refer to particles above 1 GV, at which rigidities, the available power spectral density information is scanty and unreliable (some indication exists that it is constant at frequencies below 5×10^{-4} Hz corresponding to rigidities above 5 GV), the magnetic field information, presently available, is not useful to derive any conclusions regarding the propagation of high rigidity cosmic ray particles.

(3) Even though the magnitude of the interplanetary field as well as its power spectral density show significant variations on a day to day basis, the annual mean interplanetary magnetic field ($\sim 5\ \gamma$) and probably also the annual mean power spectral density essentially show time invariance over the solar cycle of activity.

(4) The properties of the interplanetary field enumerated above relate to the conditions near Earth and reasonable extrapolations to other parts of solar system is required before application to the cosmic ray phenomena. Besides, the observed data on the field fluctuations, are in reality, the fluctuations experienced by a stationary observer as different tubes of magnetic lines of force are convected past the observer by the solar wind and again extrapolation is needed to apply the results to infer the fluctuations along the tubes of force. In other words, the presently known properties of the interplanetary field can only serve as boundary conditions and a complete solution of the modulation phenomena will have to wait till simultaneous measurements of plasma and fields at different helio-distances are available.

2.4. Gross properties of solar wind

Since the first direct observations of the solar wind by Gringauz *et al.* (1960) on Lunik 2, a large number of measurements on the properties of the solar wind have been made in various spacecrafts at different epochs. Number of excellent reviews are available in literature (ex. Axford, 1968; Parker, 1969; Hundhausen, 1970) describing, in detail, the observational evidence on solar wind obtained from direct measurements and their theoretical implications. Table II summarizes the average properties of the quiet day solar wind. Figure 5 which illustrates the observed daily

TABLE II

Average properties of solar wind

Parameter	Typical quiet day value
Bulk velocity	350 km/s
Proton and electron density	8 cm^{-3}
Proton temperature	5×10^4 K
Electron temperature	1.5×10^5 K
Kinetic energy density	8×10^{-9} erg cm^{-3}

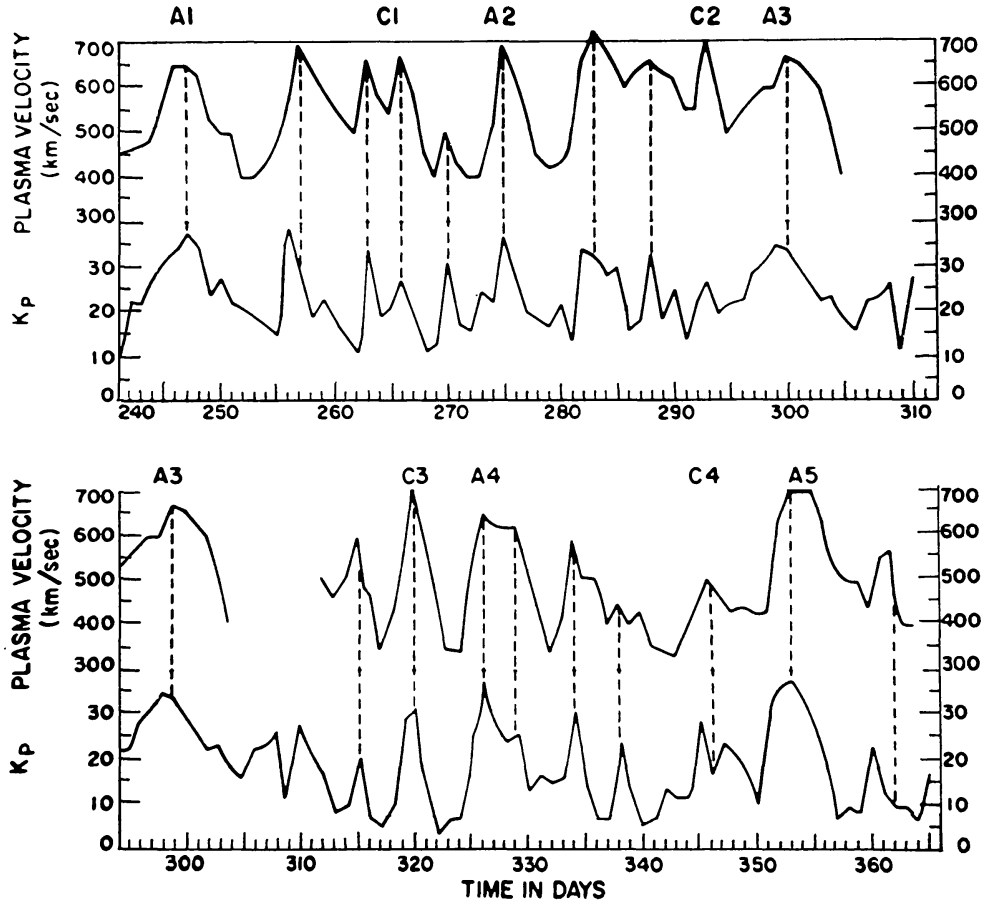

Fig. 5. The daily average solar wind velocity and the ΣK_p index during August, 1962–January, 1963 plotted on a 27 day scale. The 27 day recurrence in both the wind velocity and in K_p is clearly seen in the figure (after Snyder *et al.*, 1963).

mean bulk solar wind speed during August–December 1962, clearly demonstrates the large variability in the magnitude of the solar wind speed on a day to day basis which is also typical of the other physical parameters of the solar wind. Thus, for example, the observed solar wind speed ranges from 250–850 km s^{-1} and the number density varies from 1–120 cm^{-3} even though the typical quiet day values are about 350 km s^{-1} and 8 cm^{-3}. From a large number of observations (Strong *et al.*, 1967), the solar wind has been shown to be largely radial, the off radial angle being usually less than 5°.

Figure 5 also demonstrates an excellent correlation between $\sum K_p$ indices, the index of the geomagnetic disturbance and the solar wind velocity. A pronounced 27-day recurrence tendency in both $\sum K_p$ and the solar wind velocity (Snyder *et al.*, 1963) indicate the association of enhanced wind velocity with *M* region storms. The existence of strong correlation between $\sum K_p$ and solar wind velocity has been further confirmed by later observations (Pai *et al.*, 1967). Such a relationship, in principle,

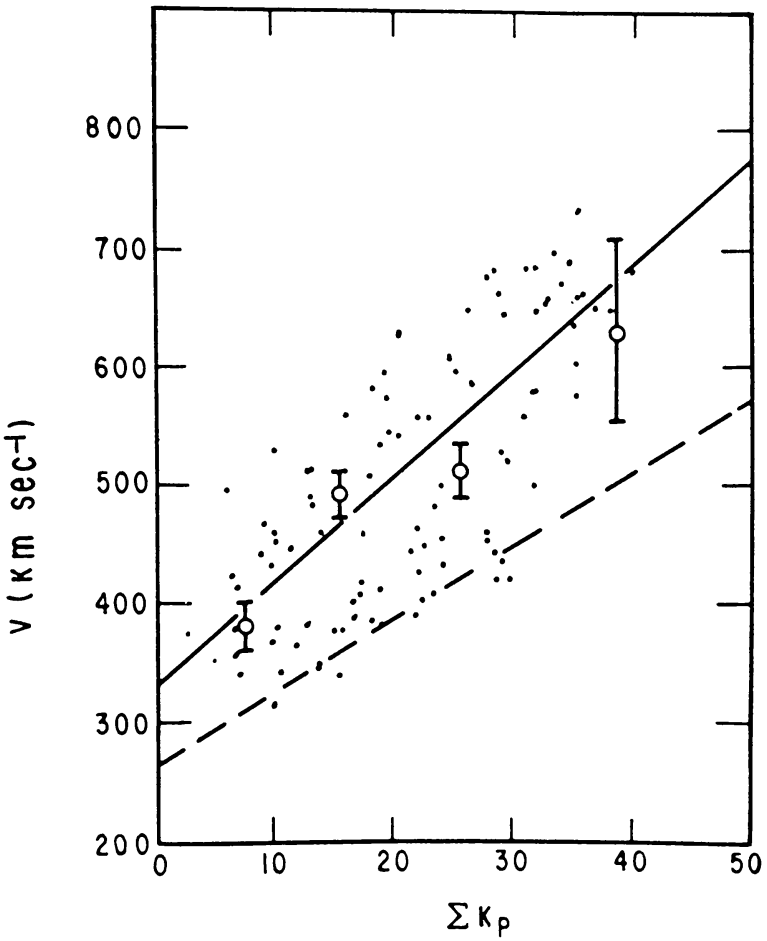

Fig. 6. Illustrating the correlation between ΣK_p and the solar wind velocity. The black dots and the solid line correspond to the daily mean values and the best fit regression line $V = (8.44\ \Sigma K_p + 330)$ km s^{-1}, obtained from Mariner 2 data during late 1962 (Snyder *et al.*, 1963) and the broken line corresponds to the regression fit obtained from IMP 1 data during 1963 (Pai *et al.*, 1967). The open circles represent the wind velocity values obtained from comet tail data (Brandt, 1967) with their error bars (after Axford, 1968).

permits us to extrapolate the solar wind values even during periods when direct observations are not available. Figure 6 shows the regression line defining the relationship between $\sum K_p$ and the solar wind velocity as observed on two different periods by Snyder *et al.* (1963) and Pai *et al.* (1967). On the basis of these observations, one would expect a variation of the solar wind velocity from about 300 km s^{-1} to 530 km s^{-1} (Snyder *et al.*, 1963) over a solar cycle which would agree with the theoretical prediction (Parker, 1963).

However, close examination of the experimental observations conducted at different times during 1962–1967 by various workers clearly shows that the long term variation of solar wind velocity is not consistent with the predictions made from the data on a short time basis. Figure 7 shows the histograms of the frequency of occurrence of different solar wind speeds (Gosling *et al.*, 1971) during each year in the period 1962–1970. A significant feature of the figure is the relative constancy of the mean

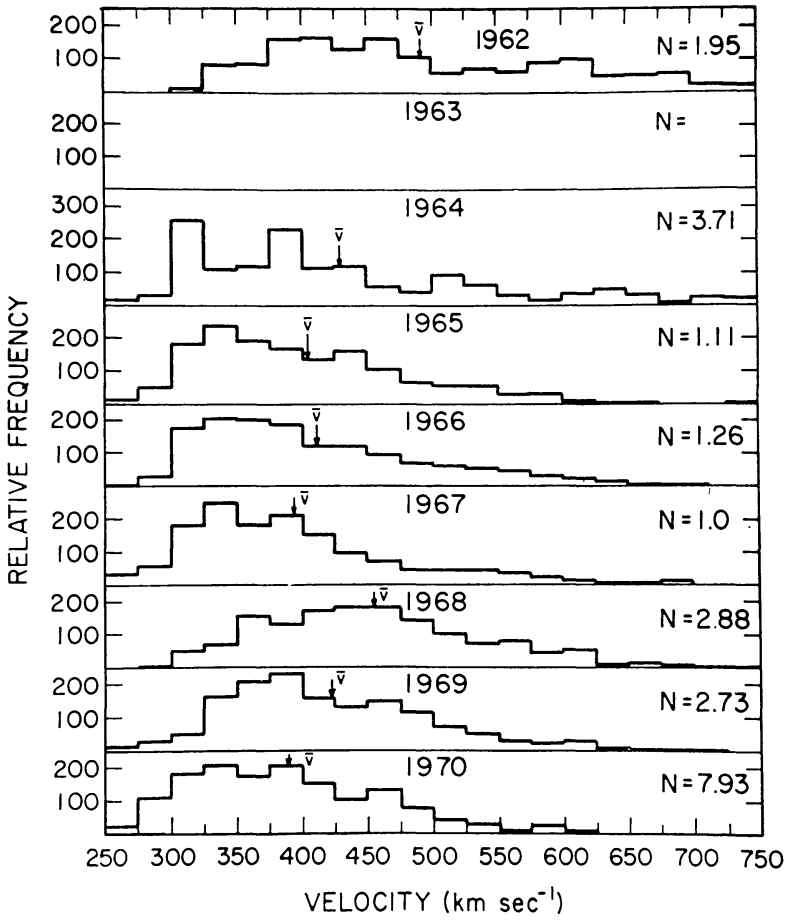

Fig. 7. Histograms showing the frequency of occurrence of different solar wind speeds in each year during 1962–1970. The mean values of the solar wind speed for each year is marked by an arrow in the diagram. The data points shown in the figure includes observations from various workers (Neugebauer and Snyder, 1966; Wolfe *et al.*, 1966; Pai *et al.*, 1967; Coon, 1968) after Gosling *et al.* (1971).

solar wind speed from year to year (shown by an arrow in the figure) indicating a very small variation in the mean speed over a solar cycle. Similar analysis done for solar wind temperatures and proton densities during 1964–1967 have further strengthened the conclusion regarding the relative constancy of the physical parameters of the solar wind over the solar cycle. In summary, the experimental observations seem to indicate that both the interplanetary physical parameters, namely the magnetic field and the solar plasma do not exhibit significant variations on a long term basis (Mathews *et al.*, 1971).

In all our discussion, so far, we have considered only the near Earth measurements in the ecliptic plane. At present no direct measurements are available of magnetic field and solar wind at different heliolatitudes away from the plane of ecliptic. Consequently our present knowledge of the interplanetary medium away from the plane of ecliptic and at large distances from the Earth's orbit are derived mainly from indirect observations such as comet tails and radio scintillations (Axford, 1968). Such indirect data being not very reliable, a complete understanding of the cosmic ray modulation effects must await the direct measurements of the interplanetary parameters by off-ecliptic space probes.

3. Motion of Cosmic Rays Through Interplanetary Space

3.1. Introduction

Various theoretical models have been proposed to account for the experimental observations of cosmic ray modulation, the radial density gradient, the radial anisotropy and their interconnection in terms of either the electric fields in the interplanetary space or the interplanetary magnetic field structure. All the models and processes that have been advanced to explain the galactic cosmic ray modulation, fall into mainly two classes – (1) Electric Field Models, and (2) Diffusion-Convection Models.

The possibility of heliocentric electric fields causing energy modulation of cosmic rays was first proposed by Alfvén (1949) and has since been modified by a number of workers (ex. Nagashima, 1951; Ehmert, 1960; Nagashima *et al.*, 1966; Frier and Waddington, 1965). According to this model, the cosmic ray particles undergo large energy changes as they are transported into the solar system due to the electric fields which may arise either from an electrostatic potential in the interplanetary space or by the time variation of the interplanetary magnetic field. The energy loss per nucleon produced by the heliocentric electric fields (or large scale $\mathbf{V} \times \mathbf{B}$ electric fields) can be calculated using Liouville's theorem and is found to be characterised by

$$\Delta E = \left(\frac{Ze}{A}\right) V' \tag{3.1}$$

where V' is the equivalent potential energy loss. The energy loss is energy independent, if the electric field is only due to an electrostatic potential. Even the early results on the modulation of high energy cosmic rays, clearly revealed that the modulation was rigidity dependent. The original approach has since been considerably modified (Singer *et al.*, 1962; Frier and Waddington, 1965; Nagashima *et al.*, 1966; Webber, 1969) by including the diffusive energy loss processes due to betatron and Fermi deceleration associated with fluctuating magnetic fields in which case Liouville's theorem is not applicable. Since both types of loss processes are strongly dependent on the form of input galactic spectrum (Nagashima *et al.*, 1966), a detailed comparison of the theory with experiment is extremely difficult without a good knowledge of the input spectrum.

Using simple form for the input spectra such as $E^{-\gamma}$, Parker (1966) has derived an

expression for the cosmic ray distribution $U(r, E)$ at a heliocentric distance r which includes energy losses due to adiabatic deceleration in terms of the distribution at infinity $U(\infty, E)$ as

$$U(r, E) = U(\infty, E)\left\{1 - \frac{V(L-r)}{K}\left[1 + \tfrac{1}{3}(\gamma + \beta - 1)\right]\right\} \tag{3.2}$$

where L is the dimension of the modulating region, and V is the solar wind velocity. The factor $\frac{1}{3}(\gamma+\beta-1)$ in the above expression represents the effect of energy loss. Since the difference in the predictions on long term modulation (Quenby, 1965, 1967) from both classes of theories are quite small, especially if the input energy spectrum is the same, and the diffusion-confection model with energy losses included has led to an elegant mathematical formulation besides demonstrating the interconnection between the long term modulation and the radial density gradient and anisotropy, we discuss this model in a greater detail and then proceed to compare the deductions from this model with the experimental observations.

3.2. Diffusion-convection model

The simple diffusion-convection model which was originally proposed by Morrison (1956) and Parker (1958) has since been revised greatly by a number of workers (Gleeson and Axford, 1967; 1968a; 1968b; Fisk and Axford, 1968; 1969; Jokipii, 1967; Jokipii and Parker, 1967; 1968a; Skadron, 1967) on the basis of pioneering work by Parker (1965, 1966) on the effect of energy losses due to adiabatic deceleration. According to this theory, the modulation of the galactic cosmic ray intensity is attributed to the motion of cosmic ray particles in a spherically symmetric model of the interplanetary medium in which the cosmic ray particles undergo convection, diffusion and energy changes as they move in the irregular magnetic fields. The cosmic ray particles undergo considerable energy losses due to adiabatic deceleration in the expanding solar wind, the deceleration resulting from repeated scattering by the magnetic field irregularities which are moving outward from the Sun at the solar wind velocity. Jokipii and Parker (1967) and Jokipii (1971) have treated the cosmic ray transport problem assuming adiabatic deceleration; whereas Gleeson and Axford (1967) and Fisk and Axford (1969) have treated this problem by considering the scattering processes, both treatments leading to essentially similar equations.

The theoretical formulation of the solar modulation of galactic cosmic rays has been recently reviewed in great detail by a number of authors (Parker, 1969; Gleeson, 1971; Jokipii, 1971). In this review, we therefore attempt to give only a brief summary of the theoretical development and compare the predictions on radial density gradient, radial anisotropy and the long term modulation of intensity with the experimental observations.

Assuming an isotropic velocity distribution of cosmic ray gas, the differential number density $U(r, E)$ and the differential streaming current density $S(r, E)$ in a steady state at kinetic energy E and at a radial distance r from the Sun is given by

(Gleeson and Axford, 1967; Fisk and Axford, 1969, 1970; Gleeson, 1971)

$$\frac{1}{r^2}\frac{\partial}{\partial r}(r^2 S) + \frac{V}{3}\frac{\partial^2}{\partial r\,\partial E}(\alpha E U) = 0 \tag{3.3}$$

and

$$S(r, E) = C(r, E)\,VU - K\frac{\partial U}{\partial r} \tag{3.4}$$

where

$$C(r, E) = 1 - \frac{1}{3}\frac{1}{U}\frac{\partial}{\partial E}(\alpha E U) \tag{3.5}$$

is the Compton-Getting factor (Gleeson and Axford, 1968b; Forman, 1970a), $V(r)$ is the solar wind velocity, $K(r, E)$ is the diffusion coefficient and

$$\alpha = \frac{E + 2m_0c^2}{E + m_0c^2},$$

m_0c^2 being the rest energy of the particles under consideration. Eliminating S between Equations (3.3) and (3.5), we obtain the Fokker-Planck equation

$$\frac{1}{r^2}\frac{\partial}{\partial r}(r^2 VU) - \frac{1}{3r^2}\frac{\partial}{\partial r}(r^2 V)\frac{\partial}{\partial E}(\alpha E U) - \frac{1}{r^2}\frac{\partial}{\partial r}\left(r^2 K\frac{\partial U}{\partial r}\right) = 0. \tag{3.6}$$

This is identical to the equation derived by Parker (1965) and Jokipii and Parker (1967) using the concept of adiabatic deceleration. The second term on the left-hand side of Equation (3.6) includes the result of energy changes suffered by cosmic ray particles in the expanding solar wind. The above equation reveals that the intensity at any point and epoch can be derived knowing the diffusion coefficient valid for that energy and epoch.

If the energy loss term in Equation (3.6) is neglected, we can obtain the solution of the equation in the steady-state convection-diffusion theory. Assuming spherical symmetry, Equation (3.6) can be solved (neglecting second term) to yield the well-known expression for the modulated cosmic ray density $U(R, \beta, t)$ at a time t at the orbit of the Earth

$$U(R, \beta, t) = U_0(R, \beta, t)\exp - \int_r^L \frac{V(r, t)}{K(R, \beta, r, t)}\,dr \tag{3.7}$$

where V is the solar wind velocity, K is the isotropic diffusion coefficient and L is the dimension of the modulating region beyond which the cosmic ray flux is assumed to be the interstellar cosmic ray density $U_0(R, \beta, t)$.

(1) Assuming K to be a separable function of R and r, given by $K = K_1(r, t)\,K_2(R, t)\,\beta$, Equation (3.7) is usually written as

$$U(R, \beta, t) = U_0(R, \beta, t)\exp - \left[\frac{\eta(r, t)}{f(R, \beta)}\right]$$

where

$$\eta(r, t) = \int_r^L \frac{V(r, t)}{K_1(r, t)}\, dr \tag{3.8}$$

is the modulating parameter, and $f(R, \beta)$ has the same form as $K_2(R, \beta)$. The cosmic ray intensity at any point therefore depends on the solar wind velocity, the dimension of the modulating region and the diffusion coefficient which may be a function of rigidity, time and distance.

(2) Besides the prediction of the absolute intensity, the diffusion-convection theory also predicts the change in modulation at any given rigidity, the change being caused by the changes in V, L or K. Whereas the changes in V are easily measured, the changes in L and K are to be inferred from the observed changes in the inter-relationship between cosmic ray solar activity parameters and the changes in the power spectral density of the interplanetary magnetic field respectively. The change in modulation at times t_1 and t_2, at any rigidity R is given by

$$M = \beta \ln \frac{U_1}{U_2} = \frac{3}{c}\left[\frac{V_2(L_2 - r)}{\lambda_2} - \frac{V_1(L_1 - r)}{\lambda_1}\right] \tag{3.9}$$

where λ is the mean free path equal to $3\, K/c\beta$

(3) The radial gradient of cosmic ray intensity for simple convection-diffusion, is given by

$$G = \frac{1}{U}\frac{\partial U}{\partial r} \approx \frac{V(r, t)}{K(R, \beta, r, t)}. \tag{3.10}$$

The rigidity dependence of the radial gradient will depend on the rigidity dependence of K.

(4) The fractional changes of any species $\beta \ln(U_1/U_2)$ being dependent on rigidity, the relative modulation of protons, electrons and helium nuclei, at any given rigidity, should be identical, if simple convection-diffusion theory is applicable.

If energy losses, which may be quite significant particularly at low energies, are considered, it is not possible to obtain explicit analytic soluiions to Equation (3.6) valid at all energies. On the other hand, usefull deductions regarding the behaviour of particles can be made assuming simple forms for the diffusion coefficient K. Jokipii (1967), and Fisk and Axford (1969) have tried to obtain approximate analytic solution to the above equation at constant α assuming the diffusion coefficient K to be a separable function of r and R which implies that the scattering mean free path is also a separable function of r and R. Since the value of α changes continually with E approximating to ≈ 2 at very low energies and to ≈ 1 at relativistic energies, it is not possible to have a solution valid over the entire energy range. If, instead, simple approximations valid over limited energy intervals are used to predict the nature of cosmic ray anisotropies, more useful results are obtainable. In practice, it has been found useful to define a dimensionless quantity (Gleeson and Axford, 1968a) which may be termed as 'Reynolds number' for the modulation.

$$H = S \Big/ \left[VU - \tfrac{1}{3} V \frac{\partial}{\partial E} (\alpha E U) \right] \approx \frac{Vr}{K} \tag{3.11}$$

which is useful in defining the energy limits within which each of the approximation is valid. For particles of relativistic velocities ($E \gtrsim 1$ GeV), $H \ll 1$ and at lower energies $H \gtrsim 1$.

3.2.1. *At High Energies*

At high energies ($E \gtrsim 100$ MeV), streaming current density S and the radial anisotropy ξ are both very small and $H \ll 1$ which when applied to Equation (3.4) yields

$$VU - K \frac{\partial U}{\partial r} - \frac{V}{3} \frac{\partial}{\partial E} (\alpha E U) = 0$$

and

$$S \approx \frac{Vr}{6} \frac{\partial^2}{\partial r \, \partial E} (\alpha E U). \tag{3.12}$$

The differential radial gradient of cosmic ray intensity can be approximated by

$$G = \frac{1}{U} \frac{\partial U}{\partial r} \approx \left(\frac{V}{K} \right) C(r, E) \tag{3.13}$$

with $K \approx 9.3 \times 10^{21}$ cm^2 s^{-1}, the radial density gradient at 5 GeV works out to be about 9%/AU which compares well with the experimental observations (O'Gallagher, 1967).

Equation (3.13) relates the radial density gradient directly to the spectral distribution of the cosmic ray flux (through the Compton-Getting factor C) and to the diffusion coefficient. Substituting the value of the density gradient in Equation (3.6), the radial anisotropy ξ for particles of velocity v is given by

$$\xi = \frac{3S}{vU} - \frac{Vr}{6} \frac{\partial^2}{\partial r \, \partial E} (\alpha E U) \approx - \frac{V}{2v} \frac{1}{U} \frac{\partial}{\partial E} \left[\alpha E C U \left(\frac{Vr}{K} \right) \right]. \tag{3.14}$$

From the above equation, it is clear that one can use the unmodulated spectrum for determining ξ for values of $(Vr/K) \ll 1$. Assuming the cosmic ray spectrum to be represented by a spectrum of the type $E^{-\gamma}$, the expression for the radial anisotropy can be reduced to (Fisk and Axford, 1970)

$$\xi \approx - \gamma \alpha \left(\frac{V}{2v} \right) \left(\frac{r}{U} \frac{\partial U}{\partial r} \right). \tag{3.15}$$

Figure 8 shows the plot of the theoretically estimated value of the radial density gradient and radial anisotropy for particles of energies greater than 200 MeV which will be compared with the experimental observations later.

3.2.2. *Approximation at Low Energies*

At low energies, due to the decrease of the diffusion coefficient with energy, the

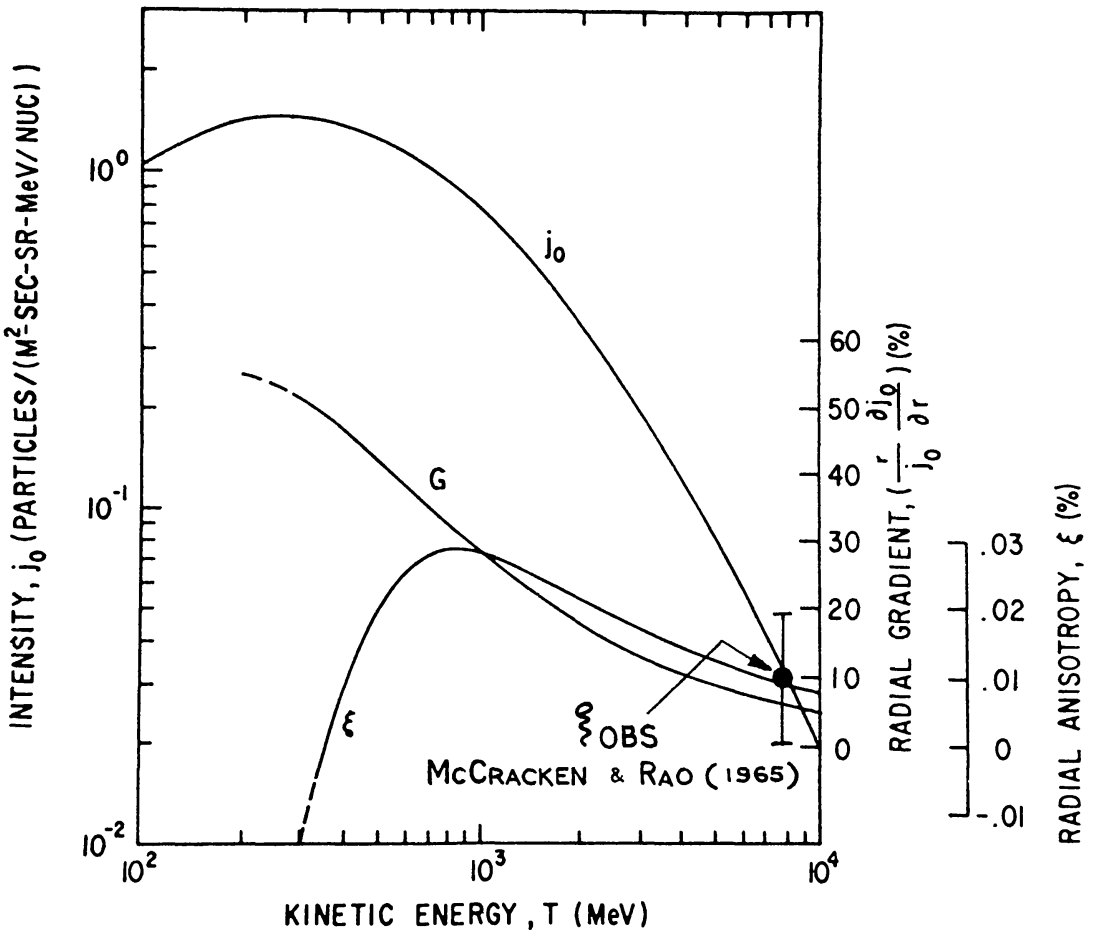

Fig. 8. Showing the theoretically estimated radial density gradient and the radial anisotropy of cosmic radiation at energies above a few hundred MeV. The calculations are based on (1) the input spectrum of type $E^{-\gamma}$ given by Gloeckler and Jokipii (1967), (2) the diffusion coefficient to be proportional to $R\beta$ and (3) $V = 400$ km s^{-1} (after Fisk and Axford, 1970). The experimentally observed value of radial anisotropy (McCracken and Rao, 1965) at high energies is also plotted in the figure.

condition $H \ll 1$ is no more valid. In fact, at energies below 50 MeV/nucleon, $H > 1$ (about 3). Under this condition, the approximation depends very crucially on the magnitude of the radial density gradient and the streaming current vector.

3.2.3. *Case 1: Large Radial Density Gradients*

If the radial density gradients at low energies are very large, the term containing the streaming current density $2S/r$ in Equation (3.3) can be neglected yielding

$$\partial S/\partial r \approx -\frac{V}{3}\frac{\partial^2}{\partial r\,\partial E}(\alpha E U) \tag{3.16}$$

which on integration and assuming V to be a constant reduces to

$$S \approx -\frac{V}{3}\frac{\partial}{\partial E}(\alpha E U). \tag{3.17}$$

TABLE III

Observed heliocentric radial gradients for galactic particles of different energies and species during various epochs

	Year	Spacecraft	Particles	Kinetic energy MeV/nucleon	Radial range r(AU)	r(AU)	Gradient % per AU	Reference
1	1960	Pioneer 5	Protons and Helium	75	1.0–0.9	0.1	0.0 ± 20	Simpson *et al.* (1962)
2	1962	Mariner 2	Protons and Helium (Ionization chamber)	10	1.0–0.71	0.29	12.0 ± 4	Neher and Anderson (1964)
3	1962	Mariner 2	Protons an Helium (GM counter)	10	1.0–0.71	0.29	0.0 ± 15	Anderson (1965)
4	1962	Zond 1	Protons and Helium (GM counter)	Integral	1.0–1.25	0.24	0.0 ± 12	Vernov *et al.* (1964)
5	1965	Mariner 4	Protons	Integral	1.0–1.56	0.56	9.6 ± 0.9	O'Gallagher and Simpson (1967)
6	1965	Mariner 4	Protons	430	1.0–1.56	0.56	3	Krimigis (1968)
7	1965	Mariner 4	Protons and Helium	10	1.0–1.28	0.28	6.8 ± 1.6	Anderson (1968)
8	1965	Mariner 4	Protons and Helium	50	1.0–1.56	0.56	-14.4 ± 2	Krimigis and Venkatesan (1969)
9	1965	Zond 3 and Venus 2	Protons and Helium (GM counter)	Integral	0.9–1.28	0.39	$4 \pm ?$	Vernov *et al.* (1966)
10	1965	Mariner 4	Protons	1–15	1.0–1.56	0.56	< 500	O'Gallagher and Simpson (1967)
11	1965	Mariner 4	Protons	20–30	1.0–1.56	0.56	500 ± 135	O'Gallagher and Simpson (1967)
12	1965	Mariner 4	Protons	30–60	1.0–1.56	0.56	187 ± 63	O'Gallagher and Simpson (1967)
13	1965	Mariner 4	Protons	70–100	1.0–1.56	0.56	145 ± 63	O'Gallagher and Simpson (1967)
14	1965	Mariner 4	Helium	100–300	1.0–1.56	0.56	65 ± 8	O'Gallagher and Simpson (1967)

Tabel III (continued)

	Year	Spacecraft	Particles	Kinetic energy MeV/nucleon	Radial range r(AU)	r(AU)	Gradient % per AU	Reference
15	1965	Mariner 4	Helium	300–420	1.0–1.56	0.56	55 ± 5	O'Gallagher and Simpson (1967)
16	1965	Zond 3 and Venus 2	Protons	1–5	1.1–0.87	0.23	~ 220	Vernov *et al.* (1968)
17	1967	Mariner 5	Protons	> 0.32	1.0–0.7	~ 0.30	-400 ± 100	Krimigis (1970)
18	1968	Pioneer 8	Protons	> 2000	1.0–1.12	0.12	-1.5 ± 6	Lezniak and Webber (1970)
19	1968	do	do	1250–2000	1.0–1.12	0.12	0 ± 7	
20	1968	do	do	660–1250	1.0–1.12	0.12	23 ± 8	
21	1968	do	do	334– 660	1.0–1.12	0.12	28 ± 9	
22	1968	do	do	240– 334	1.0–1.12	0.12	-7 ± 11	
23	1968	do	do	63– 107	1.0–1.12	0.12	20 ± 15	
24	1968	do	do	> 60	1.0–1.12	0.12	0 ± 5	
25	1968	Pioneer 8	Protons	12– 25	1.0–1.12	0.12	0 ± 25	
26[a]	1970	Meteorite Study	Protons	> 400 MeV	1 –2	–	60 ± 25	Forman *et al.* (1971)
27[a]	1967–68	Cosmic Rays	Protons	$\sim$ 5 Gev	–	–	8	Bercovitch (1971)
28[a]	1965–70	Cosmic Rays	Protons	$>$ 1 Gev	–	–	8	Rao *et al.* (1971)

[a] These are rough estimates inferred from indirect measurements.

The radial anisotropy ξ can be written (Fisk and Axford, 1970) as

$$\xi = -\frac{V}{v}\left(\alpha \frac{\partial \ln j_0}{\partial \ln E} + 1\right) \tag{3.18}$$

where $j_0 = vU/4\pi$ is the mean differential intensity.

3.2.4. *Case 2: Small Radial Density Gradients*

Small radial density gradient usually means that the scattering is very large and the particles are effectively frozen into the solar wind. If the density gradient is small, particles will undergo severe deceleration in the adiabatically expanding solar wind, the radial anisotropy being mainly produced by Compton-Getting effect due to the bulk motion of the particles with the solar wind velocity. Under this condition, the term space $K(\partial U/\partial r)$ can be neglected in Equation (3.4) which then yields

$$\xi = \frac{4CV}{v} - \frac{V}{v}\left(\alpha \frac{\partial \ln j_0}{\partial \ln E} - 2\right). \tag{3.19}$$

The expression for the radial gradient, is similarly shown to be (Fisk and Axford, 1970)

$$G \approx \frac{-2C}{r} \approx \tfrac{2}{3}\left(\alpha \frac{\partial \ln j_0}{\partial \ln E} - 2\right). \tag{3.20}$$

These results also apply in the case of purely convective transport (Gleeson, 1971).

3.3. Radial density gradient of cosmic ray intensity

A prediction of considerable importance to the modulation phenomena arising out of the diffusion-convection model relates to the existence of a positive radial density gradient outward from the Sun during periods when Sun itself is not a source of particles. Such a radial density gradient would depend on the magnitude of the residual modulation, the larger the modulation, the larger being the gradient. In spite of the several attempts that have been made in the past to measure the radial density gradient of both protons and alpha particles, the experimental observations, particularly at low energies, have proved to be inconclusive.

Table III summarizes all the presently available data on the radial gradients of particles of different energies and species at various epochs. It is seen from the table that the mean radial gradient at relativistic energies during 1962–1967 was generally of the order of 8% per AU. Occasional reporting of the negative gradients (Krimigis and Venkatesan, 1969; Krimigis, 1970; Vernov *et al.*, 1970a) are attributable to the presence of particles of solar origin. Major discrepancy, however, exists at lower energies, particularly between the observations of O'Gallagher and Simpson (1967) and of other workers (Anderson, 1968). O'Gallagher and Simpson report a radial gradient of $\sim 50\%$ per AU even for particles having their $R\beta$ between 0.4 and 1.2 which is about five times larger than Anderson's observations.

The large divergence observed amongst various experimental observations is un-

doubtedly due to the inherent difficulties involved in the measurement of radial gradients. A correct estimation of the gradient can only be obtained through simultaneous measurements of differential intensity of cosmic ray particles on two or more spacecrafts situated at different radial distances. In addition, a reasonable estimate of the azimuthal gradient of particle density must also be known since such azimuthal gradients (McCracken *et al.*, 1967, 1971), unless corrected for, will vitiate the radial gradient measurements. Part of the discrepancy is to be attributed to the general practice of deriving the radial density gradients through comparison of spacecraft data with the ground based observations. For example, if the observations of O'Gallagher and Simpson were compared with data from OGO spacecraft (Kane and Winckler, 1969), instead of climax neutron monitor observations, the radial density gradients so obtained will be considerably smaller than the values given in Table III and will probably agree better with the recent estimates of Lezniak and Webber (1970).

The radial density gradient, being a function of the diffusion coefficient, an examination of the variation of the radial gradient with rigidity and distance is desirable. In spite of the disagreements between various gradient measurements, the observations

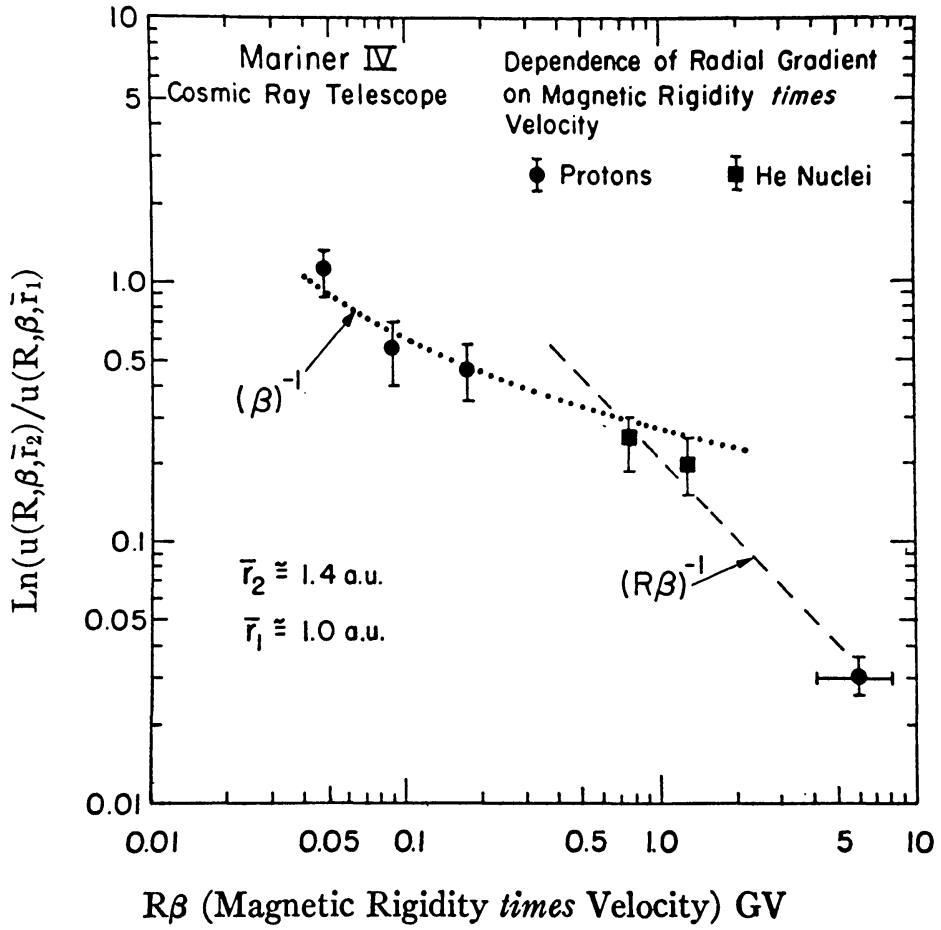

Fig. 9. Radial density gradient of protons and He nucleii observed during 1965 plotted as a function $R\beta$. U_2 and U_1 represent the cosmic ray density measurements at 1.4 AU and 1.0 AU respectively (O'Gallagher, 1967).

made on Mariner 4 (O'Gallagher and Simpson, 1967; O'Gallagher, 1967) can be utilised to draw certain broad conclusions regarding the properties of the density gradient.

(1) From a comparison of the density gradient between 1–1.28 AU and 1.28–1.56 AU, the radial density gradient has been shown to be practically invariant with distance, at least in the limited range of heliocentric distance employed.

(2) The density gradient, according to the theory, is inversely proportional to the diffusion coefficient which varies as $R\beta$, $R^{1/2}\beta$ or β depending on the power spectral density of the magnetic field. Examination of the O'Gallagher's observations (Figure 9) shows that the radial gradients of both protons and He nucleii are proportional to $1/R\beta$ at $R>0.5$ GV and to $1/\beta$ for $R<0.5$ GV. The fact that the density gradients for both protons and He nuclei are observed to obey the same law, can be taken as an experimental evidence, at least near Earth, for the validity of the usual assumption that $K(R, \beta, r, t)$ can be considered to be a separable function of distance and rigidity, i.e.

$$K(R, \beta, r, t) = K_1(r, t)\, K_2(R, t)\, \beta .$$

(3) The existence of a residual gradient during 1965 confirms the existence of a residual modulation even during the period of minimum sunspot activity.

3.4. Experimental observation on long term modulation

(a) *General Characteristics*

Since the discovery of the inverse relationship between the sunspot activity and cosmic ray intensity by Forbush (1958), much has been learnt concerning the 11 yr modulation of cosmic ray intensity. In particular, a large amount of data concerning the rigidity dependence of the long term variation and its functional relationship with

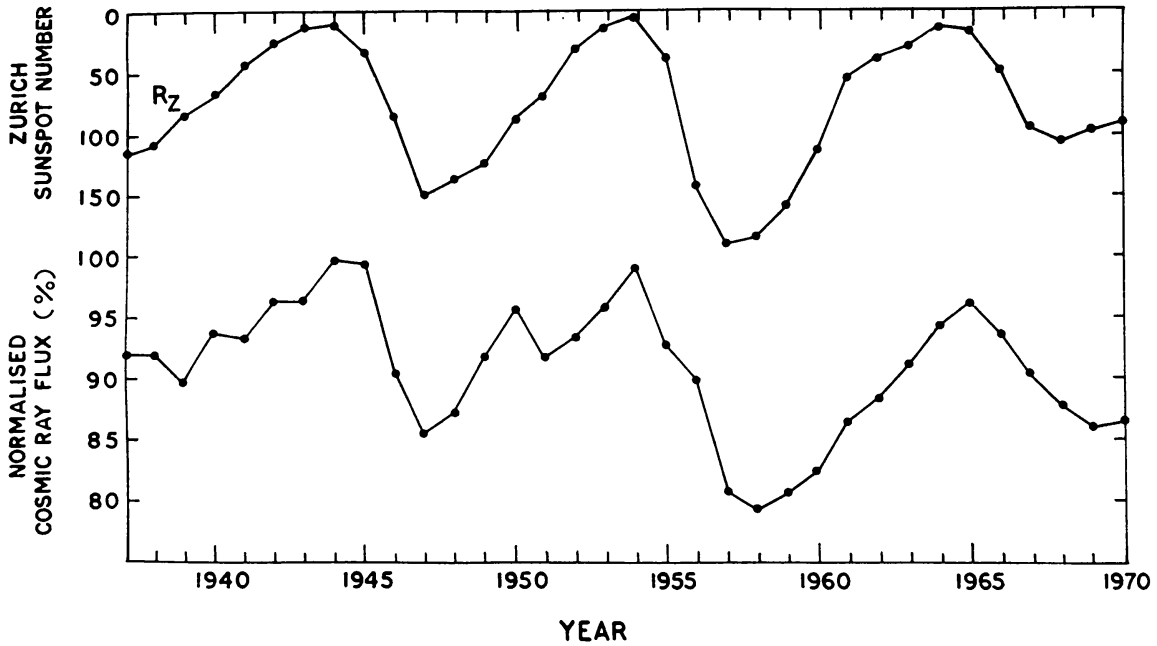

Fig. 10. The plot showing the inverse relationship between the solar cycle of activity and the cosmic ray intensity. Normalised cosmic ray neutron intensity at a station like Deep River (see text) is plotted along with the Zürich sunspot number over three solar cycles from 1937–1970.

other solar and terrestrial parameters have now been gathered to facilitate strict comparison with various theoretical predictions. Figure 10 shows the long term variation of normalized cosmic ray neutron intensity at a station like Deep River and of sunspot number beginning from 1937–1970. The normalized intensity between 1937–1957 has been obtained from ion chamber data (Forbush, 1958) and the normalized intensity after 1957 has been deduced from the neutron monitor data from Ottawa and Deep River. The figure shows that the intensity maximum in 1965 as observed at a middle latitude station like Deep River was within about 2% of the

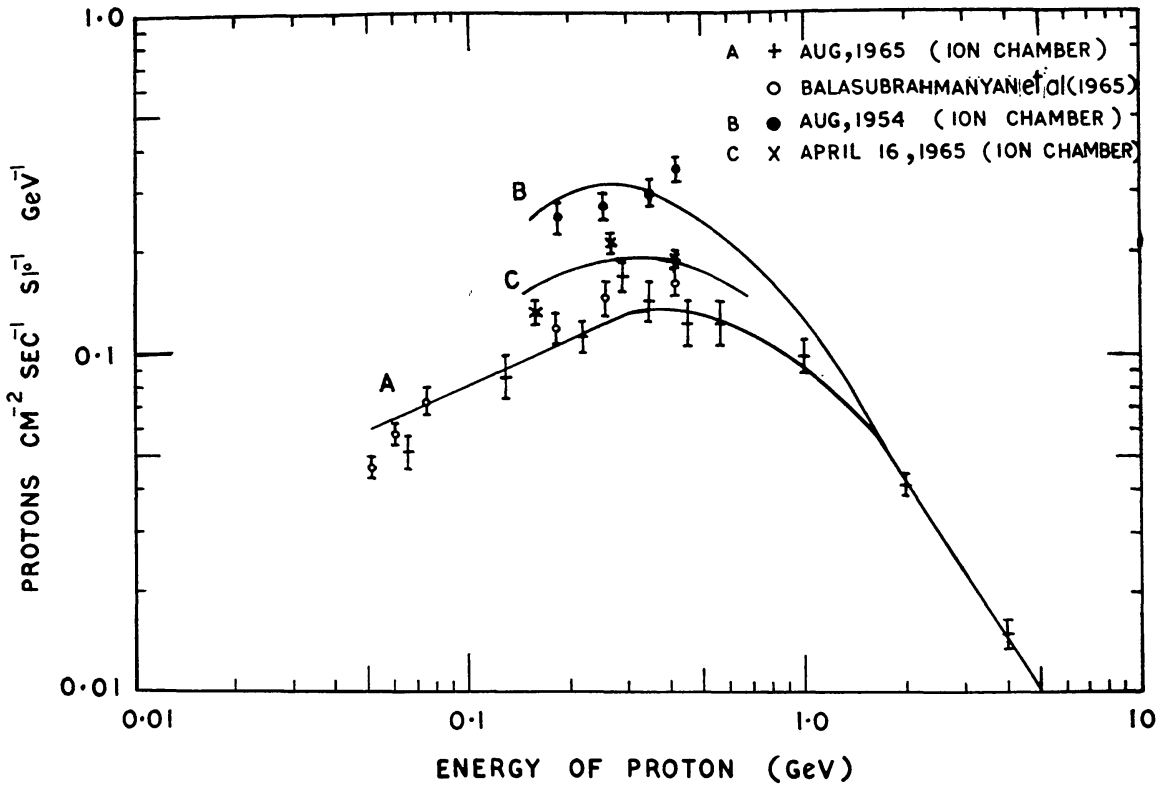

Fig. 11. Differential proton intensities measured with ion chamber at balloon altitudes during different levels of solar modulation (after Neher, 1967).

corresponding intensity maximum in 1954. But the decrease in intensity from the solar minimum activity in 1965 to maximum activity in 1969–1970 (solar cycle No. 20) was only about 12% as compared to the change of $\gtrsim 20\%$ observed from 1954 to 1958 for solar cycle No. 19.

From systematic measurements of proton intensity at different latitudes using balloon borne ion chambers, Neher (1967) has computed the differential proton spectra at different levels of solar modulation. Figure 11 shows that the deduced differential proton intensities at balloon altitudes, particularly at low energies (<1 GeV), varies very significantly with the level of solar modulation. Computing the integral proton intensity during different years from the above data, Neher (1967) concludes that the increase in intensity from 1958 to 1965 was only a factor 3.1 as compared to the observed decrease of a factor of 4.2 from 1954 to 1958.

Even though the large difference in the modulation of cosmic ray intensity in the two different solar cycles can be attributed to the different levels of solar activity prevailing during the two cycles, the maximum sunspot number during the present cycle (cycle No. 20) being about 140 as compared to the maximum sunspot number of 250 reached during 1958 – two major conclusions emerge from an examination of the above data.

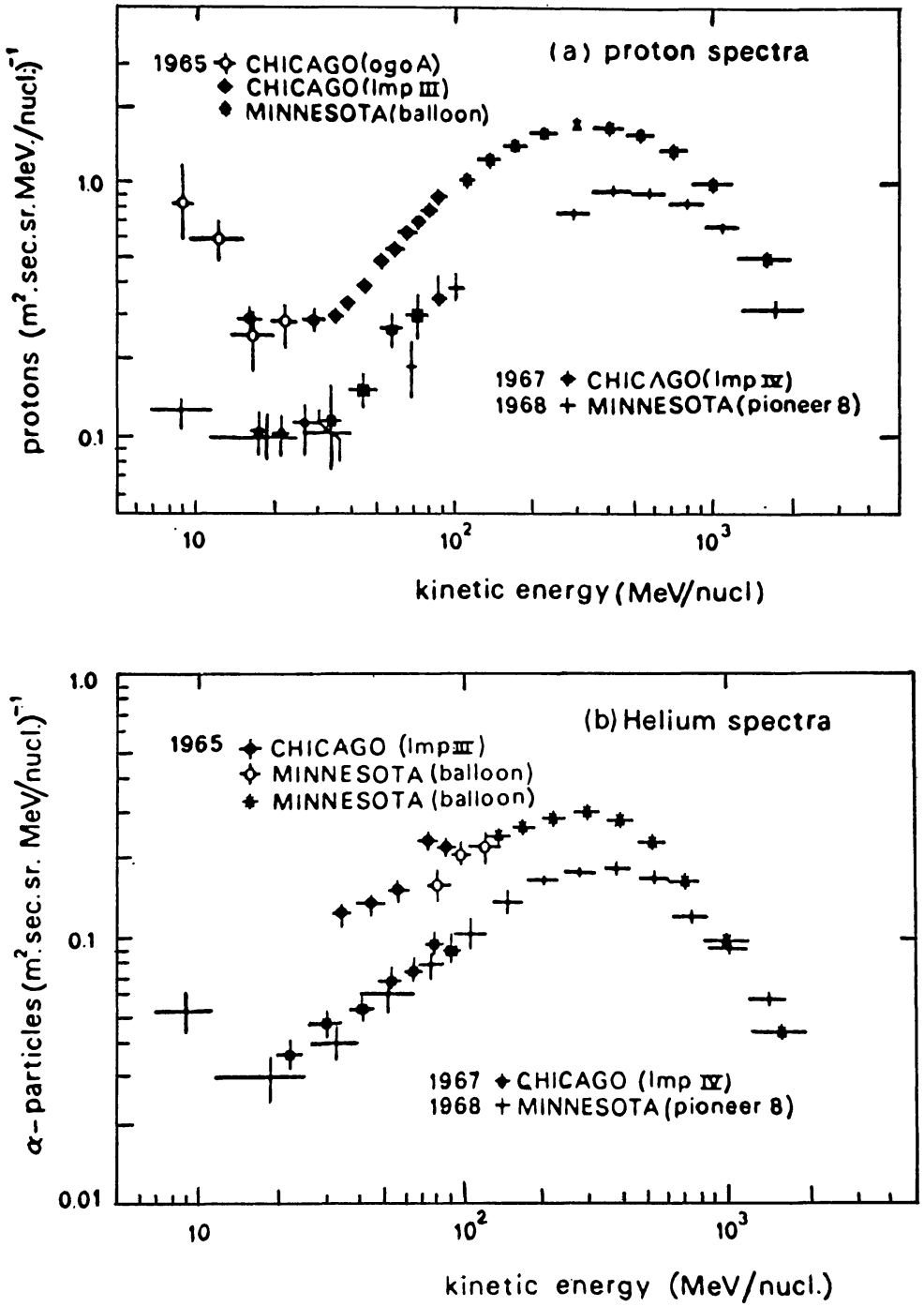

Fig. 12. Differential primary spectrum of protons and He nucleii during 1965 and 1968. 1965 data includes balloon measurements by Ormes and Webber (1968) at higher energies ($\gtrsim$ 100 MeV) and of Fan *et al.* (1966b) at lower energies. The Pioneer 8 data and IMP 4 data are taken from Lezniak and Webber (1969) and Hsieh (1969) respectively.

(1) Largest amount of modulation takes place at low energies.

(2) Even during the sunspot minima, the observed intensity is very likely to be lesser than the interstellar intensity, the difference being a function of the level of solar activity. In other words, even during the solar minimum, there exists a residual modulation of cosmic ray intensity.

3.5. Experimental observations on long term modulation

a. *Specific Variations of Protons, He nuclei and Electrons:*

The available observations from various spacecrafts have enabled us to examine the long term modulation of different species of cosmic ray particles down to very low

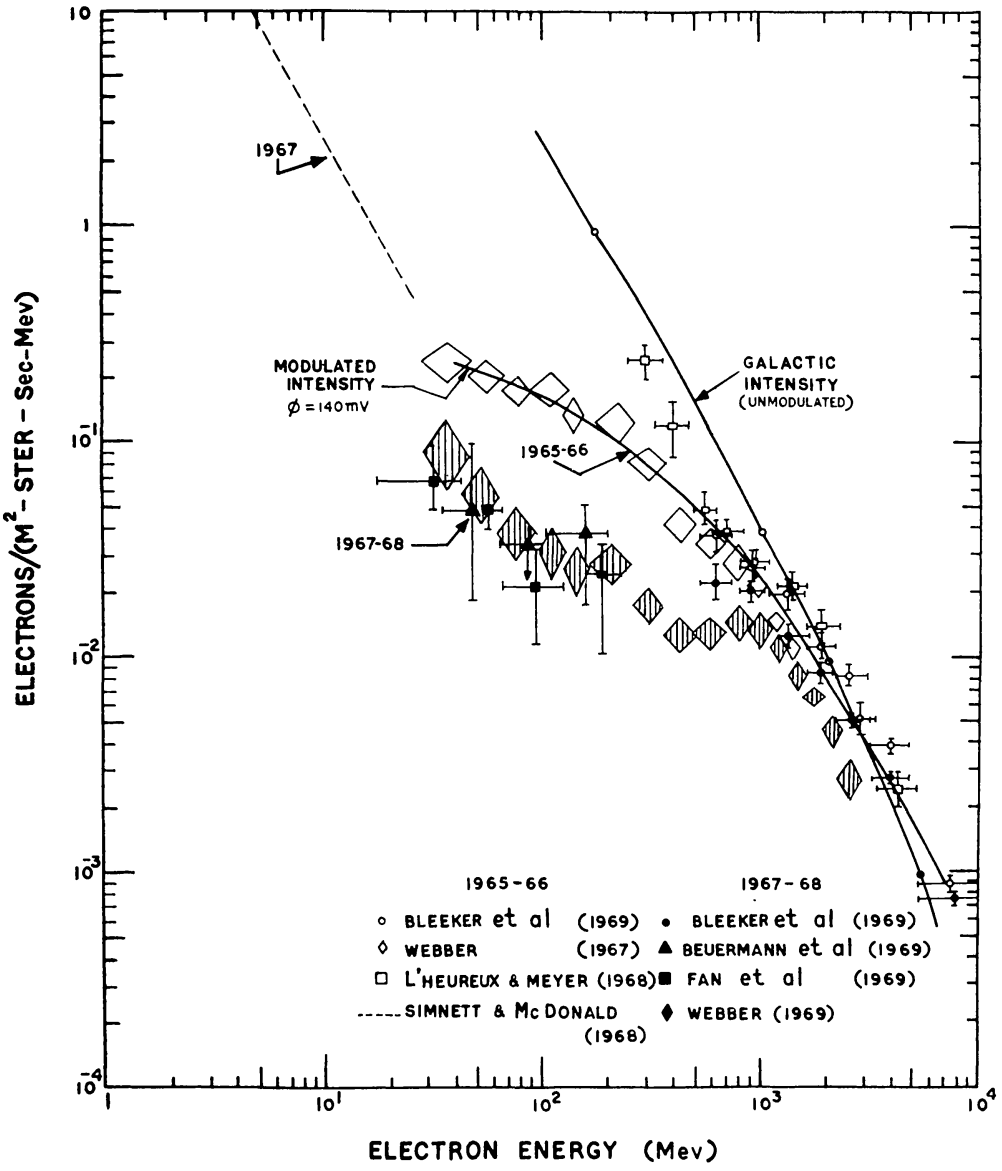

Fig. 13. Differential primary spectrum of electrons during 1965–1966 and 1967–1968. The sources of various observations are indicated in the figure. W corresponds to the theoretical unmodulated spectrum and the modulated spectrum obtained assuming $\varphi = 140$ MV.

rigidities. A number of critical reviews (Nagishima *et al.*, 1966; Quenby, 1967; Frier and Waddington, 1965; Webber, 1969) are available summarizing the experimental data on the long term modulation of the different species of particles, the observations covering upto the end of 1968. In this review we will present only a very brief summary of these results and compare with the predictions of the diffusion-convection model.

Figures 12 and 13 show the differential energy spectrum of the primary protons, He nuclei and electrons measured both during 1965, the year of minimum sunspot activity and during 1968. All the three species of particles show a larger modulation of intensity at lower energies. The fractional change in the observed flux of primary particles (both protons and He nuclei) are compared in Figure 14 as a function of particle velocity times the particle rigidity ($R\beta$) for two different periods during 1963–1965. At rigidities below ~0.1 GV, the experimental observations on both protons and

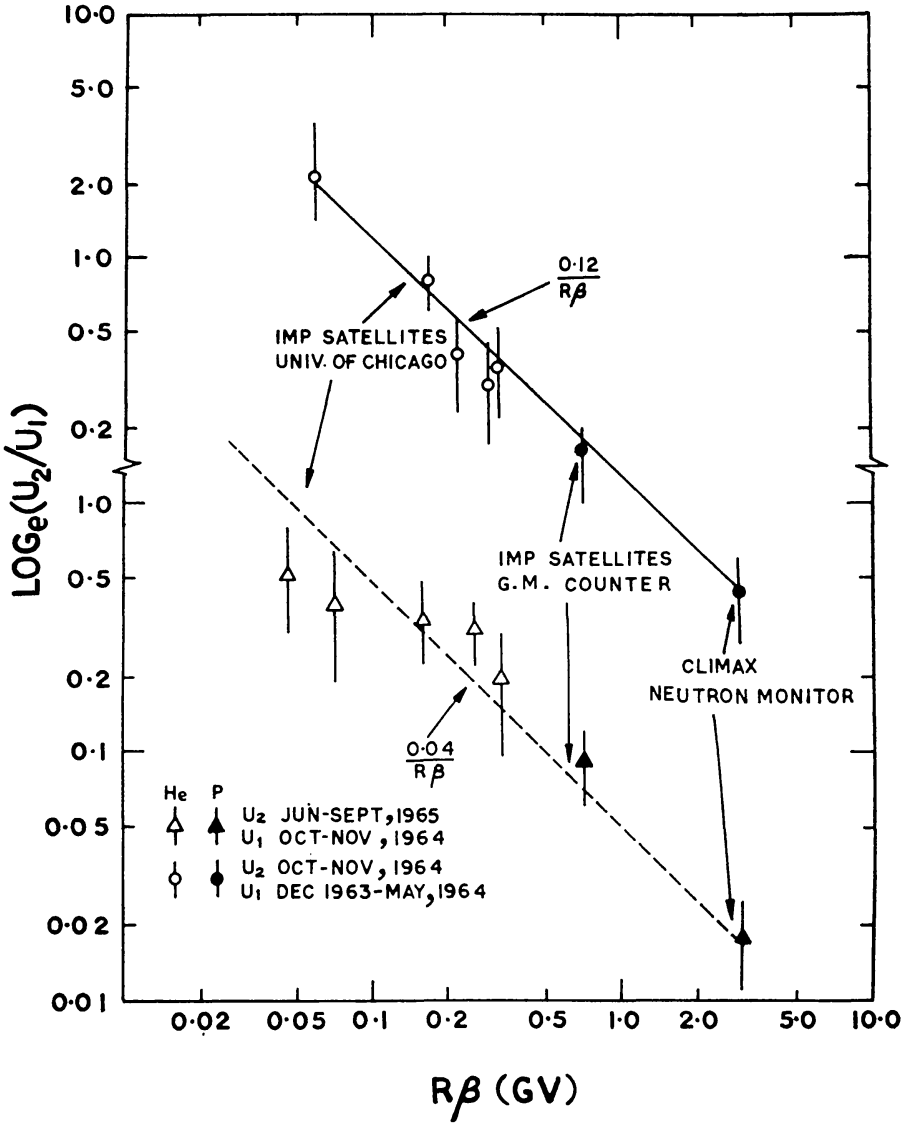

Fig. 14. Fractional change in observed primary cosmic ray flux during different periods plotted as a function of $R\beta$ (after Gloeckler and Jokipii, 1966).

He nuclei seem to show (Gloeckler and Jokipii, 1966) that the fractional change in intensity varies as $1/R\beta$. All the observations made by different workers (O'Gallagher, 1967, 1969; Ormes and Webber, 1968; O'Gallagher and Simpson, 1967) are in general agreement with each other and show that $f(R, \beta) \propto 1/R\beta$ or $1/\beta$ for rigidities $\lesssim 1$ GV and $f(R, \beta) \propto 1/R$ at rigidities $\geqslant 2$ GV.

Comparison of relative changes observed in protons, He nuclei and electrons at the same rigidity can serve as a crucial test to prove the diffusion-convection model. Since the spectral shape of any species, particularly at low rigidities, is dependent on the level of modulation (Webber, 1969), it is very important to ensure such com-

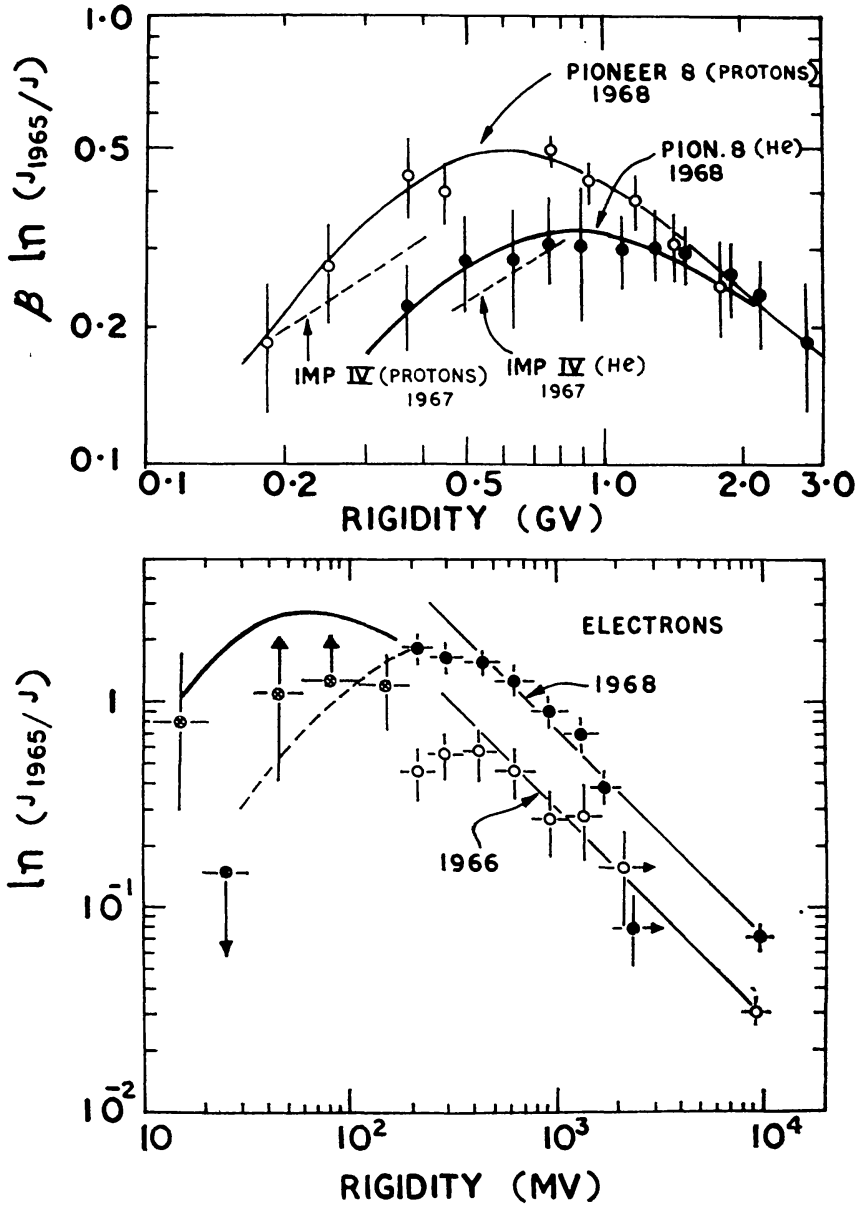

Fig. 15. (a) Fractional modulation of protons and He nucleii between 1965 and 1968 plotted as a function of rigidity. The observed changes on IMP 4 between 1965–1967 are also shown by dotted lines. (b) Fractional modulation of electrons during 1965–1968 plotted as a function of rigidity (after Webber, 1969 and Rockstroh and Webber, 1969).

parisons are made at the same level of solar modulation. Due to the larger charge to mass ratio, separation of rigidity dependent modulation from the velocity dependent modulation is easier for electrons than for other species of particles. In Figure 15a, the fractional change in the differential intensity of protons and He nuclei from 1965 to 1968 is plotted as a function of rigidity. In Figure 15b, the fractional modulation of electrons between 1965–1966 and 1966–1968 are shown, the two periods corresponding to a change of $\sim 3.6\%$ and 7.1% respectively in the Mt. Washington neutron intensity. The corresponding observed change in electron intensity between 1966–1968 (Webber, 1968; Beuermann *et al.*, 1969) is ~ 2.5 times larger than the change during 1965–1966.

Examination of Figure 15 reveals that

(1) Upto a rigidity of ~ 2 GV, the rigidity dependence of the modulation factor of protons, He nuclei and as well as of electrons are practically identical.

(2) The fractional modulation of each of the species shows identical behaviour. Steep upto about 2 GV rigidity and a considerable flattening at lower rigidities.

From the experimental observations, Webber (1969) concludes that the transition rigidity corresponding to the peak modulation factor (Figure 15) is different for different species of particles, the peak modulation occurring at the lowest rigidity for electrons (~ 0.5 GV) and at increasingly higher rigidities for protons (~ 1 GV) and He nuclei (~ 2 GV). This is consistent with the occurrence of the peaks in the

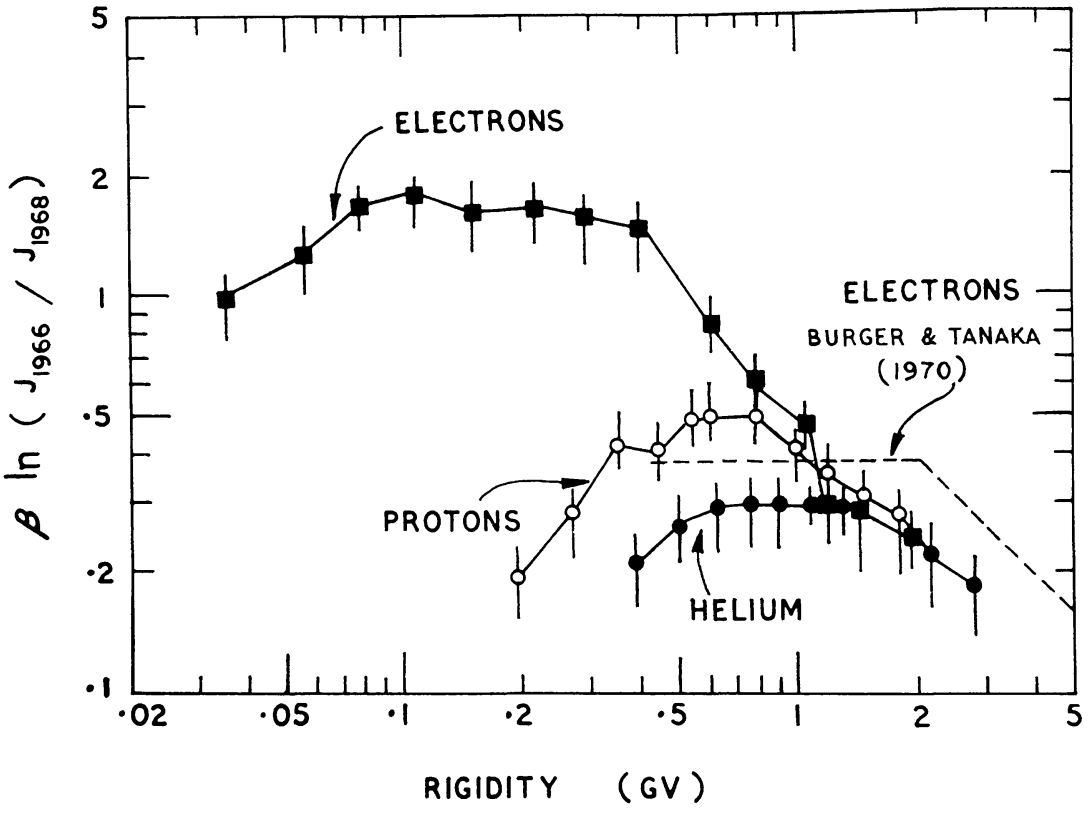

Fig. 16. Fractional modulation of protons, He nucleii and electrons between 1965 nad 1968 (after Webber, 1969). The dashed curve represents the best fit to the fractional modulation of electrons during 1966–1968 as observed by Burger and Tanaka (1970).

differential spectra for electrons, protons and He nuclei at successively higher rigidities. However, in all such comparisons involving finer details, one must bear in mind the existence of considerable uncertainties in the experimental observations. For example, Burger and Tanaka (1970) find that the transition rigidity ($\sim$2 GV) is practically the same for all three species and probably does not exhibit any significant variation over the solar cycle, a conclusion which is at variance with the earlier result quoted by Webber who finds that the transition rigidity, besides being charge dependent, also depends on the level of modulation.

(3) Figure 15 clearly shows that at lower rigidities ($\sim$2 GV), the modulation of protons is greater than for helium nuclei of same rigidity. Even though such a splitting is not expected on the basis of simple convection-diffusion theory, the results are in good agreement with the predictions of the model (Gleeson and Axford, 1968b; Gleeson, 1971) which includes energy losses of particles due to deceleration in the expanding solar wind. In Figure 16, the fractional modulation suffered by all the three species of particles, namely protons, He nuclei and electrons are plotted as a function of rigidity, which clearly demonstrates the charge dependent splitting evident below $\sim$2 GV rigidity. It should be pointed out that unlike the evidence for protons and He nuclei, the conclusion regarding electron modulation should be treated as tentative. From both balloon observations and OGO-5 observations, L'Heureux *et al.*, 1968; L'Heureux and Meyer, 1968; Bleeker *et al.*, 1968, 1969; Burger and Tanaka (1970) conclude that the fractional modulation of electrons is much less than that reported by Webber and his co-workers (see Figure 16) and has a rigidity dependence which is in fairly good agreement with the proton curve. More measurements on electrons are needed to confirm the difference in the modulation factor for electrons as compared to that of protons.

b. *Discussion of Experimental Results*

The two important pieces of observational evidence, namely the flattening and the charge dependence of the modulation parameters at lower rigidities are not easily explainable by simple convection-diffusion theory. The steepening of the power spectral density of magnetic field irregularities above frequencies corresponding to the particles of 'transition rigidity' can be invoked to explain the fattening of the modulation. The change in the form and the spectral behaviour of the power spectral density of magnetic fields, from epoch to epoch, should also cause a change in the rigidity dependence of this modulation factor. However, the observational data on the power spectra being rather meagre and their interpretation being ambiguous, the available data, at present, is not adequate to support these conclusions. Neverthless, we may recall from Equation (2.2) that for rigidities lower than R_l, whose mean free path approximates or is lower than the correlation length D of the magnetic field, the diffusion coefficient K is given by $\frac{1}{3}cD\beta = \text{const}$. This clearly indicates that at lower rigidities, the modulation may never be steeper than that corresponding to $c\beta$.

The charge dependency and the flattening of the fractional modulation parameter at low rigidities finds natural explanation in terms of the energy losses due to

deceleration of the particles. Since the expression for modulation due to electric field models is identical with the expression for diffusion-convection models with energy loss term included, it is instructive to qualitatively examine Equation (3.2) before going into the quantitative details of the energy losses. At medium and high energies when the exponent γ in the differential spectrum $E^{-\gamma}$ is positive, the energy loss will provide an additive factor increasing the fractional modulation. At non-relativistic energies, the spectral exponent γ may be negative in which case the energy loss will tend to cancel the modulation effect due to diffusion-convection, thereby causing the flattening of the fractional modulation. The rigidity corresponding to the peak fractional modulation should be the same as the rigidity at which the differential spectra for each species shows the peak (where the spectral exponent changes sign). Similarly, the 'splitting' should be explainable in terms of the energy loss and the relevant differential primary spectrum appropriate to each species of particles.

The energy loss term in the theoretical treatment of the transport of cosmic radiation in the irregular magnetic fields and the various numerical or analytic solutions of the equations described earlier in Section 3.2 do not clearly bring out the

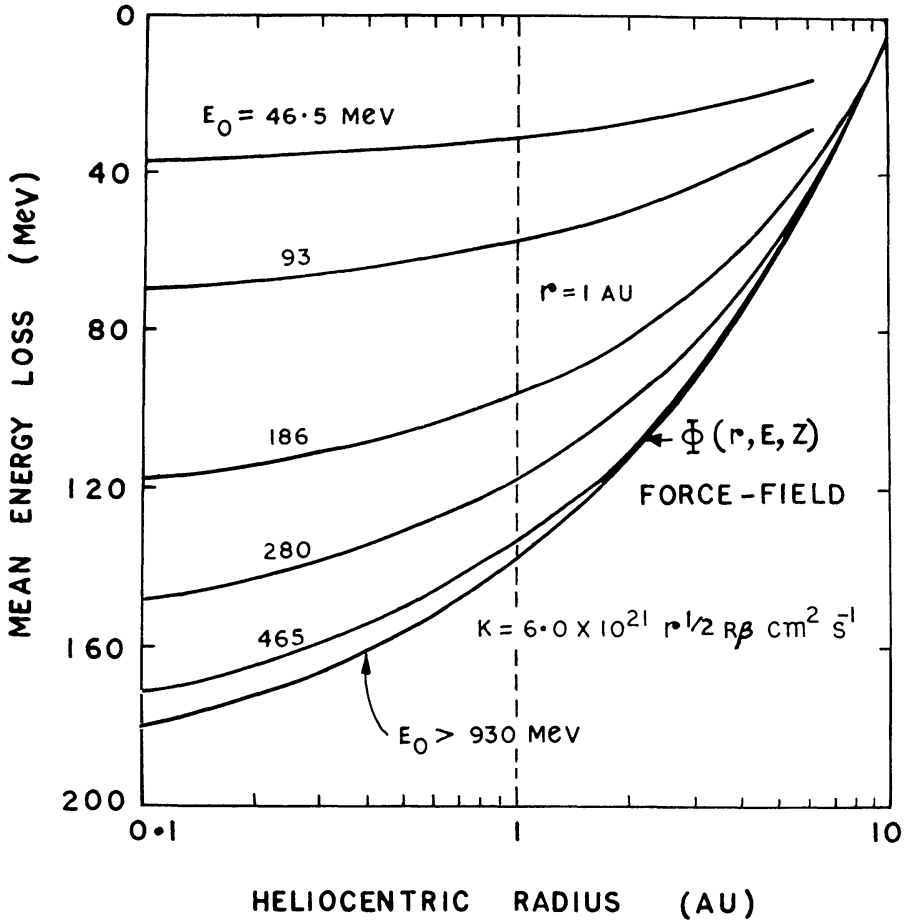

Fig. 17. The mean energy loss suffered by particles of different energies due to deceleration in the interplanetary medium plotted as a function of heliocentric distance. For each curve, a Gaussian distribution of differential number density with a central energy W, and width 0.1 W at half maximum is assumed. The dimension of the modulating region is assumed to be at 10 AU and the diffusion coefficient to be given by $6 \times 10^{21} r^{1/2} R\beta$ cm^2 s^{-1} (after Gleeson and Urch, 1971).

importance of energy losses (which appears through the Compton-Getting factor) in predicting the cosmic ray modulation. The only treatment amongst these which explicitly derives the energy loss suffered by cosmic ray particle at different injection energies are the ones which use the force field equation (Gleeson and Axford, 1968b; Gleeson and Urch, 1971).

Assuming the diffusion coefficient K to be a separable function of the heliocentric distance r and rigidity R given by

$$K = K_1(r)\, K_2(R)\, \beta$$

the differential intensities at r and L for particles of charge Ze is given by

$$\frac{j(r, W)}{W^2 - W_0^2} = \frac{j(L, W + \Phi)}{(W + \Phi)^2 - W_0^2} \tag{3.18}$$

where L is the dimension of the modulating region, $W = E + W_0$ the sum of the particle kinetic and rest energies, and Φ is energy dependent 'potential energy' term which for $K_2 \propto R\beta$, is given by

$$\Phi = |Ze|\, \varphi(r) \tag{3.19}$$

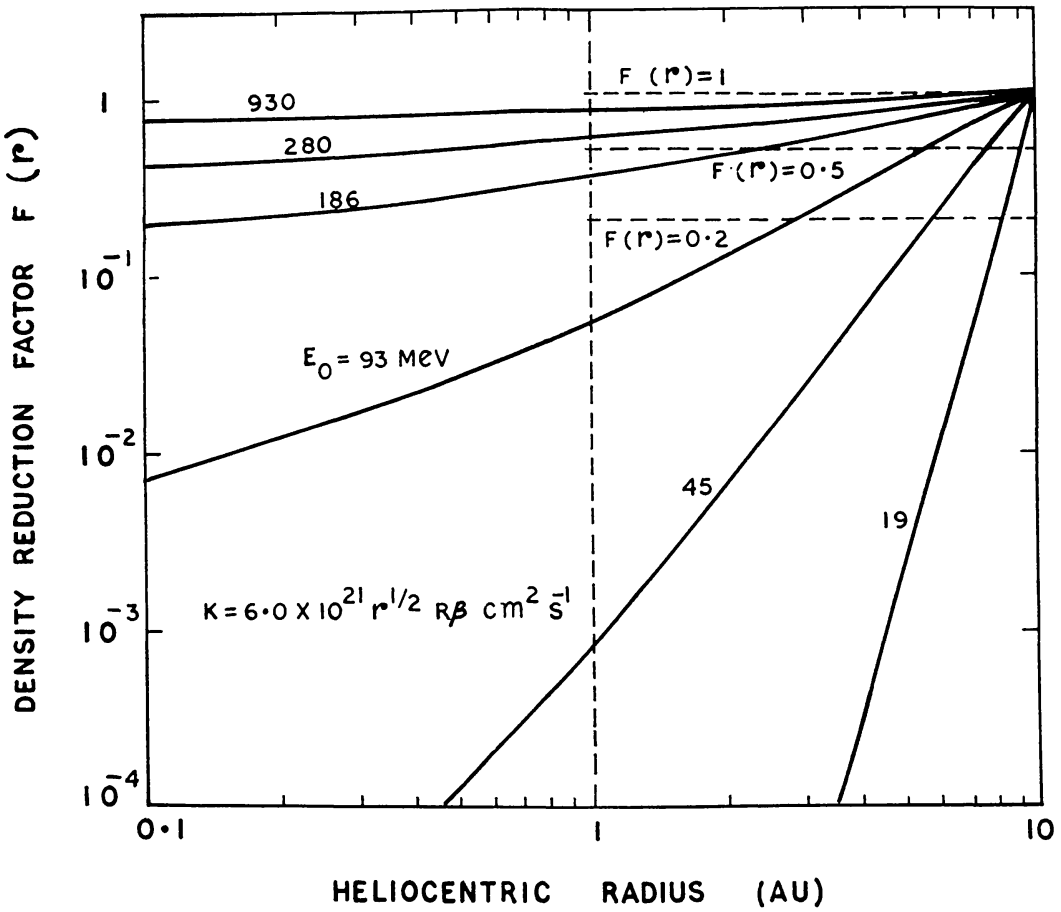

Fig. 18. The fractional reduction in the density of particles of different energies injected at the boundary of the modulating region assumed to be at a heliocentric distance of 10 AU (see text) (after Gleeson and Urch, 1971).

where $\varphi(r)$ is the modulation potential given by

$$\varphi(r) = \int_r^L \frac{V(x)}{3K_1(x)}\,\mathrm{d}x. \tag{3.20}$$

The above approximate solution is good to $E \sim 100$ MeV/nucleon (Fisk *et al.*, 1970). Note that $\varphi(r)$, being independent of charge, can be used for characterising modulation. Φ is the mean energy loss suffered, due to adiabatic deceleration, by particles which are injected at the boundary of the modulation region with an energy $(W+\Phi)$.

Assuming a spherically symmetric model, Gleeson and Urch find that for the types of diffusion coefficients commonly derived, the effect of energy loss for particles of energy $\lesssim 100$ MeV is very significant and galactic protons and helium nuclei with kinetic energies below 80 MeV/nucleon are virtually excluded from the inner solar system. Figures 17 and 18 show the mean energy loss suffered and the reduction in number density of particles of different energies as observed at different distances from the sun derived assuming $L=10$ AU and the diffusion coefficient $K=6.0\times10^{21}\, r^{1/2}\, R\beta$ cm^2 s^{-1}. At the orbit of the Earth ($r=1$ AU), it is seen that particles with energies of ~ 180 MeV/nucleon are reduced to a factor 0.3 of their value in the interstellar space and particles below ~ 100 MeV are virtually removed. Similar conclusions have been arrived at by Goldstein *et al.* (1970), Fisk (1970) and Lezniak and Webber (1970) who have obtained solutions of the same equation through numerical integration.

Even though the information on the energy loss is obtained under very simplified assumptions, an important consequence of the above treatment is to point out the fact that galactic primary particles of energy $\lesssim 80$ MeV/nucleon cannot be uniquely associated with any particle observed near Earth. All particles of energy $\lesssim 80$ MeV/nucleon observed at the Earth would have had much higher energies at the time of their injection into the solar cavity. Consequently, demodulation of the spectra of particles at low energies observed near Earth to obtain the spectra of galactic particles is very much suspect particularly at energies below ~ 80 MeV/nucleon.

The fractional modulation of cosmic ray particles of different species at any time is obviously dependent on the modulation potential $\varphi(r)$ and on the form of the galactic spectrum. The value of $\varphi(r)$ necessary in 1964–1965 can be shown to vary from about 150 to 350 MV at 1 AU for K(6 GV) varying between 4×10^{22} cm^2 s^{-1} to $1.5\times$ $\times10^{22}$ cm^2 s^{-1}. Assuming electric field modulation, to account for the observed change in the fractional modulation of protons and helium nuclei, the value of $\varphi(r=1\text{ AU})$ applicable to 1964–1965 is generally accepted to be about 140 MV. Figure 19 illustrates the reasonable agreement observed between the calculated and the observed differential energy spectra of helium nuclei. The assumed unmodulated galactic spectrum and the calculated spectra using both the force field solution as well as the numerical solution (Gleeson and Urch, 1971; Lezniak and Webber, 1969) are compared in the figure with the experimental observations corresponding to the solar minimum activity in 1965 (Gloeckler and Jokipii, 1967). Similarly the agreement between theoretical calculations (Webber, 1969) assuming $\varphi \approx 140$ MV (curve W) and

the actual experimental observations on electron modulation (Figure 15) also show a reasonable agreement.

In summary, we believe that the diffusion-convection theory with energy losses included can explain the experimental observations, particularly for cosmic ray rigidities above 100 MV, provided the diffusion coefficient and the input galactic

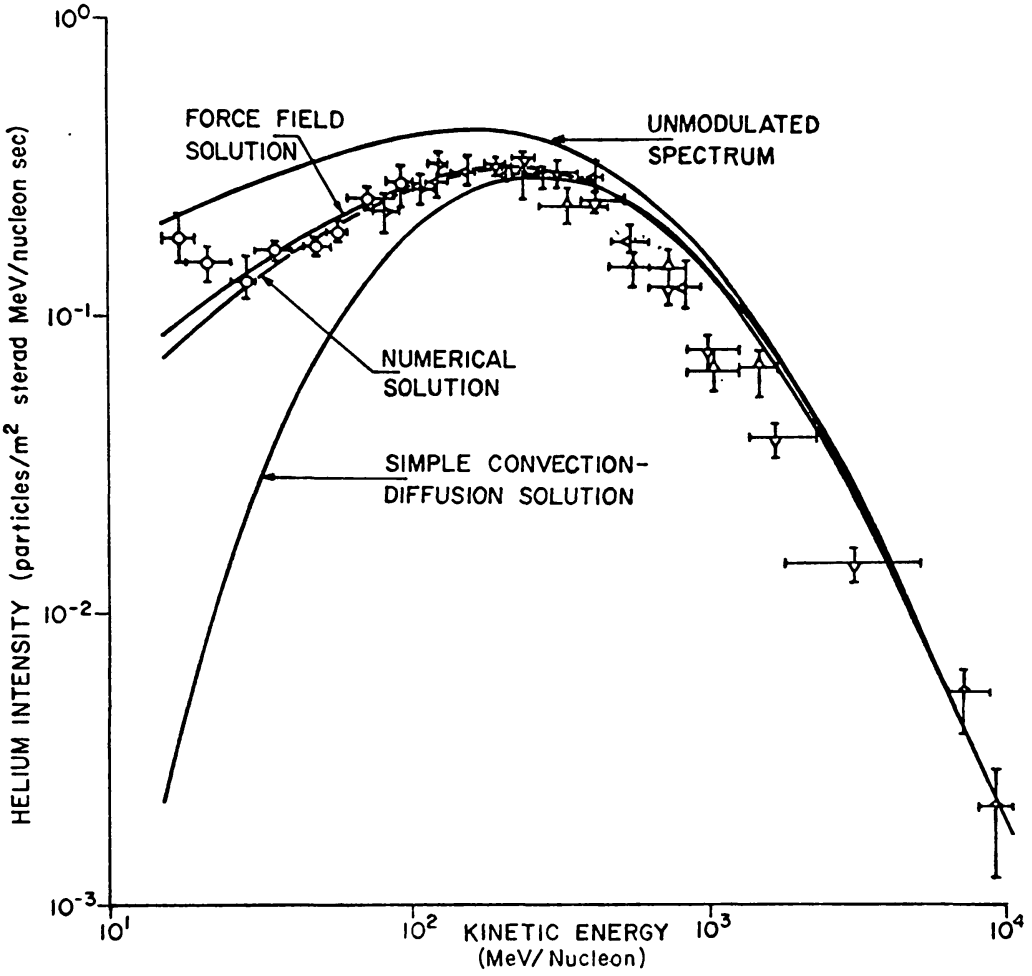

Fig. 19. Comparison between the experimentally observed differential energy spectra of He nucleii during 1965 (Gloeckler and Jokipii, 1967) and the theoretically derived spectra obtained using both the numerical solution and the force field solution. The solution given by the simple convection-diffusion theory without the effect of energy losses included is also indicated (after Fisk, 1971).

spectra are accurately known. The calculations below 100 MV, however, are not reliable since at low energies the energy losses due to deceleration are comparable with particle energies. The discrepancies between the experimental observations and the theoretical calculations partly arise due to our imperfect knowledge of the magnetic field and the injection spectrum. Even the assumption of K being a separable function of r and R needs to be confirmed in view of the doubts raised by some workers (Krimigis and Venkatesan, 1969; Lezniak and Webber, 1969; Gleeson and Axford, 1968b).

3.6. Residual modulation and dimension of modulating region during sunspot minimum

The presence of a continuous solar wind throughout the solar cycle indicates that the cosmic ray intensity sampled at the Earth even during minimum solar activity is modulated considerably. The generally observed lag of about 1–2 months between the solar activity minimum and the cosmic ray intensity peak can only be interpreted in terms of the existence of a residual modulation. The preceding discussion has clearly indicated that the cosmic ray flux measured during 1965 requires the modulating potential $\varphi(r)$ to be ~ 140 MV and an associated mean energy loss of 140 Ze at higher energies.

For obtaining a quantitative estimate of the residual modulation, the value of the modulating parameter η applicable to the solar minimum has been determined by many workers. Biswas *et al.* (1967) have estimated $\eta \approx 0.6$ GV during 1965 by comparing the He^3/He^3+He^4 ratio measured at the Earth with the corresponding values derived for the local interstellar medium. Recently the same authors (Ramadurai,

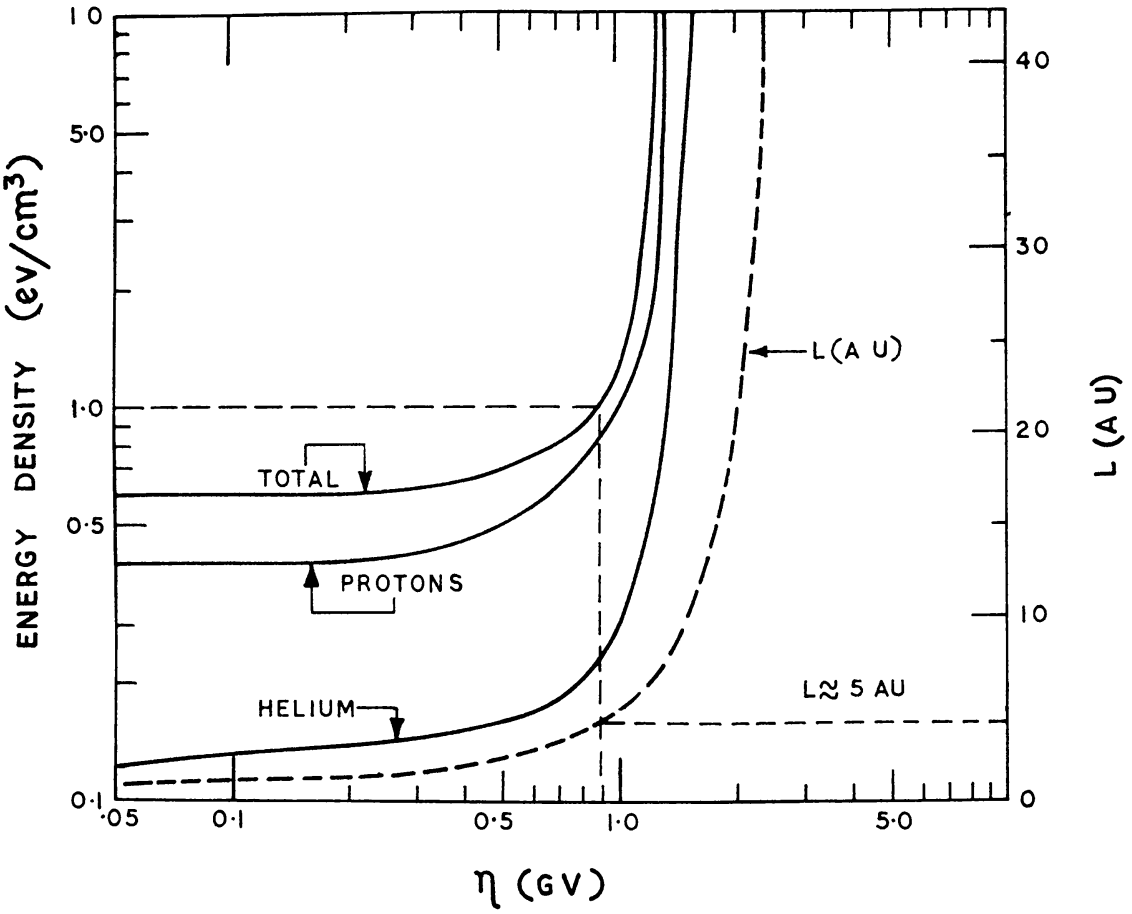

Fig. 20. The local interstellar energy density plotted as a function of the modulation parameter η (after Gloeckler and Jokipii, 1967). L, the dimension of the modulating region in AU is also plotted as a function of η, L being derived from Mariner 4 observations in 1965 (after O'Gallagher, 1967).

1970), however, have revised their original estimate of η and give a new value of $\eta = 0.25$ GV for 1965. Independent estimate of by Ramaty and Lingenfelter (1968) obtained by comparing the observed and the calculated He^3 and deutron spectra during the solar minimum has yielded a value of $\eta = 0.35$ GV.

Taking a mean value of 0.4 GV for η during 1965, one can roughly estimate the fractional decrease in cosmic ray intensity that would be registered by an ion chamber to be about $(e^{0.4/0.75} - 1) \approx 50\%$ assuming the mean rigidity of response of the chamber to be about ~ 1 GV ($R \sim 0.75$ GV). A radial density gradient $\sim 10\%$ per AU would then yield $L \approx 5$ AU for the dimension of the modulating region during solar minimum.

Gloeckler and Jokipii (1967) have estimated the value of L in 1965 independently

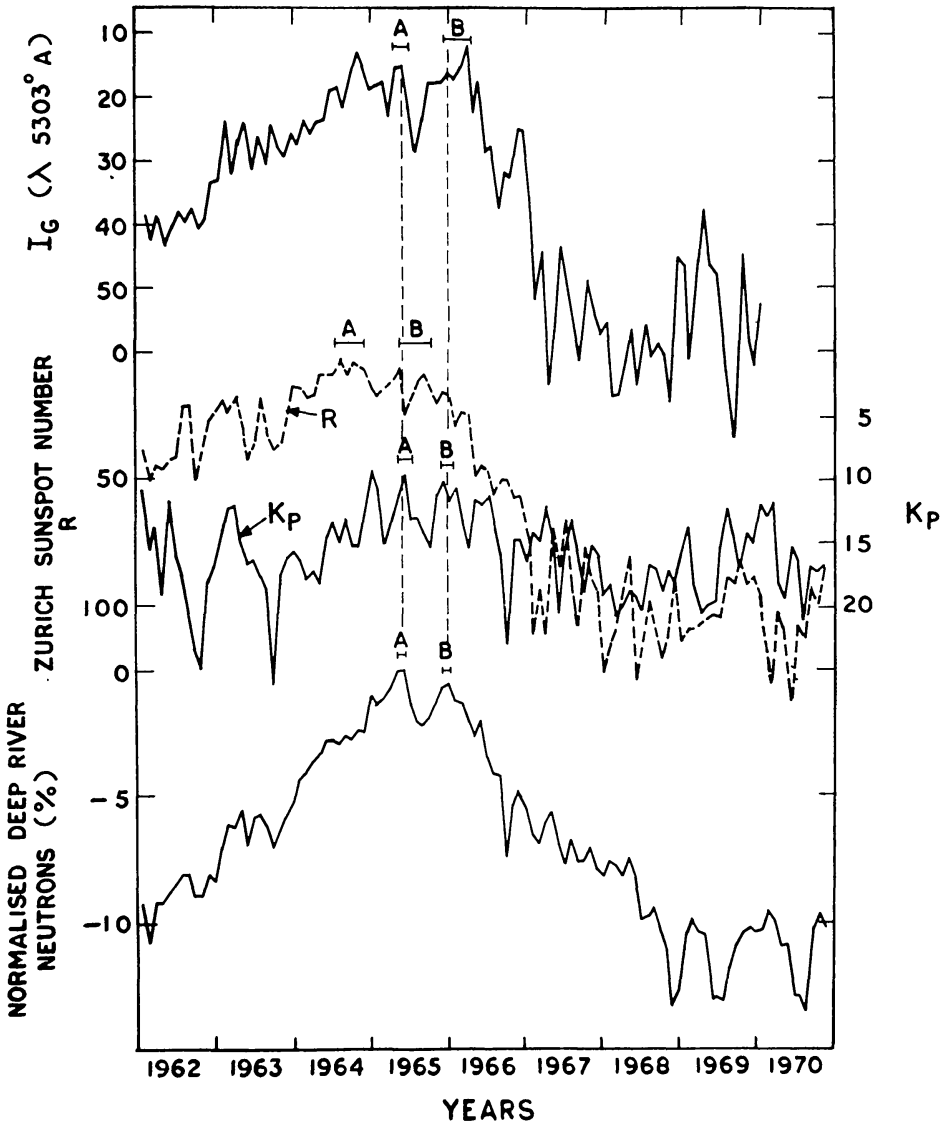

Fig. 21. Illustrating the inter-relationship between monthly mean cosmic ray activity (Deep River neutron intensity) sunspot number, K_p index and the intensity of green coronal line 5303 Å during 1962–1970. The figure shows that whereas the lag between sunspot number and cosmic ray activity is of the order of 9–12 months (comparing peaks marked A and B), the lag between other solar activity parameters and cosmic ray index is only 1–2 months during 1965.

from energy considerations. Since L determines the depth of modulation region, the local interstellar energy density is very sensitive to the value of η. Figure 20 illustrates the manner in which the energy density varies with η. For values of $\eta \gtrsim 0.7$ GV, the energy density increases rapidly and exceeds 10 eV/cm^3 for $\eta \approx 1.3$ GV. An energy density of 1 eV/cm^3 corresponds to a value of $\eta \approx 0.9$ GV which is consistent with other estimates obtained for L.

The lag between the peak cosmic ray intensity and the minimum in solar activity can be utilised to estimate the value of L. Such a lag can be theoretically understood as due to the 'time constant' of the modulating region around the Sun, i.e. the time required for the solar plasma disturbance to propagate through the modulating region. The original estimates of lag time of 9–12 months (Forbush, 1958) between maximum cosmic ray intensity during sunspot minimum and the sunspot activity yielded a radius of ~ 100 AU for the modulating region, a value which is an order of magnitude greater than the value derived from other evidences.

The erroneous estimation of the dimension of the modulating region derived from the lag between the solar activity and cosmic ray intensity has been attributed to the use of sunspot number as an index of solar activity. It is quite obvious that the relevant parameter should be the solar wind velocity. In the absence of the availability of solar wind velocity values for the entire cycle of solar activity, we can profitably utilise the existence of strong correlation between K_p index and the solar wind velocity given by Snyder *et al.* (1963) and compare the time lag between the cosmic ray intensity and K_p index. Figure 21 shows, on a monthly basis, the relationship between the cosmic ray intensity, sunspot number and K_p index. Unlike the considerable time lag which exists between the minimum sunspot number and cosmic ray intensity, the time lag between the lowest value of the mean K_p index and the peak cosmic ray intensity is observed to be only about ~ 1 month.

The intensity of the green coronal emission line 5303 Å which is representative of the coronal temperature has also been recently suggested (Sarabhai and Subramanian, 1965; Hatton *et al.*, 1966) as a good parameter to describe the solar activity. The demonstration of a fairly good correlation between the intensity of 5303 Å and the solar wind velocity for limited periods when solar wind velocity data is available (Pathak and Sarabhai, 1970) adds some significance to such a comparison. Figure 21 also shows the monthly mean values of intensity of green coronal emission line plotted for the period 1962–1970. Both K_p index and the intensity of green coronal emission line indicate that the lag between the cosmic ray intensity and solar activity changes during sunspot minimum is of the order of ~ 1 month which corresponds to a value of about ~ 7 AU for the dimension of the modulating region in agreement with other cosmic ray evidence.

3.7. Cosmic ray hysteresis and dynamics of the long-term modulation

Referring to Equation (3.8), the long-term modulation of cosmic ray intensity can be either caused by a time variation of the modulation parameter $\eta(t)$ or of the modulation function $f(R, \beta)$. We shall examine the available experimental observations to

determine which of these two parameters changes over a cycle resulting in the long-term variation of cosmic ray flux.

3.7.1. *Change in* $f(R, \beta)$

Any change in $f(R, \beta)$ (which has the same dependence as the diffusion coefficient) over a long-term period can be caused due to a change in the spectral shape of the power spectrum of the magnetic field which can arise due to a marked difference in the distribution of the size of magnetic irregularities during different portions of the

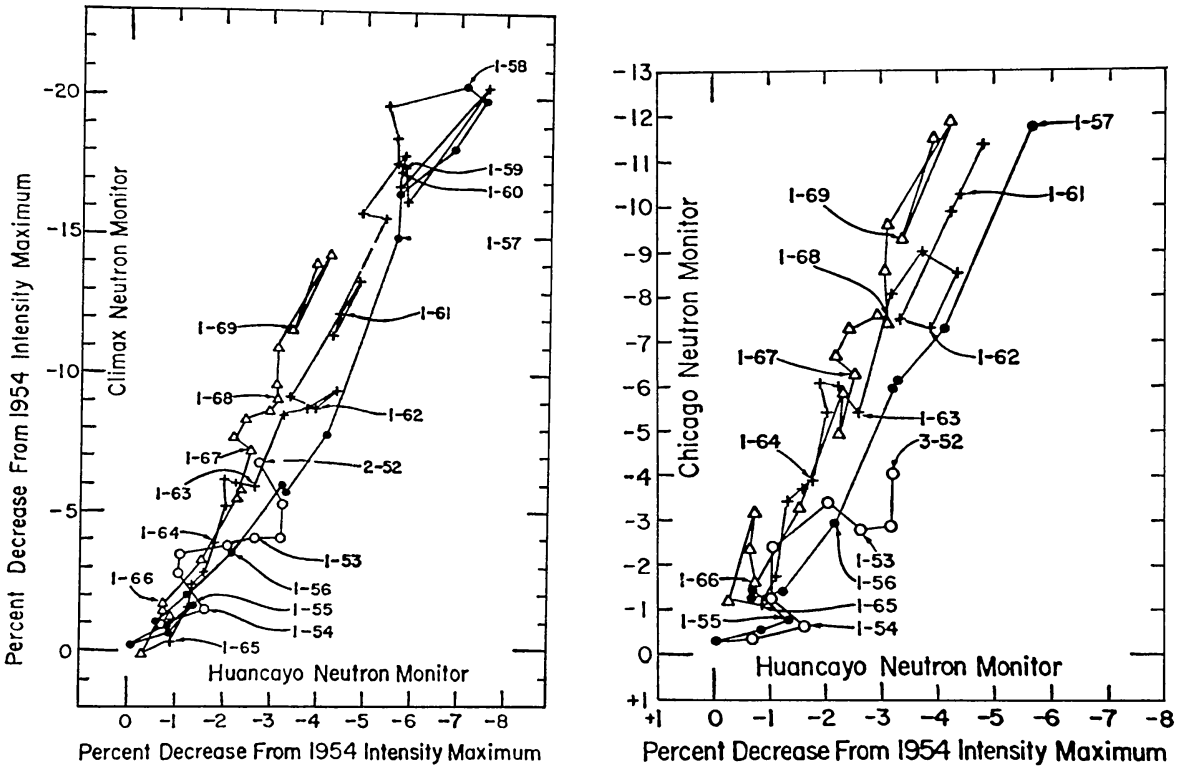

Fig. 22. Correlation of Climax and Chicago neutron monitor intensity variations with Huancayo neutron monitor variations during 1952–1969. The data points representing 3 monthly means demonstrate the validity of a single regression line during both the ascending and descending parts of the solar cycle (after Simpson and Wang, 1970).

solar cycle. Such a change, if present, might result in producing a 'hysteresis' effect in the cosmic ray particles, i.e. different intensity changes at the same level of modulation leading into and out of the period of solar minimum activity. Even though a 'hysteresis' effect was reported by earlier workers (Simpson, 1963; Hatton *et al.*, 1963), careful examination of the data from several neutron monitoring stations by Simpson and Wang (1967, 1970) and Wang (1970) has indicated the virtual absence of any hysteresis if due allowance is made for the long-term drifts of the monitors. Figure 22 shows the neutron intensity changes observed at Climax and Chicago (mean rigidity of response ~ 10 GV) plotted as a function of percent change observed at Huancayo neutron monitor (mean rigidity of response ~ 40 GV) during 1952–1969. The appli-

cability of a single regression curve during both the ascending and the descending portions of the solar cycle clearly indicates the absence of hysteresis for cosmic ray particles of energies $\gtrsim 2$ GeV.

At energies lower than ~ 2 GeV, however, the evidence seems to indicate the existence of a hysteresis. Both the comparison of low energy particles measured in IMP-OGO with neutron monitor data (Balasubrahmanian *et al.*, 1968) as well as intercomparison of modulation of protons, ^{3}He and ^{4}He at energies between 20–100 MeV per nucleon obtained from satellite measurements at different levels of solar modulation (Hsieh, 1970) indicate a change in the form of the modulation function at these energies during the ascending and the descending part of the solar cycle.

3.7.2. *Change in* $\eta(t)$

Since the modulation function of $f(R, \beta)$ is essentially constant at the orbit of the earth for particles of rigidity $\gtrsim 2$ GV, the long-term variation of cosmic ray flux at higher energies can only be understood in terms of the time variation of the modulating parameter η. To account for the changes in cosmic ray flux observed by Gloeckler

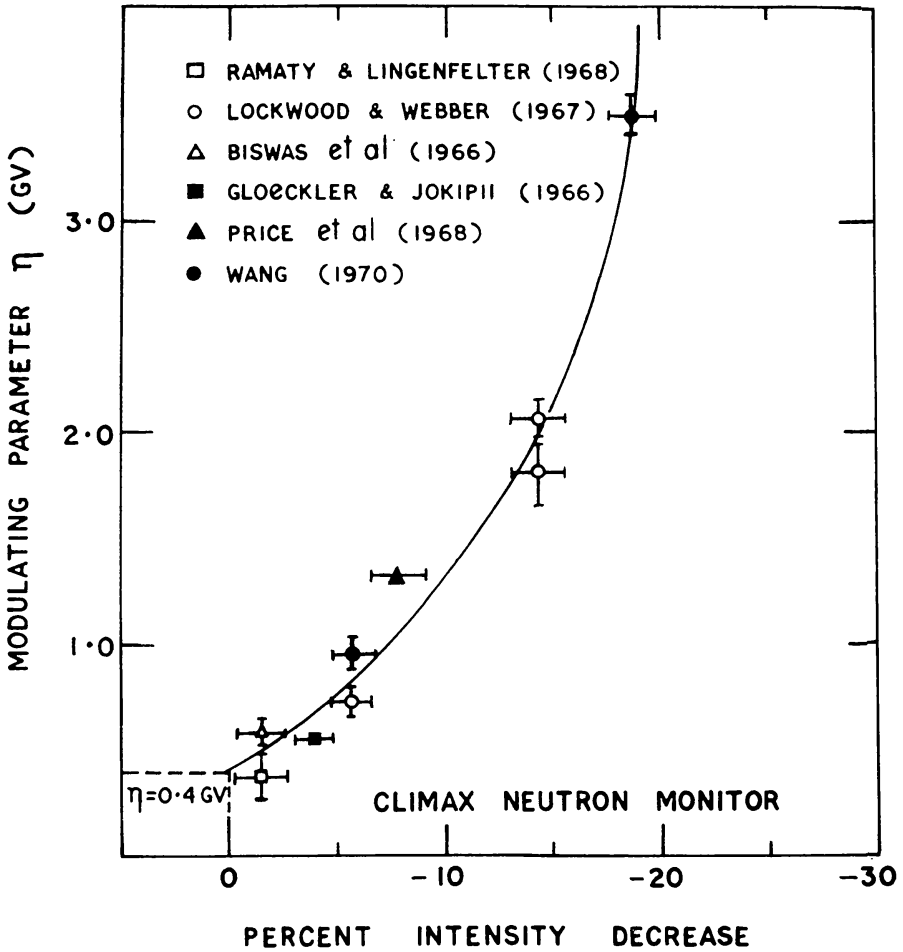

Fig. 23. Illustrating the variation of the modulation parameter η with the level of solar modulation. Decrease in Climax monitor intensity from the maximum intensity level observing during 1965 is used for indicating the level of solar modulation (after Wang, 1970).

and Jokipii (1966, 1967) from the solar minimum to maximum, a change in η of the order of $\Delta\eta = 3.10 \pm 0.10$ GV is estimated (Wang, 1970) for the period 1957–1968. Considering the mean value of η during 1965 to be equal to 0.4 GV, it would appear that the long-term modulation of cosmic ray flux above 1 GV would correspond to a change from 0.4 GV to 3.5 GV in the value of η. The values of η derived from the cosmic ray measurements by various workers are plotted in Figure 23 as a function of the neutron intensity measured by Climax neutron monitor which illustrates the variation of η over a solar cycle (see also Table IV). We wish to emphasize that it has been possible to derive the variation of η with solar cycle only under the assumption that $f(R, \beta)$ is only a function of rigidity and does not vary significantly with time.

Assuming that the power spectral density and hence K_1 does not appreciably change with time, change of $\eta(t)$ with time naturally leads us to the conclusion that the dimension of the modulating region L also changes with time. Assuming the density gradient applicable to the solar minimum period as 10% per AU, L was estimated as 5 AU during 1965. Similarly, the value of L applicable to the solar maximum activity

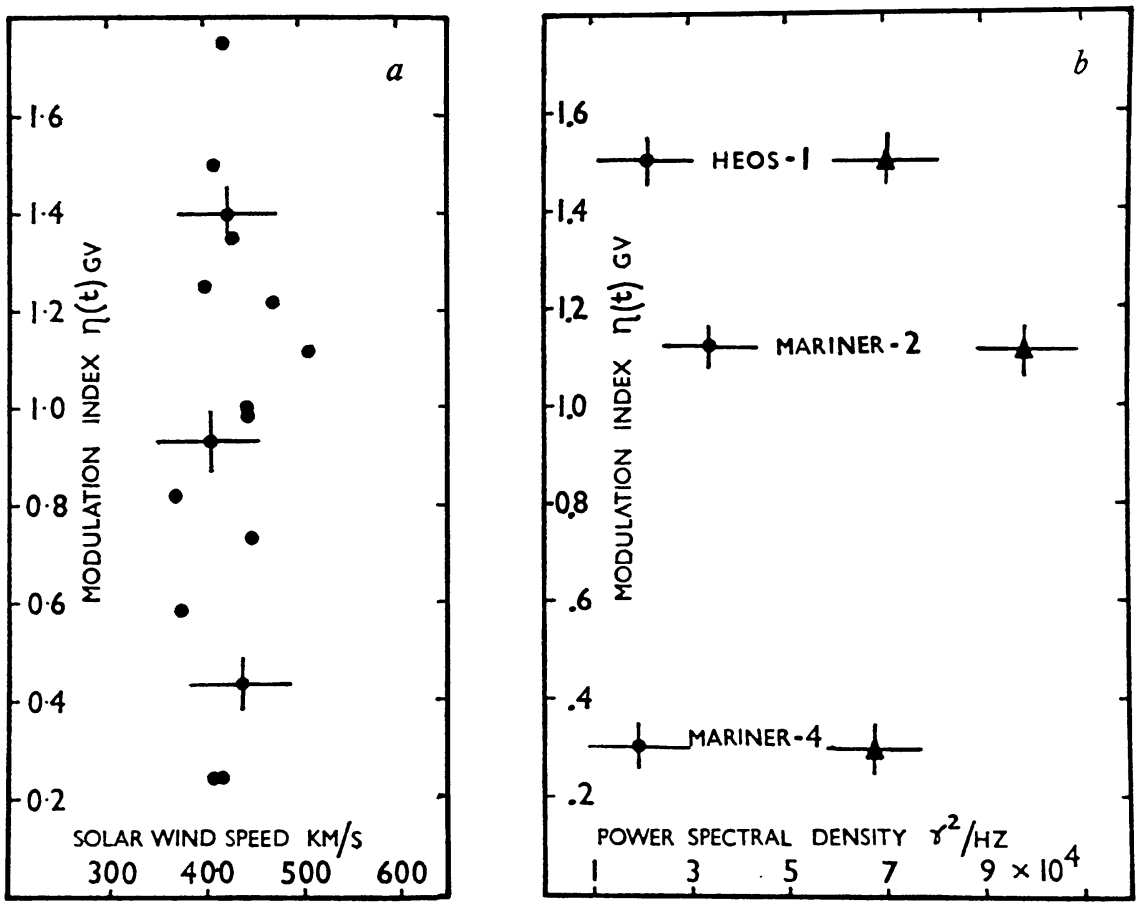

Fig. 24. Cosmic ray modulation parameter plotted as a function of solar wind speed and power spectral density of the interplanetary magnetic field at two frequencies namely 4.6×10^{-5} and 1.7×10^{-4} Hz during selected periods in 1962–1969. The interplanetary parameters used have been obtained from the observations on Mariner 2, Mariner 4 and HEOS-1 spacecrafts (after Mathews *et al.*, 1971).

TABLE IV

Time variation of the modulating parameter (after Wang, 1970)

Dates	Climax Neutron Monitor Rate	Particles measured		η(GV)	Reference
		Type	Rigidity range (GV)		
1957, Sept. 27 and 1958, Jan. 29 and 30	2750	High-altitude nucleonic intensity	1.0–5.0	3.50 ± 0.10	Wang (1970)
1959, June	2893	Protons and Helium	0.7–4.0	1.80 ± 0.15	Lockwood and Webber (1967)
1959, June	2893	Sea-level neutron monitor	2.0–11.0	2.05 ± 0.08	Lockwood and Webber (1967)
1967, July	3109	Heavy nuclei, $Z > 12$	1–2	1.3	Price *et al.* (1968)
1963, July	3183	Sea-level neutron monitor	2.0–11.0	0.74 ± 0.04	Lockwood and Webber (1967)
1956, Aug. 2, 1966, Aug. 15, and 1967, June 22	3187	High-altitude nucleonic intensity	1.0–5.0	0.95 ± 0.10	Wang (1970)
1963, Dec.– 1964, May	3249	Helium and neutron monitor neutron monitor	0.3–5.0	0.56	Gloeckler and Jopikii (1966)
1965, June–Sept.	3331	Protons and Helium	0.5–3.5	0.25 ± 0.05	Ramadurai (1970)
1965, June–Sept.	3331	Deuterons and ^{3}He	0.3–1.0	0.35	Ramaty and Lingenfelter (1968)
1954, Aug.–Sept.	3371	–	–	0.4	Extrapolated

has been estimated as ~ 50 AU using $\eta = 3.5$ GV and the appropriate value for the density gradient. Even though a firm estimate of the change of L over the solar cycle requires a knowledge of the radial and time dependence of the diffusion coefficient, and the density gradients, the experimental observations seem to suggest a variation of L from ~ 5 AU to ~ 50 AU from sunspot minimum to maximum. Such a conclusion is consistent with the estimate of L derived from the lag between the solar activity and the cosmic ray activity. Employing standard regression technique, Wang (1970) has observed a phase lag of nearly 6 months between 5303 Å maximum and the cosmic ray minimum suggesting a value of ~ 50 AU for the dimension of the modulating region during maximum solar activity.

However, the experimental evidence for the time variation of the volume of the modulating region is mainly derived from indirect observations of the time lag between the solar activity as represented by coronal observations and cosmic ray intensity changes. It must be remembered that quantitative calculation of L requires a consideration of the helio-latitude of the active region (Stozkov and Charakhchyan, 1970) and part of the change in delay between the cosmic ray activity and solar activity could result from the displacement, with time, of active regions on the Sun, from high to low helio-latitudes (Guschina *et al.*, 1969). The direct experimental measurements of solar wind and interplanetary magnetic field unfortunately do not support the time variation of L. The mean solar wind velocity and solar wind density seem to be practically invariant (Gosling *et al.*, 1971) with time. Figure 24 shows the observed variation in the modulation index plotted as a function of solar wind speed and power spectral density of the magnetic field (Mathews *et al.*, 1971). The interplanetary observations have been obtained from instrumentation on Mariner 2, Mariner 4 and HEOS-1 spacecrafts during selected periods in the interval 1962–1969. The figure seems to indicate that the modulation parameter is almost independent of either the solar wind or the interplanetary field parameters, on a long term basis.

A change in the value of η can be achieved through either a change in the value of L, the dimension of the modulating region or a change in the amplitude of the power spectral density of the magnetic field. The experimental observations of the power spectral density, near Earth, do not show significant change over a solar cycle. Thus, we find that the known variation of interplanetary parameters are not easily reconcilable with the observed long-term variation of cosmic ray intensity. The problem can be resolved if we assume the density gradient during sunspot maximum ($\gtrsim 100\%$ per AU at $R \sim 1$ GV) to be much larger compared to that at solar minimum. Since the experimental observations do not show such a large density gradient at 1 AU, the large density gradient would have to be located beyond 1 AU.

Another area where our understanding is yet incomplete is in the quantitative estimation of the contribution of microstructures or discontinuities to the power spectral density of the magnetic field. It is evident from the above discussion that a complete understanding of the long-term modulation of cosmic ray intensity must await better measurement of density gradients at and beyond 1 AU and a better knowledge of the interplanetary field structure both in and out of the plane of ecliptic.

4. Anisotropic Variations of Galactic Cosmic Radiation *

4.1. Introduction

Cosmic ray particles of all energies exhibit significant anisotropies, the magnitude of anisotropy being dependent on the particle energy. The predominant anisotropy which has been rather extensively studied is the anisotropy due to solar modulation of galactic cosmic radiation. All cosmic ray particles upto energies of 500 GeV are seriously affected by the Sun and the interplanetary magnetic fields in the solar system which completely obliterate the galactic (Sidereal) anisotropy for these particles. Particles of energy greater than 500 GeV can, however, be expected to exhibit sidereal anisotropy. Investigations of the anisotropy of very high energy particles, using underground meson monitors have shown (Jacklyn, 1965; Jacklyn and Vrana, 1969; Peacock *et al.*, 1970) the existence of a small sidereal anisotropy ($\sim 0.05\%$) oriented along the spiral arm magnetic field. Poor statistics, uncertainty in the determination of energy response functions of the underground monitors and difficulty in the exact determination of the contribution due to solar modulation have prevented us, in the past, from determining the actual magnitude of sidereal anisotropy which is of great relevance to the understanding of the origin and propagation of cosmic radiation in the Galaxy. Since the sidereal anisotropy is beyond the scope of this review article, we concentrate our main attention to the discussion of only the anisotropies due to solar modulation. Consequently, whenever we refer to anisotropy, we mean only anisotropy due to solar modulation.

4.2. Asymptotic cones of acceptance and their application to cosmic ray variations

Most of our information on anisotropies is derived from an analysis of data from ground based montors. As mentioned in Section 1, a knowledge of atmospheric transition effects and the geomagnetic effects is essential before one can interpret the ground based data in terms of the anisotropy of primary cosmic radiation. Dorman (1963) has given an excellent summary of these effects and of the earlier results on the cosmic ray variations.

Even after allowing for the changes in cosmic ray flux caused by changing meteorological factors, a knowledge of the asymptotic directions of approach of particles (Brunberg and Dattner, 1953; Brunberg, 1958) i.e. particle velocity vectors outside the magnetosphere, must be known in order to relate the anisotropy observed at the Earth with the primary cosmic ray anisotropy in space. A significant advance in our understanding of the cosmic ray anisotropy has been made during the last few years with the introduction of the concept of the 'asymptotic cone of acceptance' of detectors by Rao *et al.* (1963) which incorporates the trajectory information in the Earth's magnetic field as well as the differential response function of the monitor into a single parameter. The asymptotic cone of acceptance of a detector is nothing but the solid

* While this article was in press, another review on 'cosmic ray diurnal anisotropy' by Pomerantz and Duggal (1971) has appeared.

angle containing all the asymptotic directions of approach which make a significant contribution to the counting rate of the detector.

Before proceeding with a rigid mathematical formulation of the asymptotic cones of acceptance, a qualitative consideration of the problem would be very useful in understanding the physical problem. In Figure 25 the asymptotic directions of approach for particles of selected rigidities between 2 and 100 GV and incident on the top of the atmosphere from 0°, 16° and 32° in the north-south and east-west geomagnetic planes are plotted on the geographical scale of coordinates. The four detector locations considered are sufficient to illustrate, qualitatively, the importance of application of the concept of asymptotic cone of acceptance to the physical problem of cosmic ray variations. The asymptotic directions of approach have been calculated by tracing particle trajectories in a simulated geomagnetic field (McCracken *et al.*, 1962, 1965; Shea *et al.*, 1968) which includes spherical harmonic terms upto the 6th degree. From a close examination of Figure 25, we can draw the following conclusions.

(1) The width and the mean position of the acceptance cone is dependent on the geographic location of the station. The cones of acceptance of equatorial and mid-latitude stations like Ahmedabad and Mt. Wellington are much wider in longitude compared to that of a high latitude station such as Mawson. Consequently an anisotropy in space having a limited angular extent will be recorded with a much lower amplitude at an equatorial station than at a high latitude station. The narrower the asymptotic cone of acceptance of a detector, the more faithful would be the reproduction of the spatial anisotropy, or the observed amplitude of the anisotropy at any station is a strong function of the angular spread of its asymptotic cone of acceptance. This effect results in an appreciable latitude dependence of the amplitude of observed variation even if the initial anisotropy is not. The latitude variation of amplitude caused by smearing would be more pronounced for higher harmonics.

(2) Equatorial as well as middle latitude stations (upto 55° lat., Figures A and B) essentially scan a narrow band of declination close to the equatorial plane. To obtain asymptotic cones of acceptance making a substantial angle with the equatorial plane, it is necessary to go to very high geomagnetic latitudes.

(3) The observed phase of the anisotropy at any given station is dependent on the relative angular difference between its asymptotic cone of acceptance and the station meridian. The cone of acceptance at Mawson is almost coincident with its meridian whereas the cone of acceptance of a station shown in *D*, which is at the same geomagnetic latitude as Mawson, but 120° away from it in geographic longitude, is 50° E of its meridian. This implies that any anisotropy in space would be observed by a station corresponding to *D* approximately three hours earlier in local time as compared to Mawson, i.e. different stations along constant geomagnetic latitude at 70° S (or N) would see 'an anisotropy' at local times differing by as much as 3 hr. The origin of this spurious phase difference is traceable to the non-coincidence of geographic and geomagnetic planes. This phase difference would be quite large at higher geomagnetic latitudes whereas they would still be appreciable at lower latitudes.

Extensive computations of asymptotic cones of acceptance have been made by

McCracken *et al.* (1965). Table V lists the mean asymptotic latitude and longitude for a few selected stations. Given the various properties of an anisotropic flux of primary cosmic radiation, i.e. the rigidity dependence of the anisotropy, its spatial distribution etc. one can calculate the amplitude and phase of the variation that will be recorded at any station as the Earth rotates (Rao *et al.*, 1963). By comparing the

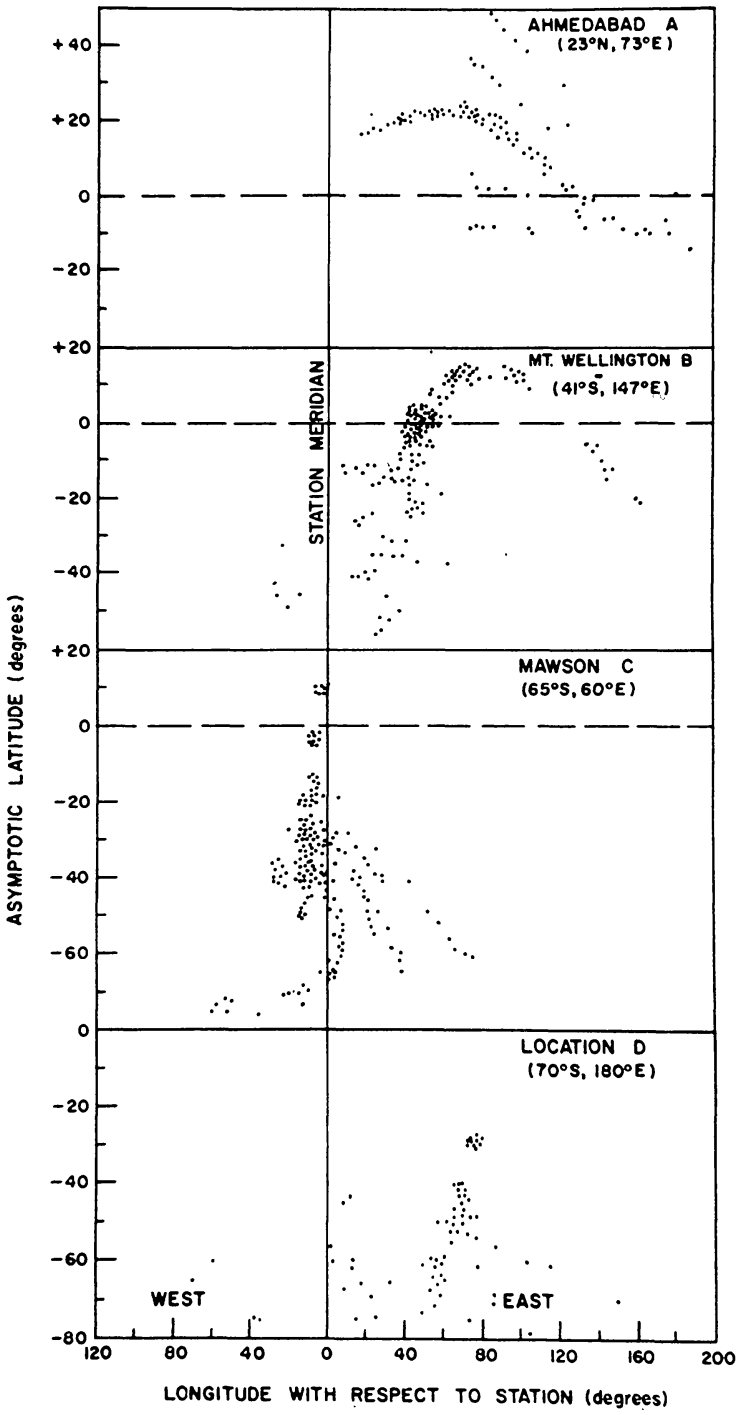

Fig. 25. The asymptotic directions of approach for particles arriving at four different locations. Location D has the same geomagnetic latitude as Mawson (after McCracken *et al.*, 1965).

1972SSRv...12..719R

TABLE V

Geographic and asymptotic coordinates and the expected relative amplitudes and phases of diurnal and semi-diurnal components for a few selected neutron monitor stations

No.	Stations	Geographic coordinates		Cut-off rigidity	Mean asymptotic coordinates		Daily variation			
		lat. (in degrees)	long.	in GV	lat. (in degrees)	long.	I Harmonic Amplitude (Relative)	Phase in hours	II Harmonic Amplitude (Relative)	Phase in hours
1	Ahmedabad	23.0	72.6	15.94	19	125	60.44	3.6	31.49	2.5
2	Alert	82.5	297.7	<0.05	77	331	9.90	2.0	4.20	3.1
3	Alma Ata	43.2	76.9	6.69	25	143	60.17	4.5	23.32	4.0
4	Calgary	51.1	245.9	1.09	28	269	85.09	1.6	76.85	1.6
5	Chacaltaya	−16.3	291.9	13.10	−17	341	66.14	3.6	28.21	2.6
6	Churchill	58.8	265.9	0.21	40	286	73.02	1.3	65.67	1.3
7	Climax	39.4	253.8	3.03	26	296	71.18	3.2	48.28	2.7
8	Dallas	32.8	263.2	4.35	25	316	69.47	3.5	45.63	3.3
9	Deep River	46.1	282.5	1.02	27	319	84.48	2.3	73.46	2.4
10	Denver	39.8	255.0	2.91	26	294	77.43	2.8	56.90	2.6
11	Durham	43.1	289.2	1.41	25	332	83.44	2.8	68.06	2.8
12	Goose Bay	53.3	299.6	0.52	35	339	77.91	2.4	68.23	2.5
13	Huancayo	−12.0	283.1	13.49	−16	333	63.56	3.6	27.82	2.5
14	Inuvik	68.4	226.3	<0.18	47	233	64.46	0.6	57.13	0.6
15	Kerguelen Is.	−49.4	70.2	1.19	−26	87	86.39	1.2	77.55	1.2
16	Leeds	53.8	358.5	2.20	31	52	74.61	3.5	58.01	3.5
17	Mawson	−67.6	62.9	0.22	−42	55	70.18	−0.3	61.76	−0.4
18	McMurdo Sound	−77.9	166.6	<0.05	−74	261	11.49	6.1	9.74	7.2
19	Mt. Norikura	36.1	137.6	11.39	26	195	57.83	3.9	27.92	2.9
20	Mt. Washington	44.3	288.7	1.24	25	331	82.14	2.9	67.90	2.9
21	Mt. Wellingotn	−42.9	147.2	1.89	−25	193	80.71	3.1	62.08	3.0
22	Resolute	74.7	265.1	<0.05	66	274	34.56	0.6	26.62	0.6
23	Rome	41.9	12.5	6.31	26	80	60.35	4.6	22.22	4.1
24	Sulphur Mountain	51.2	244.4	1.14	27	270	84.61	1.7	75.15	1.7
25	Uppsala	59.9	17.9	1.43	35	63	75.58	3.0	62.79	3.1
26	Wilkes	−66.4	110.5	<0.05	−56	107	51.82	−0.2	44.34	−0.2

observed amplitudes and phases of anisotropy at a number of stations with the above calculations, one can obtain a best fit to the anisotropy. This method called the method of 'variational coefficients' has been extensively made use of in the study of both the diurnal and semi-diurnal anisotropies of cosmic radiation assuming the anisotropy to be time invariant for at least a day.

If the anisotropic cosmic ray flux within the solid angle Ω_i is $J_0(1+A_i R^\gamma)$ and J_0 is the flux from all other directions, the increase in the counting rate ΔN over the normal counting rate N due to the excess anisotropic flux will be

$$\frac{\Delta N}{N} = V(\Omega_i, \gamma) A_i \tag{4.1}$$

where the anisotropy is assumed to vary with rigidity as R^γ. Equation (4.1) demonstrates that the count rate deviation from normal due to an anisotropy can be calculated if the variational coefficient $V(\Omega_i, \gamma)$ for all possible solid angles Ω_i are known. Note that for an anisotropy which is independent of both declination and energy ($\gamma=0$), the variational coefficient just indicates the manner in which the total count rate of a station is contributed from different asymptotic longitudes.

Variation coefficients for a large number of stations and for different values of γ, the spectral exponent of variation varying from $-1.5 \leqslant \gamma \leqslant 2.0$ are available in the form of tabulation in literature (McCracken *et al.*, 1965; Shea *et al.*, 1968). Figure 26 shows the variational coefficients plotted as a function of asymptotic longitude for a few representative stations assuming $g(\Lambda)=\cos\Lambda$ where $g(\Lambda)$ represents declination dependence of the anisotropy of cosmic radiation flux. Employing the variational coefficients, the predicted amplitudes and phases of both the diurnal and semi-diurnal variations at a number of stations for different forms of assumed primary anisotropies have been calculated (McCracken *et al.*, 1965; Mori, 1968). Table V lists these parameters for a number of selected stations obtained for an energy independent anisotropy.

4.3. Experimental observations on diurnal variation of cosmic rays

Even though occasional attempts (Rao and Sarabhai, 1964) have been made by a few workers to study the cosmic ray daily variation in its entirety without resorting to divide it into its harmonics, most of our information on the cosmic ray daily variation has been derived through a study of the diurnal and the semi-diurnal components. A great body of experimental observations has been accumulated in the past 30 yr concerning the daily variation of cosmic radiation. Even though the uncertainty in the application of atmospheric corrections introduced a large ambiguity in the interpretation of earlier meson observations, Elliot and Dolbear (1951), and Rao and Sarabhai (1961) were able to prove beyond any doubt, the existence of a small diurnal component of cosmic radiation using crossed meson telescopes. Meteorological effects being the same for east and west (or N and S) telescopes inclined at the same zenith angle (true only to a first degree of approximation), the residual variations due to the diurnal anisotropy can be estimated by comparing the data from crossed

telescopes. With the availability of data from neutron monitors for which the atmospheric effects are fairly well understood, it has been possible to examine the daily variation of cosmic radiation in a great detail. The improved statistics provided by the high counting rate super neutron monitors has further improved our knowledge of the daily variation.

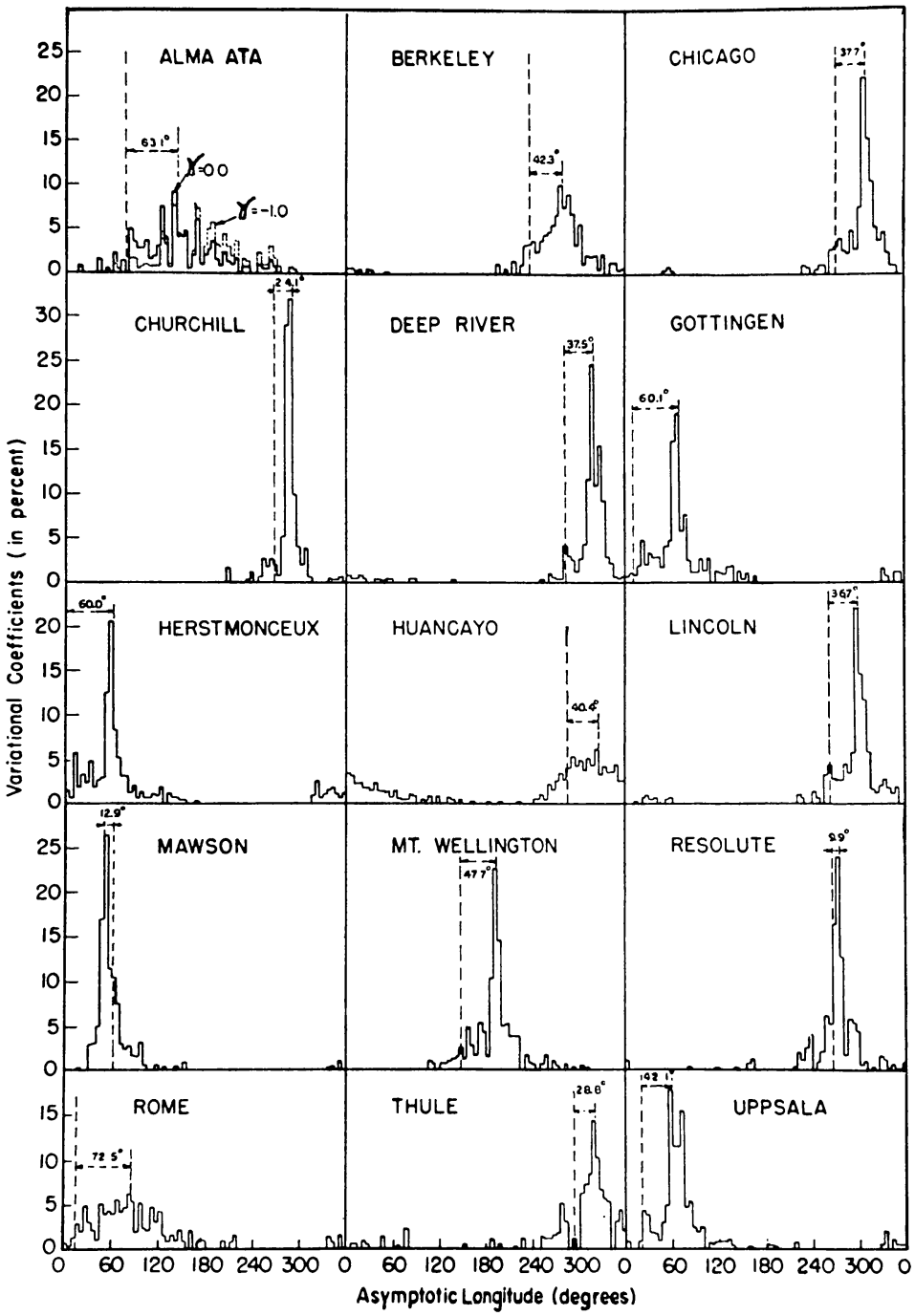

Fig. 26. The variation coefficients at a few selected stations plotted as a function of their asymptotic longitude for $\gamma = 0$ and $g(\Lambda) = \cos \Lambda$. The station meridian is also indicated in the diagram. The variational coefficients for $\gamma = 1.0$ and $g(\Lambda) = \cos \Lambda$ are also plotted (dotted curve) for Alma Ata (after Rao *et al.*, 1963).

4.3.1. *Average Properties of Diurnal Variation*

From an extensive analysis of data from a large number of neutron monitors that were in operation during IGY and later, the average properties of the diurnal variation such as its time of maximum, its dependence on declination and energy have been investigated by several workers (Duggal *et al.*, 1961; Rao *et al.*, 1963; McCracken and Rao, 1965).

In Figure 27, the average diurnal variation observed by various detectors during the period 1957–1965 obtained after correcting for the width of the asymptotic cone of acceptance of each detector is plotted as a function of its mean asymptotic latitude of viewing. The figure clearly demonstrates that the observed amplitude of diurnal variation at any station varies as the cosine of the mean asymptotic latitude of that station. The superimposed continuous curve indicates the expected distribution of the amplitude of the average anisotropy derived assuming a cosine dependence of declination.

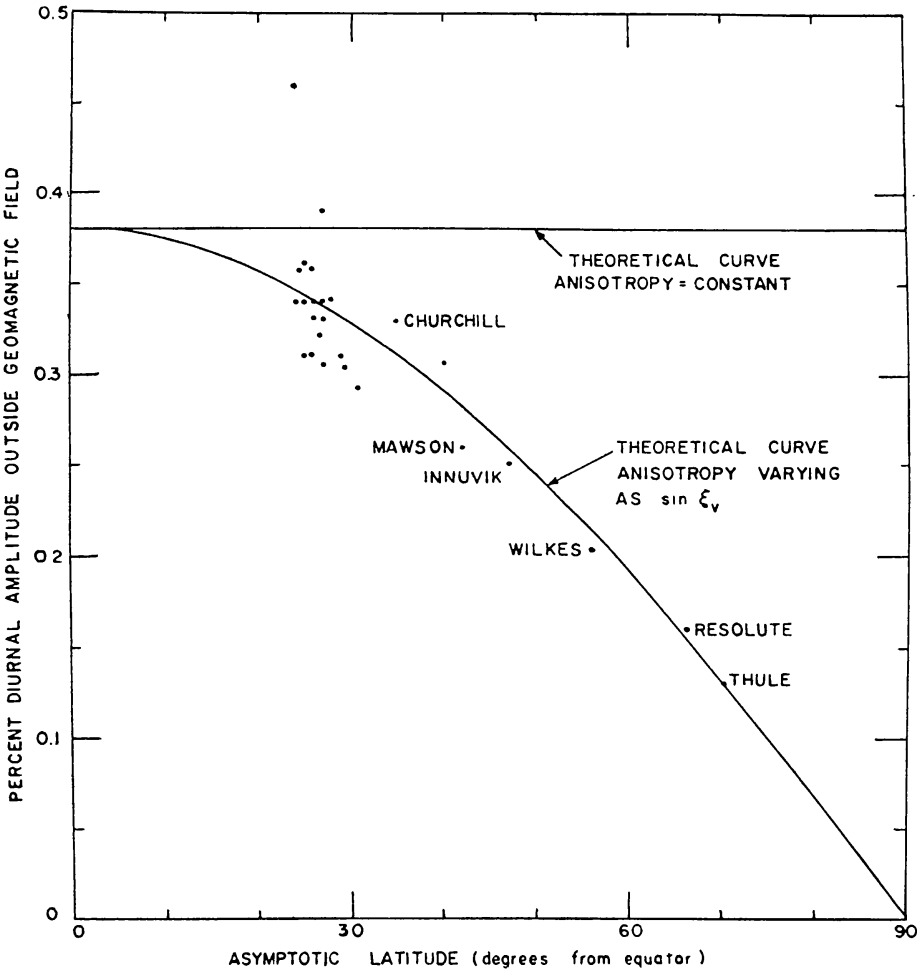

Fig. 27. The observed average diurnal amplitude at various stations corrected for the width of their asymptotic cones of acceptance are plotted as a function of their mean latitude of viewing. The theoretical curves for anisotropy independent of declination $g(\Lambda) =$ constant and anisotropy varying as cosine of declination $g(\Lambda) = \cos \Lambda$ are also plotted in the figure. (after McCracken and Rao, 1965).

Extensive analysis of all the neutron monitor data during 1954–1965 (Rao *et al.*, 1963; McCracken and Rao, 1965) has conclusively proved that the average diurnal variation of cosmic ray intensity can be adequately expressed by

$$\frac{\partial J(E)}{J(E)} = AE^{-\gamma}\cos(\psi - \psi_0)\cos\Lambda, \quad \text{for} \quad E \lesssim E_{\max}$$
$$= 0 \quad \text{for} \quad E \gtrsim E_{\max} \tag{4.2}$$

where A is a constant equal to $(0.38 \pm 0.02) \times 10^{-2}$, $\gamma = 0$, $\psi_0 = 89 \pm 1.6°$ measured anticlockwise from the noon meridian, Λ is the declination and $E_{\max}$ is usually of the order ~ 100 GeV. In other words, the average diurnal anisotropy of cosmic radiation is (a) energy independent in the energy range 1–100 GeV; (b) varies as cosine of the declination; (c) has an average amplitude of about $0.38 \pm 0.02\%$ and (d) has a maximum flux incident from $89 \pm 1.6°$ E of the Earth-Sun line.

$E_{\max}$ in Equation (4.2) which is the upper limit of energy above which the modulation becomes insignificant has been investigated by several authors. Since less than 20% of the counting rate of a high latitude neutron monitor originates in primary particles of energy $E \gtrsim 100$ GeV, neutron monitors are not very sensitive to changes in $E_{\max}$. Rao *et al.* (1963) and Jacklyn and Humble (1965) used the ratio of the amplitude of first harmonic in neutron monitor and underground meson telescope at Hobart to place the 'upper cut-off' at about 100 GeV. Subsequently, several authors (Peacock, 1970; Summer and Thomson, 1970; Jacklyn *et al.*, 1970; Ahluwalia and Erickson, 1970; Agrawal *et al.*, 1971) have followed a similar method and have concluded that $E_{\max} \lesssim 100$ GeV and that it varies with solar activity, the lowest value of 40–50 GeV being attained during solar activity minimum. It must be remarked that in the evaluation of $E_{\max}$ the differential response curve of meson monitors play a crucial role, which are not known with the same accuracy as that of neutron monitors.

4.3.2. *Long-Term Variation of Average Diurnal Variation*

The long-term changes in the average properties of the diurnal variation has also been investigated by several authors. The early work of Thambyahpillai and Elliot (1953) and Sarabhai *et al.* (1954) had indicated the existence of a solar cycle variation in particular a 22 yr cycle of variation in the time of maximum of the mean diurnal vector. However, study of the average diurnal variation as observed by neutron monitors over the period 1957–1965 by McCracken and Rao (1965) as well as by Duggal *et al.* (1967) has shown that it has been remarkably constant over these years, except for a small decrease in the amplitude to 0.3% in 1965. Figure 28 shows the yearly mean amplitude and the time of maximum of the diurnal anisotropy during 1957–1969 derived from the neutron monitor data. The figure clearly demonstrates the near constancy of the diurnal anisotropy characteristics over the solar cycle.

In an attempt to understand the diurnal variation observed by meson monitors, Forbush (1969) has analysed the ion chamber data for the last 30 yr. Comparing with the neutron observations, he concludes that the systematic long-term changes in the diurnal variation arises from the superposition of varying contribution from two

distinct components – one component having a maximum in the asymptotic direction 128° E of the Sun which exhibits a sinusoidal variation with a period of two solar cycles and a second component having a maximum in the asymptotic direction 90° E of the Sun which exhibits a periodicity of one solar cycle variation with the minimum amplitude coinciding with the minimum in solar activity.

As discussed earlier, the small changes in the amplitude of the diurnal variation, in particular the reduction of amplitude to 0.3% in 1965 can be explained as due to changes in the upper cut-off rigidity above which the diurnal variation ceases. A change in the cut-off rigidity (Agrawal and Rao, 1969) from about 40 GV in sunspot manimum of 1965 to about 100 GV in 1968 can explain the observations. Further, in view of the fact that the time of diurnal variation derived from neutron data has remained practically constant over the entire solar cycle (McCracken and Rao, 1965, also Figure 28), the conclusions by Forbush (1969) and Duggal *et al.* (1970) derived from using ion chamber data have to be viewed with caution. Both the changes in upper cut-off rigidity and the application of inadequate temperature corrections make

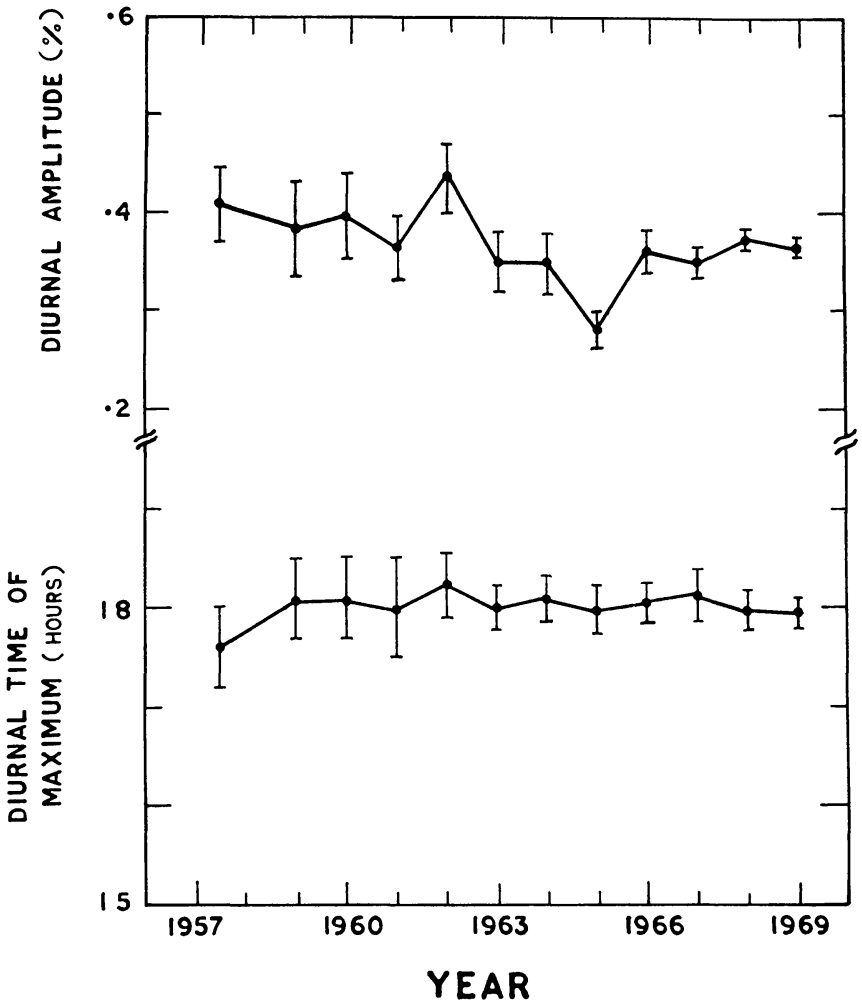

Fig. 28. Yearly mean amplitude and the time of maximum of diurnal anisotropy of cosmic radiation during 1957–1969 derived from the neutron monitor data. The error bars indicate the actual error due to the dispersion in different observations and not the statistical error, which is quite negligible.

the diurnal variation of meson component more sensitive to solar activity. Recently, Agrawal *et al.* (1971) have reported that if appropriate temperature correction is used to correct meson intensity, the diurnal anisotropy amplitude and time of maximum observed by a meson monitor shows good agreement with neutron data during 1965–1969.

4.4. Diurnal variation of cosmic radiation – theoretical treatment

The diurnal variation observed by ground neutron monitoring stations can be caused either due to the (a) diurnal variation of the asymptotic cones of acceptance of detectors, as a result of the difference in the deformation of the geomagnetic field by the solar wind between day and night or (b) as a consequence of modulation of the galactic cosmic radiation by the solar system magnetic fields.

The external currents induced by the interaction of plasma with the geomagnetic field produce a strong day night asymmetry in the geomagnetic cavity resulting in a further lowering of the geomagnetic cut off at night due to the tail currents. The diurnal variation of the cut off rigidity, in turn, can cause a diurnal variation of cosmic radiation observed at ground stations. Calculation of detailed trajectories of particles at different stations by a number of authors (Ahluwalia and McCracken, 1966; Michel, 1965; Reid and Sauer, 1967; Gall, 1968) have clearly shown that the effect of the geomagnetic field perturbation by solar wind on the cut off rigidity is not appreciable at high energies ($\gtrsim 1$ GeV) and consequently the contribution from the cut off changes to the diurnal variation observed by ground monitors is negligible.

Two major effects cause the anisotropy of cosmic radiation in space (a) the first due to the corotation of particles with the interplanetary field structure and (b) the second due to adiabatic deceleration and energy losses in the expanding solar wind. Whereas the first process is the most important process at energies above 500 MeV, the second becomes significant for particles of energies below 100 MeV.

4.4.1. *Anisotropy due to Corotation*

Assuming that under steady equilibrium conditions there is no net flux of galactic cosmic radiation inward or outward from the Sun i.e. Sun is neither a sink nor a source of cosmic ray particles, the cosmic ray particles at these energies must rigidly corotate in the Archimedes spiral magnetic lines of force. Theoretically as Ahluwalia and Desseler (1962) showed, the motion of cosmic ray particles under these conditions can be described in terms of their drift in the electric field $E = -V \times B/C$ as seen from a stationary observer.

Stern (1964)) pointed out a fundamental objection to the above simple picture. Applying Liouville's theorem which imposes the restriction that the cosmic ray density must be constant in phase space (there should be no net streaming in a steady field system for which $\partial B/\partial t = 0$) Stern showed that, in the absence of scattering, the drift term will be exactly cancelled by the density gradient which will be set up normal to the Sun's equatorial plane. The perpendicular density gradient will result in reducing the net anisotropy to zero provided electric and magnetic fields are assumed to be static.

The above theoretical picture changes drastically (Parker, 1964; Axford, 1965; Parker, 1967) with the introduction of small scale magnetic irregularities which are transported radially outward from the Sun by the solar wind. The random walk of cosmic ray particles in the moving frame of solar wind leads to diffusion which eventually will cancel out the pressure due to perpendicular cosmic ray density gradients resulting in a net streaming of the cosmic ray gas. In the ideal case of the scattering due to small scale magnetic irregularities being sufficiently large, the pressure due to the density gradients will be completely relieved and the cosmic ray gas at a heliocentric distance r will execute a rigid corotation with the Sun with a velocity equal to Ωr (Ωr being $\approx$400 km/s at 1 AU) where Ω is the angular velocity of the Sun. The anisotropy of cosmic ray particles introduced by this rigid corotation is given by the usual Compton-Getting formula (Gleeson and Axford, 1968b; Forman, 1970a)

$$\xi_{\text{COROT}} = (2 + \alpha\gamma)\frac{\Omega r}{v} \tag{4.3}$$

where

$$\alpha = \frac{E + 2m_0c^2}{E + m_0c^2}$$

where m_0c^2 is the rest energy of the particles, γ is the exponent of the differential energy spectrum of primary cosmic radiation and v is the particle velocity (corotation velocity $\Omega r \approx 400$ km/s at Earth's orbit).

Equation (4.3) for the corotation anisotropy clearly demonstrates that the anisotropy will be energy independent at energies above $\sim$1 GeV, the maximum theoretical amplitude being 0.62% for $\gamma = 2.65$ and $V \approx 400$ km/s. The direction of anisotropy will be along the 1800 h direction i.e. along the corotation vector. At lower energies, however, the reduction in the velocity of the particle will result in a larger amplitude for the observed anisotropy. Figure 29 shows the theoretically expected maximum amplitude of corotation as a function of the energy of the particle.

If the distribution of small scale irregularities are insufficient to relieve the pressure due to density gradients, the particle corotation will be correspondingly reduced below Ωr resulting in a reduction in the amplitude of the corotation anisotropy from the theoretical maximum. In the extreme case of the complete absence of small scale irregularities, the gradient drift will exactly cancel the corotation leading to zero diurnal variation in accordance with Liouville's theorem.

On the other hand, in the second extreme case when $K_\perp \simeq K_\parallel$, the particles can move across the field lines as easily as they can move along the field lines. For such a case, the particles will not be contained within the field lines and therefore will cease to corotate reducing the corotation amplitude again to zero.

4.4.2. *Radial Anisotropy due to Energy Changes*

As discussed in Section 3, the energy losses suffered by cosmic ray particles, as they execute random walk in the magnetic irregularities, will result in these particles leaving

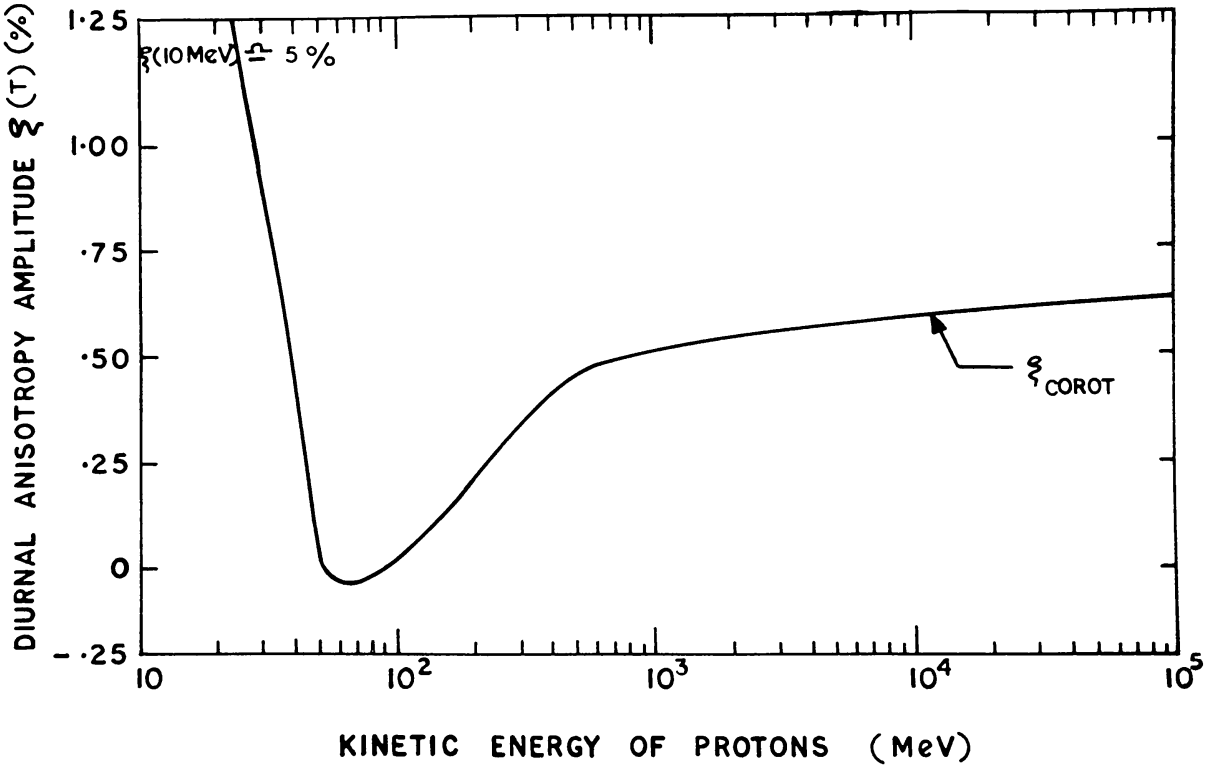

Fig. 29. Theoretically expected (maximum) amplitude of corotation anisotropy plotted as a function of particle kinetic energy.

the solar system with either increased or decreased energy resulting in a net inward or outward flux of particles. The energy loss due to deceleration resulting in a loss of energy for particles is equivalent to having a sink for those particles. The resulting radial anisotropy is dependent on both the energy of the particle and the density gradient.

The radial anisotropy at intermediate and high energies ($E \gtrsim 1$ GeV) can be estimated by substituting the observed values for various parameters in Equation (3.15). Assuming 9% per astronimical unit for the radial gradient at 5 GeV ($\alpha = 1.17$) the amplitude of the radial anisotropy is found to be $\xi \approx +0.02\%$ for $\gamma = 2.65$.

At lower energies, as described in Section 3, radial anisotropy depends critically on the value of the density gradient. Using the different approximations described in Section 3, the radial anisotropy under different conditions is plotted in Figure 30 for cosmic ray particles of energy $E \lesssim 100$ MeV. The best fit differential primary spectrum used in these calculations is also shown in the figure.

The theoretical curves (a), (b) and (c) correspond to three different cases: (a) assuming the spectrum given in the figure to be entirely due to particles of galactic origin and the radial density gradient to be large, the radial anisotropy being computed from Equation (3.18), (b) assuming the spectrum upto 10 MeV to be primarily due to particles of solar origin and the radial density gradient of the galactic protons to be small in which case the radial anisotropy can be computed using Equation (3.19) and (c) assuming the cosmic ray spectrum to be a combination of galactic and solar

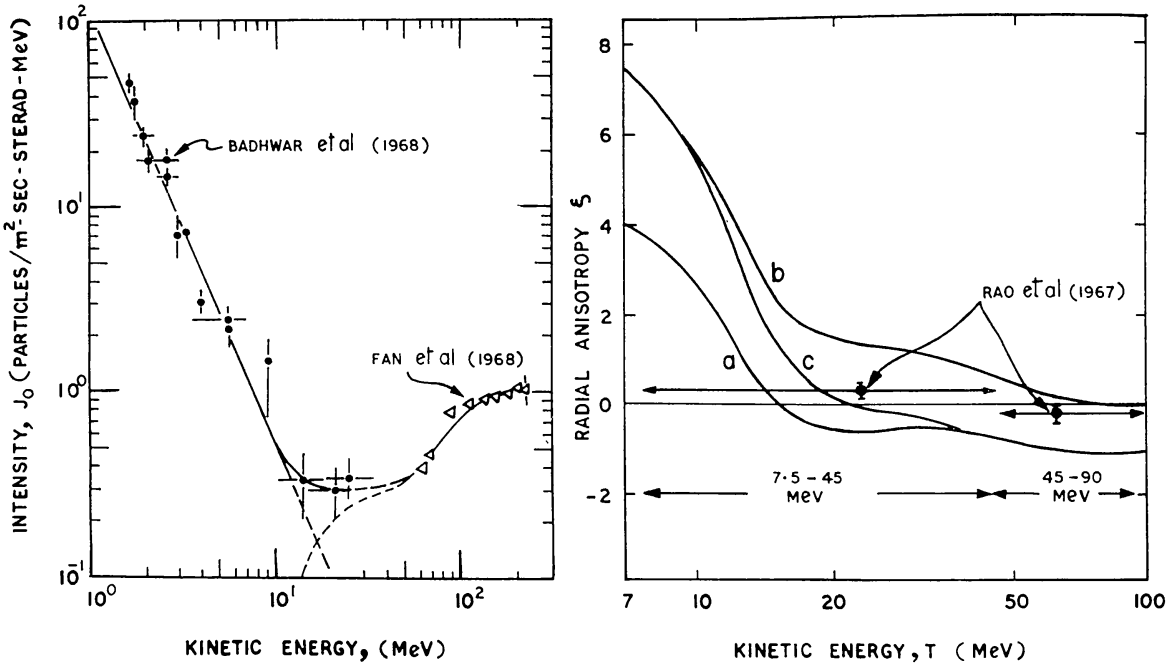

Fig. 30. (a) The best fit cosmic ray spectrum during 1966 at low energies obtained from observation of Fan *et al.* (1968) and Badhawar *et al.* (1968). (b) The theoretically estimated radial anisotropy as a function of energy under different assumptions described in the text (after Fisk and Axford, 1970). At energies $\gtrsim$ 1 GeV, the anisotropy is energy independent and has a maximum amplitude of $\sim 0.62\%$.

contribution as in (b) but with the radial density gradient of galactic flux to be large in which case the anisotropy is computed using Equation (3.19) for solar proton and (3.18) for galactic protons.

Besides the energy changes as Jokipii and Parker (1968a) and Subramanian and Sarabhai (1967) have indicated, asymmetry in the distribution of solar activity can also contribute to the radial anisotropy. Coronal observations seem to indicate a higher solar activity at 20–30° heliolatitudes as compared to that corresponding to very high latitudes or in the equatorial plane. Lower cosmic ray density associated with higher activity at higher heliolatitudes will tend to diffuse cosmic rays outward in the equatorial plane across heliolatitudes. Even though quantitative calculations which are closely dependent on the solar activity and the density of cosmic ray flux at different heliolatitudes, are not available, a rough estimate of this effect (Parker, 1969) suggests that the resulting radial anisotropy can be as large as 0.5% at MeV energies.

4.4.3. *Comparison with Experiments*

a. *Radial Anisotropy*

(i) *High energies:* The experimental observations at high energies ($E \gtrsim 1$ GeV) indicates (McCracken and Rao, 1965) that the diurnal anisotropy at these energies has an average amplitude of about 0.4% with the maximum flux incident from $89 \pm 1.6°$ E of the Earth-Sun line. This yields a value of $0.01 \pm 0.02\%$ for the radial anisotropy which is in good agreement with the theoretical prediction from convection-

diffusion theory. Figure 8 illustrates the excellent agreement between the experimental observation and the theoretically expected value of the radial anisotropy at high energies.

(ii) *Low energies:* The anisotropy of low energy cosmic radiation during 1965–1966 has been investigated by Rao *et al.* (1967a) with instrumentation on board Pioneer 6 and 7 spacecrafts. They find that particles in the energy range 7.5–45 MeV exhibit a radial anisotropy of amplitude $0.18 \pm 0.05\%$ (from 13.6° W of the Earth-Sun line) and particles in the energy range 45–90 MeV/nucleon exhibit an anisotropy of amplitude $0.20 \pm 0.15\%$ incident from a direction 173.4° E of the Earth-Sun line (anti-solar direction). We also note that particles below 100 MeV/nucleon, do not show significant azimuthal anisotropy or in other words low energy particles do not show appreciable corotation.

The theoretically predicted (Fisk and Axford, 1970; Jokipii and Parker, 1970) radial anisotropy for low energy particles under different assumptions is plotted in Figure 30 along with the available experimental observations (Rao *et al.*, 1967a). A close examination of the figure shows that the observed radial amplitudes are consistent with only the theoretical curve derived assuming the spectrum obtained by O'Gallagher (1967) to be completely due to galactic protons and the radial density gradients to be large (case a).

Equation (3.18) which can be applied to estimate the anisotropy under these conditions also predicts (Forman, 1970b) a large radial gradient of anisotropy. Even though the statistical accuracy of the experimental observations by Rao *et al.* (1967a) are not sufficient to notice small variation of anisotropy with heliocentric distance (0.8–1.1 AU), the observations do not support a large gradient of ξ that would be expected on the basis of theory. A more serious problem is the recent observation of Kinsey (1970) and Gleeson *et al.* (1970) which indicate that the Sun is essentially a quasi-continuous source of low energy particles. Even though the observation by Kinsey pertains to 1967–1968, it is reasonable to assume that even during 1965–1966 the low energy cosmic radiation was well contaminated with solar particles. The expected radial anisotropy for both large and small density gradients (cases b and c in Figure 30) derived on the assumption of the low energy part of the cosmic ray spectrum to be contaminated by solar protons, is found to be much larger than what the experimental observations of Rao *et al.* (1967a) suggest. Thus the observed low energy anisotropy measurements cannot be reconciled with the theory and we, therefore, believe that a further confirmation of the low energy anisotropy observations is very crucial to verify the validity of the diffusion-convection theory.

b. *Azimuthal anisotropy*

Comparing the characteristics of the average diurnal variation of cosmic ray intensity with the predictions of Axford-Parker theory, we observe that the agreement between the theory and the experiment on the spectral exponent, the time of maximum and the declination dependence is very impressive. The only discrepancy is found to be in the observed diurnal amplitude ($\sim 0.4\%$) being much less than the theoretically predicted amplitude of $\sim 0.62\%$. If the value of E_{max} the particle energy above which

corotation is negligible is less than 200 GeV, the observed diurnal amplitude would be reduced considerably below 0.6% (Subramanian, 1971a). As has already been discussed, the full corotation effect is realisable only if the perpendicular pressure gradient is relieved by scattering in irregularities. If the pressure gradient is only partially relieved, the resulting corotation amplitude will be less than the theoretical maximum. Since the cosmic ray pressure gradients can be relieved only by diffusion perpendicular to the lines of force, ($K_\perp$), the observed average diurnal variation can be profitably utilized to infer the properties of $K_\perp$. The near constancy of the mean diurnal amplitude during 1957–1969 points out to the near constancy of $K_\perp/K_\parallel$ during the solar cycle (McCracken and Rao, 1966).

The reduction in the amplitude of the diurnal variation during 1965 has been attributed (Ahluwalia and Erickson, 1970; Jacklyn *et al.*, 1970) to the reduction in the upper cut off rigidity from 100 GV–40 GV. Such a reduction in E_{max}, however, is difficult to understand in view of the available interplanetary field data. During the entire period 1965–1968, the sector structure configuration of the magnetic field was practically the same, the field data showing two predominant sectors (Wilcox and Colburn, 1969), even though the sectors were just evolving in 1965. The alternate hypothesis of change in the scale sizes of the field inhomogeneities during the two periods is also not well supported by the power spectral measurements discussed earlier. We believe that our understanding of the origin of E_{max} is still incomplete.

The preceding discussion, shows that, on the whole, the average picture of the diurnal variation is well explained by Axford–Parker theory of corotation. The absence of any significant azimuthal anisotropy (Rao *et al.*, 1967a) at energies below 100 MeV/nucleon can be interpreted in terms of $K_\perp < K_\parallel$ at these energies. However, such interpretations are in contradiction with the low energy (~ 10 MeV) flare observations (McCracken *et al.*, 1971) which clearly indicate that the transverse gradients at these energies are negligible. Further, Subramanian (1971a), who has made accurate calculations taking the appropriate E_{max} into consideration, has shown that the observed average diurnal amplitude is not significantly different from the expected amplitude which also indicates that $K_\perp \ll K_\parallel$ at energies above 1 GeV. In order to reconcile some of these discrepancies, Forman and Gleeson (1970), Rao *et al.* (1971b) and Hashim *et al.* (1971) have proposed a new explanation for the diurnal variation in terms of summation of simple convection and diffusion. According to this concept, the radial convective flow will be exactly balanced by the inward diffusion, under equilibrium conditions, thus causing the net radial current to be zero (i.e. Sun is neither a sink nor a source), which produces the observed corotational anisotropy on an average basis. At lower energies, however, the condition of net radial streaming current density being zero may not hold good which might cause a reduction in the azimuthal anisotropy. Since this theory also provides an elegant explanation for the day to day variations of diurnal anisotropy, a further discussion of the theory is postponed to the next (4.6.3) section.

4.5. Semi-diurnal variation of cosmic radiation

4.5.1. *Experimental observations*

The presence of a semi-diurnal variation in primary cosmic ray intensity had been inferred from crossed meson telescopes many years ago (Elliot and Dolbear, 1951; Rao and Sarabhai, 1961). Even though, the close correlation between the second harmonic amplitude in atmospheric pressure variations and neutron monitor counting rate changes (Katzman and Venkatesan, 1960) raised some doubts about its existence, with the use of high count rate super neutron monitor data and sophisticated analytical techniques involving power spectral analysis and numerical filtration, Ables *et al.* (1965) were able to conclusively establish the existence of a small semi-diurnal anisotropy ($\sim 0.1\%$). Figure 31 demonstrates the existence of two significant peaks in the power spectral density of Deep River neutron monitor data during 1964 – the first peak corresponding to the diurnal variation and the second to the semi-diurnal variation. The semi-diurnal anisotropy was further shown to have a positive spectral exponent (Ables *et al.*, 1965; Patel *et al.*, 1968; Lietti and Quenby, 1968; Fujii *et al.*, 1970) with the excess flux oriented along a direction perpendicular to the general direction of the interplanetary magnetic field.

Due to the small magnitude of the semi-diurnal anisotropy, and the contamination

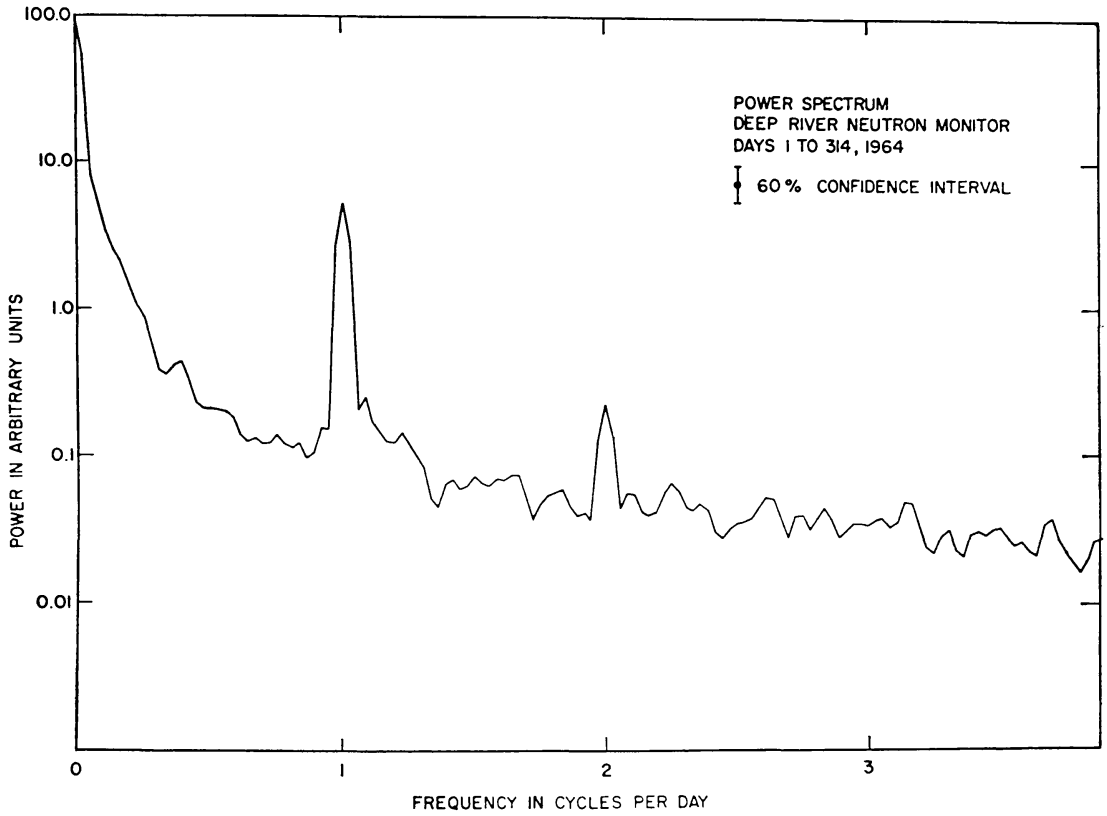

Fig. 31. Power spectral analysis of Deep River neutron monitor data during 1964 showing the presence of two significant peaks in the daily variation corresponding to periods of 1 and 2 cycles/day (after Ables *et al.*, 1965).

due to atmospheric effects, systematic study of the semi-diurnal variation has only been done recently. From an extensive analysis of data from several neutron monitors, including super neutron monitors, over a ten year period 1958–1968 Rao and Agrawal (1970) have been able to derive the properties of average semi-diurnal variation, summarized below.

(1) The average semi-diurnal variation varies as R^{γ} where γ, the exponent of variation is 1.0 ± 0.2. In other words the observed average semi-diurnal anisotropy varies as the first power of rigidity. Consequently the observed semi-diurnal component at equatorial stations and for meson monitors, both having higher energy response, will be greater than that observed at high and middle latitude stations.

(2) The annual mean amplitude of the semi-diurnal anisotropy is about $0.11 \pm 0.2\%$ the maximum flux incident from 0300 h direction that is from a direction perpendicular to the average interplanetary field vector.

(3) The amplitude of the anisotropy varies as $\cos^n \Lambda$ where $n \geqslant 2$. Even though the statistical accuracy of the data cannot unambiguously decide between $n=2$ and $n=3$, the experimental observations (Figure 32) favour a $\cos^2 \Lambda$ dependence on declination.

(4) The experimental observations indicate an upper cut off rigidity R_{max}, above

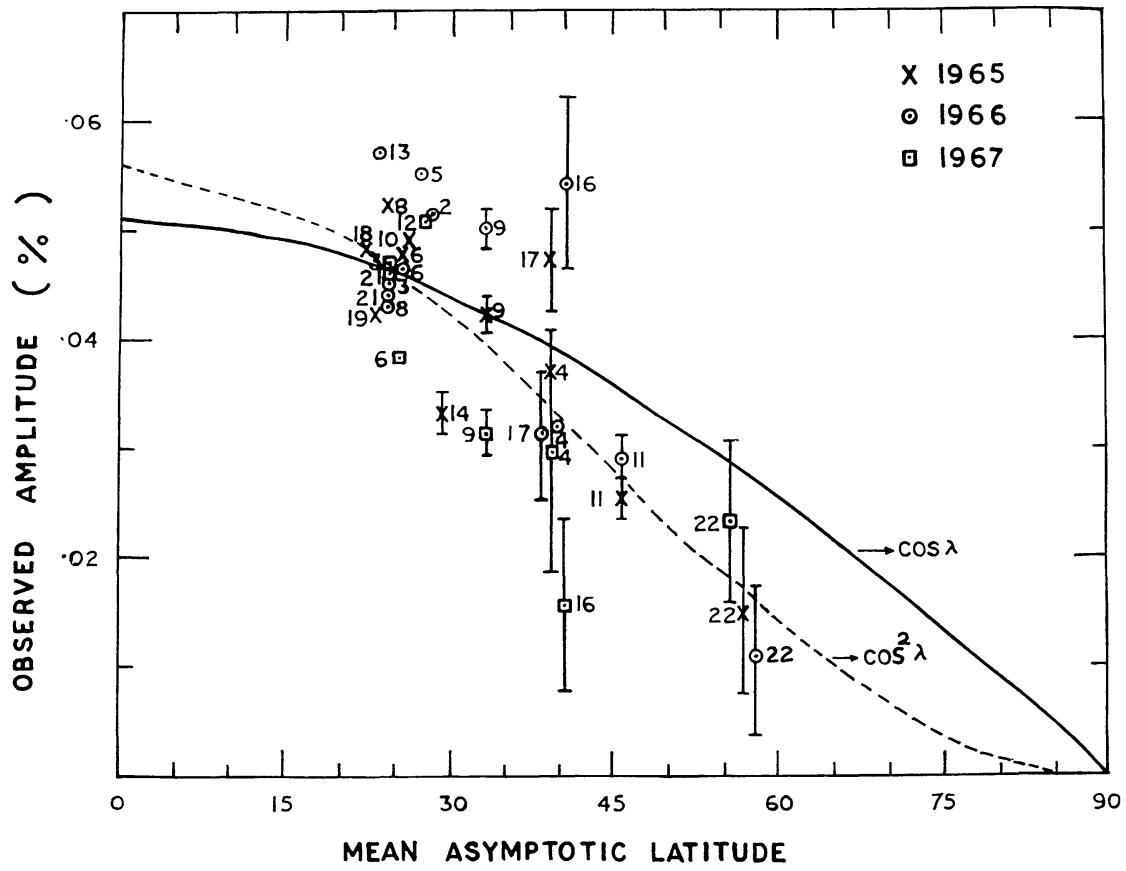

Fig. 32. Amplitude of the semi-diurnal anisotropy observed at each station (after correcting for the width of the asymptotic cone of acceptance of the detector) plotted as a function of the mean asymptotic latitude of the detector. The figure demonstrates that the observed data is consistent with $\cos^2 \Lambda$ dependence with declination (after Rao and Agrawal, 1970).

which particles do not exhibit the semi-diurnal anisotropy. Rao and Agrawal (1970) estimate R_{max} to be ~ 200 GV during 1966.

(5) The amplitude as well as the time of maximum of the semi-diurnal anisotropy during 1958–1968 show very little time variation. Figure 33 illustrates the time invariance of the amplitude and phase of the semidiurnal component.

Summing, we may conclude that the semi-diurnal anisotropy of cosmic radiation can be expressed as

$$\begin{aligned} \frac{\partial J(R)}{J(R)} &= AR\cos^2\Lambda\cos 2(\psi-\psi_0) \quad \text{for} \quad R \lesssim 200 \text{ Gv} \\ &= 0 \qquad\qquad\qquad\qquad\quad \text{for} \quad R \gtrsim 200 \text{ Gv} \end{aligned} \tag{4.6}$$

where A is a constant, Λ is declination and $\psi_0 = 48 \pm 6°$.

4.5.2. *Theoretical interpretation*

Subramaniam and Sarabhai (1967) and Quenby and Lietti (1968) have independently suggested that a significant semi-diurnal variation would result from a particle density gradient in the plane perpendicular to the plane of ecliptic. Assuming the

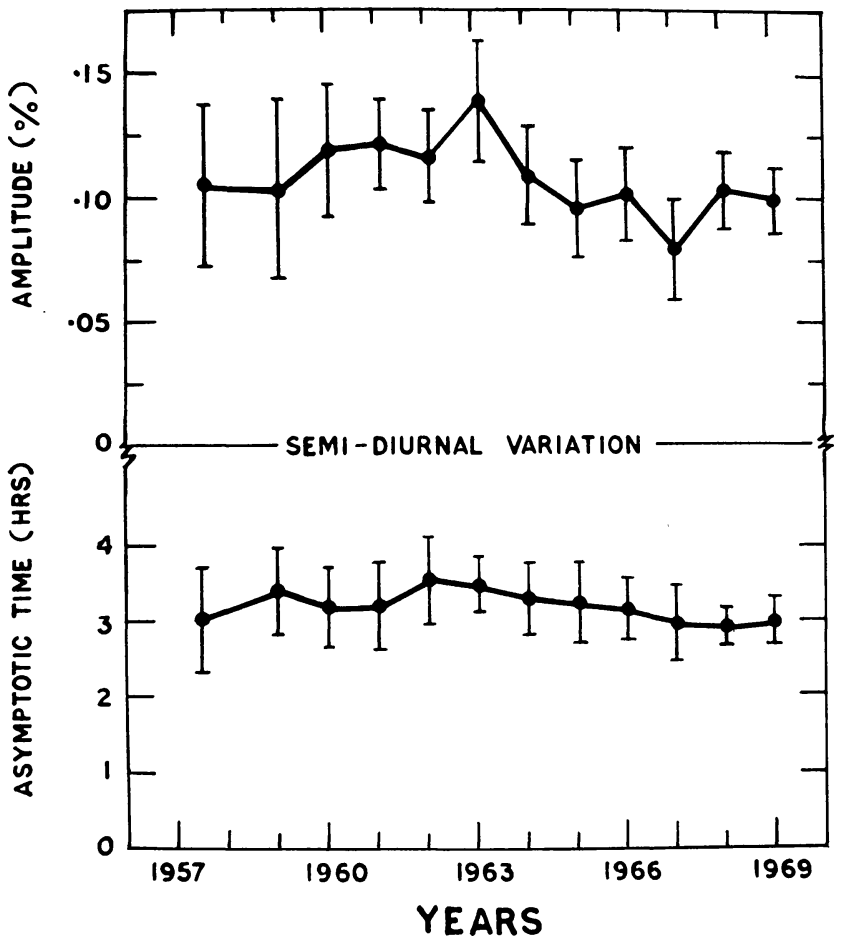

Fig. 33. The long-term variation of the amplitude and time of maximum of the semi-diurnal component during 1958–1968 (after Rao and Agrawal).

Archimedes spiral configuration for the interplanetary magnetic field and in the absence of a strong latitude dependence of magnetic irregularities, one should expect the cosmic ray particles arriving along the Sun's polar field lines to have a much easier access compared to those arriving in the equatorial plane. Consequently a significant density gradient for cosmic ray particle flux is to be expected in the plane perpendicular to the plane of ecliptic, the density increasing on both sides of the equatorial plane.

The difference between the two theoretical models proposed is mainly in the assumed nature of density gradient profile away from the equatorial plane. Lietti and Quenby have assumed a symmetrical density gradient, the density increasing uniformly above and below the solar equatorial plane, based on considerations of simple geometry of the interplanetary field and the consequent loosening of the spiral at higher heliolatitudes. Subramanian and Sarabhai, on the other hand, have adopted a density gradient profile based on the coronal observations. Both the models predict essentially similar properties for the semi-diurnal anisotropy, even though they differ in finer details which cannot be tested due to the limited statistical accuracy of the available data.

Viewing along the interplanetary magnetic field lines in the equatorial plane i.e. parallel and antiparallel to the garden hose direction, a cosmic ray monitoring instrument on Earth measures particle flux characteristic of the equatorial plane. Viewing in the perpendicular direction the detector samples particles arriving from higher heliolatitudes corresponding to the gyroradius of the particle under consideration. The higher the energy of the particles, the higher would be the heliolatitude from which they are sampled. Since any ground based cosmic ray detector scans twice a day along the field lines and twice perpendicular to the field lines, a density gradient in the perpendicular plane will introduce a semi-diurnal component in the observed cosmic ray variation. The heliolatitude of sampling being dependent on rigidity, the model readily explains the time of maximum as well as the R^{+1} dependence of semi-diurnal variation.

The general expression derived in Equation (3.8) can be used to estimate the cosmic ray flux sampled at any point r knowing the form of the unmodulated spectra and assuming the diffusion coefficient to be independent of the solar latitudinal angle. Theoretical estimates, assuming the perpendicular gradient to be of the same order as the radial density gradient in the ecliptic plane ($G \approx 12$–15% per AU) have yielded amplitudes for the semi-diurnal anisotropy in reasonable agreement with the observations.

It should be stressed here that the observed qualitative agreement between the semi-theoretical models based on latitudinal gradients and the experimental observations cannot be taken as a proof for the correctness of the model. The lack of any direct measurement of the latitudinal gradient prevents us from making accurate estimates of the semi-diurnal component that can arise from this model. Indirect estimates of the latitudinal gradient from a comparison of ground based cosmic ray measurement when the Earth's position with respect to the solar equatorial plane

changes between $\pm 7.25°$ give a value of about 6%/AU (Subramanian, 1971b) which is not adequate to explain the observed semi-diurnal variation. Furthermore, it is, in principle, possible to produce a semi-diurnal component from day to day variations of the interplanetary field. A satisfactory theoretical interpretation of the semi-diurnal component, therefore, must await till direct observations of latitudinal gradients are available and our understanding of other processes are complete.

Since the rigidity dependence of the second harmonic component essentially corresponds to the exponential modulation coefficient for the long term variation, it can be derived from the power spectral density observations of the magnetic field. As discussed in Section 2, the power spectral density at very low frequencies ($f < 5 \times 10^{-5}$ Hz corresponding to rigidities above 50 GV) falls off which might cause a reduction in the second harmonic amplitude at high energies. Further, it is also difficult to conceive the establishment of a strong density gradient beyond a distance of ~ 1 AU in the perpendicular direction, which is a distance comparable to the distance between the equatorial and the polar field lines at the orbit of the Earth. It is, therefore, reasonable to assume that particles whose rigidity is $R_{max} \gtrsim 100$–200 GV will not show significant semidiurnal anisotropy. Utilising the data from the underground semi-cubical meson telescopes at 60 MWE. Hashim *et al.* (1969) have estimated the upper cut off rigidity R_{max} to be in the range 70–100 GV which, considering the poor statistical accuracy involved in these measurements, is in good agreement with the estimates obtained by Rao and Agrawal 1970).

4.6. Daily variation on a day to day basis

Whereas the proporties of the average daily anisotropy provides a clue to the average interplanetary conditions, the cosmic ray variation on individual days has to be understood if they are to be used as probes for monitoring the interplanetary conditions on a day to day basis. Studies of daily variation on a day to day basis even before the advent of super neutron monitors (Rao and Sarabhai, 1961) showed that both the diurnal and the semi-diurnal vectors exhibit considerable variation from one day to another. The introduction of super neutron monitors has made it possible to study the day to day changes in daily variation and all its finer features with a great detail. Even though changes in the values of E_{max} or E_{min}, particle energies above or below which the corotation effect is negligible will reflect themselves as a change in the exponent of variation, large deviation from the value of $\gamma = 0$ cannot be adequately explained by azimuthal streaming and on such days, the diurnal variation must evidently be caused by other mechanisms. A word of caution is however very necessary, before one seeks a complete physical interpretation of these results. One must bear in mind the limitations imposed by the data as well as the method of deriving these quantities.

All the recent studies (Rao and Sarabhai, 1964; Sarabhai and Subramanian, 1965; Patel *et al.*, 1968) of the daily variation show that both the amplitude and the time of maximum of the diurnal as well as the semi-diurnal variation vary considerably on a day to day basis. Figure 34 shows the frequency distribution of the amplitude and phase of the diurnal and semi-diurnal variation over the years 1965–1969. The fluc-

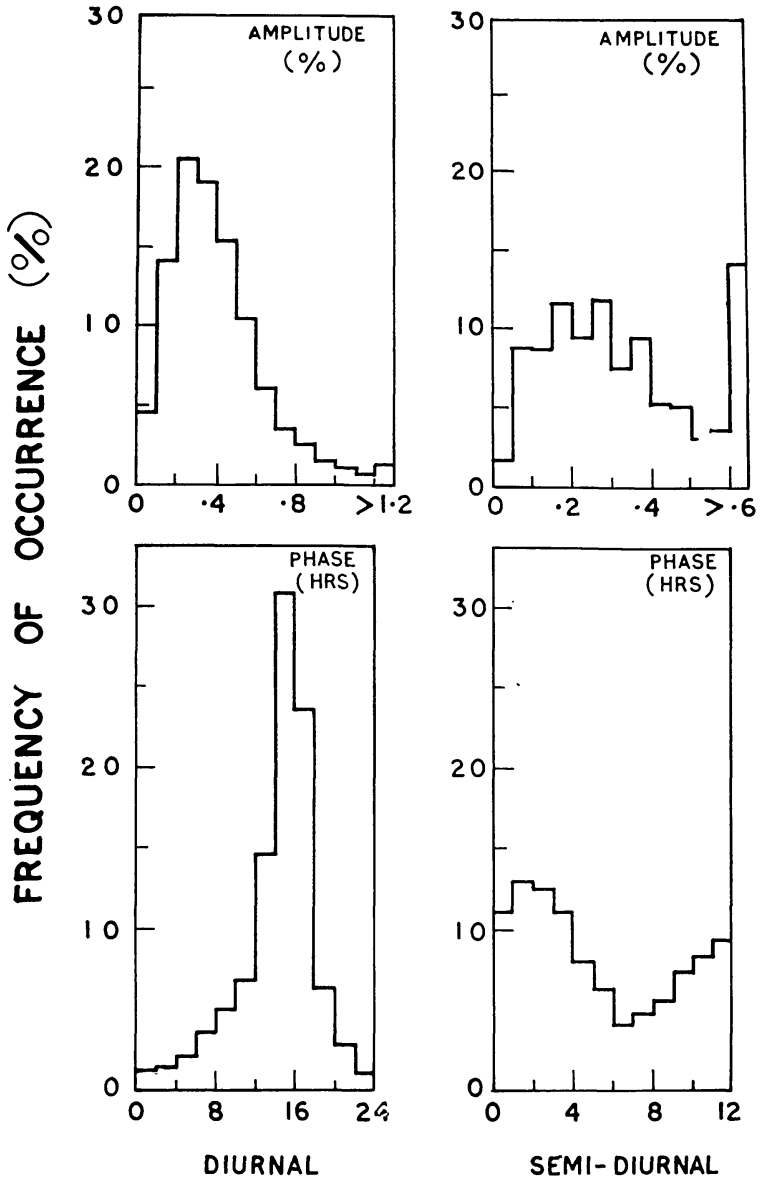

Fig. 34. Histogram showing the frequency distribution of the amplitude and the time of maximum of the diurnal and the semi-diurnal variation as observed at Deep River during 1965–1969.

tuation is far more than that can be anticipated statistically. Also note that the variability in the amplitude and time of maximum of the semi-diurnal component is much larger than that observed in the diurnal component. For example, whereas thetime of diurnal maximum is well peaked around 1600 h (1800 h in space) the semi-diurnal time of maximum shows a much broader distribution around 0100 h (0300 h in space). Further, days of large as well as small amplitudes often occur in trains. It is therefore only reasonable to seek the cause of such changes in the character of the daily variation.

Applying the method of variation coefficients to determine the energy spectrum of the diurnal variation, Patel *et al.* (1968) showed that the energy spectrum of diurnal as well as semi-diurnal variation also show a large variability on a day to day basis, the spectral exponent varying between -1 to $+2$. Figure 35 which shows the frequency

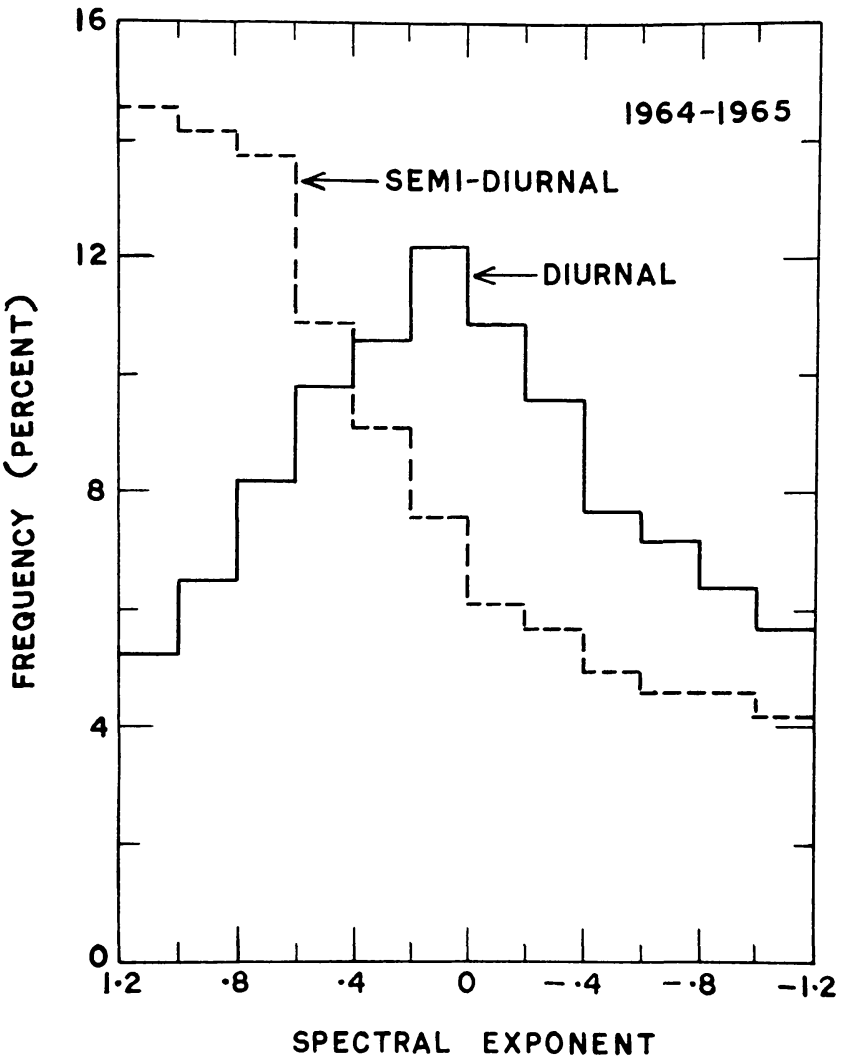

Fig. 35. The frequency distribution of the spectral exponent of variation for both the diurnal and the semi-diurnal components of cosmic radiation during 1964–1965.

distribution of the spectral exponents for both the diurnal and the semi-diurnal components for the period 1964–1965, clearly demonstrates the variability of the spectral exponents of both the components on a day to day basis. Due to the poor statistics and the nonavailability of data from equatorial stations having a high geomagnetic cut off, we must exercise caution before attaching too much importance to the magnitude of the spectral exponent on a day to day basis. Nonetheless, we observe that only on 50% of the days the diurnal ($\gamma = 0 \pm 0.4$) and the semi-diurnal ($\gamma = 1.0 \pm 0.4$) components exhibit properties that are consistent with the properties of mean anisotropy and on the rest of the days, the spectral exponents of both components show a wide variability from the mean.

Even though the variability in the amplitude of the diurnal variation can be understood in terms of the partial cancellation of the perpedicular density gradients on a day to day basis, the large variability in the spectral characteristics and the time of maximum cannot be understood by azimuthal streaming process alone. Besides the

azimuthal streaming and energy loss due to deceleration there are probably at least three more processes (Sarabhai and Subramanian, 1965) which can contribute to the anisotropy characteristics of the cosmic radiation.

4.6.1. *Streaming in Longitudinal Sector Structure.*

Additional streaming due to the difference in the solar wind velocity and in the distribution of the small scale magnetic field inhomogeneities at different helio-longitudes.

4.6.2. *Scattering at Magnetic Field Irregularities.*

If a density gradient away from the plane of ecliptic exists, scattering at magnetic field irregularities can cause a short circuiting of these latitudinal gradients. This process will produce an anisotropy with a negative spectral exponent with a minimum along the magnetic field. Depending on the pitch-angle distribution of the particles in the magnetic field, a second harmonic component can also be introduced into the observed daily variation.

4.6.3. *Latitudinal Gradients of Cosmic Ray Intensity.*

Latitudinal gradients will also produce a predominant semi-diurnal component with a positive exponent with a time of maximum aligned perpendicular to the magnetic field as described in Section 4.5. Besides, if the intensity distribution away from the plane of ecliptic has a strong N-S asymmetry a significant first harmonic component will also be introduced in the daily variation.

In Table VI, the characteristics of the diurnal and the semi-diurnal variation caused by different processes mentioned above are tabulated. Except in the case of azimuthal streaming and radial anisotropy due to deceleration, the estimates from other processes should be taken as highly tentative. Furthermore, even though some attempts have been made to isolate these effects through the observed spectral variation of daily variation on a day to day basis, the experimental observations are not really capable of yielding quantitative estimates of the effects due to individual processes.

Instead of examing the daily variation through the first and second harmonic components, several attempts have been made in the past, notably by the cosmic ray group at Ahmedabad, to examine the daily variation phenomena as a whole. One such attempt involves the examination of the time of maximum (T_{max}) and the time of minimum (T_{min}) on each day instead of its harmonic components. Just as in the case of the spectral exponent and the amplitudes and times of maxima of the harmonic components, T_{max} and T_{min} also show a large variability on a day to day basis (Rao and Sarabhai, 1964).

The advantage of considering T_{max} and T_{min} instead of the harmonic components is that they can, in general, be utilized to infer whether the anisotropy is caused by a source or a sink. One of the significant results (Rao and Sarabhai, 1964; Sarabhai and Subramanian, 1966) that emerged from a study of the T_{max} and T_{min} is that the difference ($T_{max} - T_{min}$), in general, is not 12 hr but of the order of 8 hr clearly indicating the existence of a significant semi-diurnal component. Representing in

TABLE VI

Characteristics of anisotropy of particles of energies > 1 GeV associated with different process

	Process				
	(1) Azimuthal streaming	(2) Radial anisotropy	(3) Streaming in longitudinal sector structure	(4) Scattering at irregularities	(5) Latitudinal gradient
(1) Nature of anisotropy	Diurnal	Diurnal	Diurnal	Diurnal and semi-diurnal	Diurnal and semi-diurnal
(2) Spectral Exponent					
(a) Diurnal	0	0	0	Generally negative	Positive or negative
(b) Semi-diurnal	–	–	–	?	Positive
(3) T_{max} hr	1800	1200	Variable	2100	0300 or
(4) T_{min} hr	0600	0000	Variable	0900	0900 or 2100
(5) Diurnal amplitude	0.62% maximum	0.02% maximum	–	?	Depends on density gradient
(6) Semidiurnal amplitude	–	–	–	$\sim 0.1\%$	$\sim 0.1\%$

terms of sources and sinks, T_{max} generally seems to be around 1800 h suggesting a source due to azimuthal streaming. T_{min} as seen by neutron monitors ($\sim$10 GeV) is predominantly along the garden hose direction (0900 h direction). At higher energies ($\sim$10–50 GeV), seen by meson monitors, T_{min} seems to often slip (Sarabhai *et al.*, 1965) from the garden hose to anti-garden hose direction (Figure 36) indicating that the direction of the sink is energy dependent. From an extensive analysis, Patel *et al.* (1968) conclude that $T_{max} - T_{min}$ is very nearly 12 hr on days when the diurnal variation has a zero spectral exponent and of the order 7–8 hr when the spectral exponent of diurnal variation is positive indirectly suggesting that the azimuthal streaming gives rise to a predominantly diurnal component and the latitudinal gradients are responsible for the semi-diurnal component.

An interesting feature that has been observed is that days of both abnormally large ($\gtrsim$1%) and small ($\lesssim$0.2%) amplitudes occur in trains. Figure 37 shows such examples of large and small amplitude wave trains observed by the Calgary neutron monitor. Mathews *et al.* (1969) and Hashim and Thambyahpillai (1969) have independently concluded that during many days exhibiting large amplitude waves, the anisotropy was predominantly caused by a large decrease along the garden hose direction. The possible existence of such 'sinks' in the garden hose direction have been inferred earlier by Rao and Sarabhai (1964) from their study of the distribution of times of maxima and minima. Recently attention has also been called to the wave trains with enhanced amplitudes caused by increased flux in the 18–21 hr directions (Kane, 1970; Rao *et al.*, 1971b).

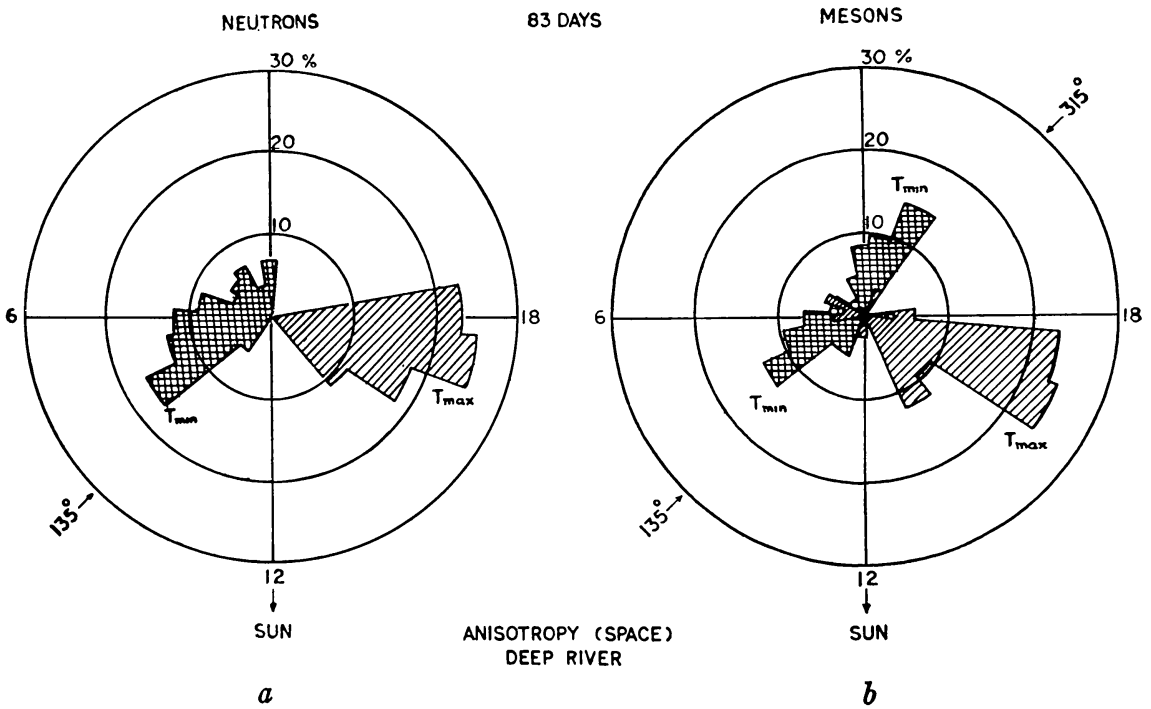

Fig. 36. Polar histogram illustrating the frequency distribution of T_{max} and T_{min}, the time of maximum and minimum of the daily variation respectively, as observed by (a) Deep River neutron monitor and (b) Deep River meson monitor (after Sarabhai and Subramanian, 1966).

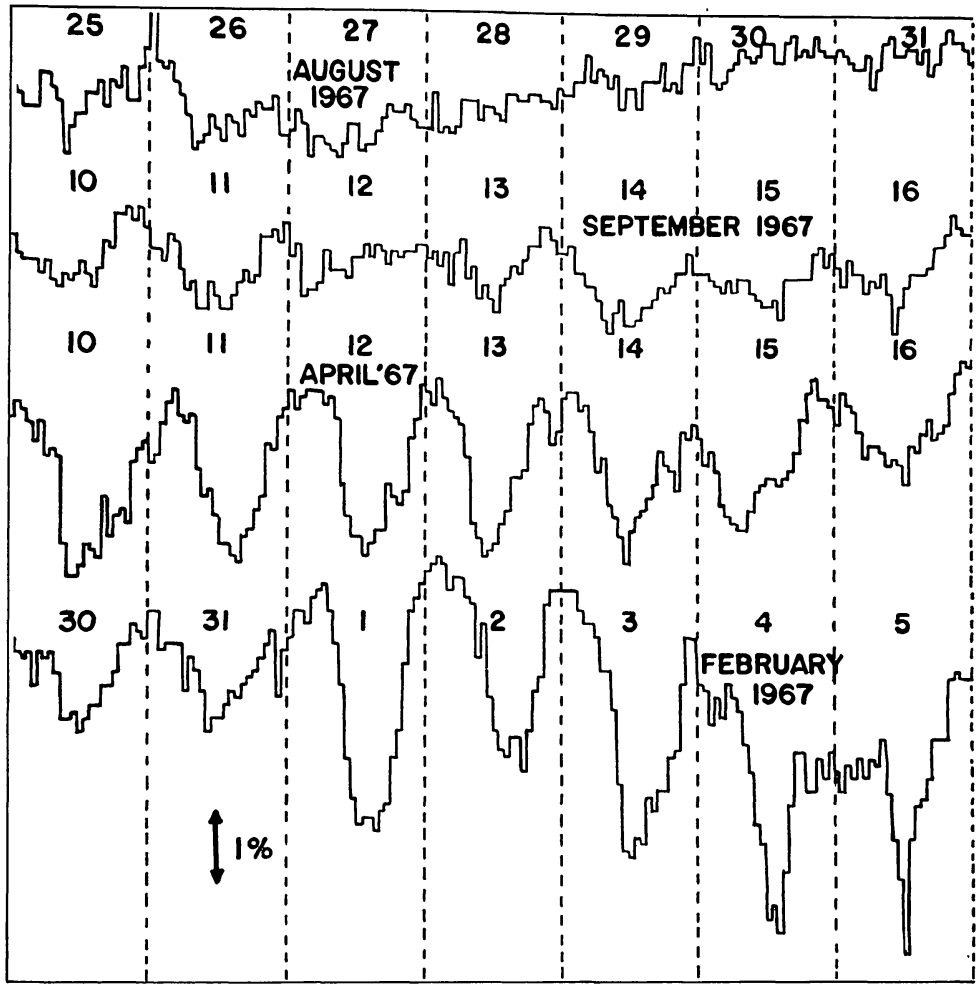

Fig. 37. The hourly values of the pressure-corrected super neutron monitor data from Calgary for different selected periods in 1967 illustrating the trains of abnormally enhanced diurnal amplitudes and trains of abnormally low amplitudes (after Mathews *et al.*, 1969).

Interpretation of daily variation in terms of sources and sinks requires rigorous analytical procedures and accurate knowledge of the background intensity over which the flux measured at each hour can be expressed as a deviation from the mean. Kane (1970) has used the difference between Alert and Deep River at each hour to study the anisotropic variation. Alert, being a high latitude station presumably reflects only the mean intensity changes related to universal time and will not record any diurnal variation. The difference curve will therefore truly represent the local time variation of the cosmic ray flux at each hour, provided no strong asymmetries in the mean intensity are present during this period. In reality, strong and highly variable asymmetries have been observed (Mathews *et al.*, 1969; Mercer *et al.*, 1971) during such periods which makes the application of difference method to study such anisotropies questionable.

An alternate method involves the construction of cosmic ray intensity profiles as a function of direction and time from the observed data from various middle latitude stations distributed at different longitudes. Using the pre-event level as the mean level,

the cosmic ray flux in each direction has been studied by a number of workers (Fenton *et al.*, 1959; Ables *et al.*, 1967; Rao *et al.*, 1971b). Since the latter method also suffers from the inherent instrumental drifts, the conclusion derived from either of the methods have to be viewed with caution.

The depletion of cosmic ray flux in the garden hose direction can be related to a possible connection of the Earth with regions of depleted cosmic ray intensity behind the rear end of a shock front which may or may not have produced a Forbush decrease at the Earth depending on the position of the shock front with respect to the Earth. Where the shock fronts do produce a Forbush decrease in the high energy cosmic radiation, large anisotropies along the garden hose direction (Fenton *et al.*, 1959) have been commonly observed. Corotating type of Forbush decrease observed at very low energies ($\sim$10 MeV) caused by recurrent active regions are known to often cause only an enhanced diurnal amplitude at high energies (McCracken *et al.*, 1966). For example, the enhanced diurnal wave train observed during 1–7 January, 1966 coincides with the corotating Forbush decrease observed (McCracken *et al.*, 1966) on Pioneer 6. Such enhanced diurnal wave trains associated with Forbush decreases which are caused by a sink along the garden hose direction have also been observed underground at 70° MWE in the muonic component (Castagnoli and Dodero, 1969).

Enhanced diurnal variation due to an excess flux coming from the $\sim$21 hr direction (Rao *et al.*, 1971b) is often observed during the later part of a Forbush decrease indicating the existence of a source in the anti-garden hose direction. Such a source can be caused by a positive density gradient following a strong convective removal of particles. Thus during the later part of the diurnal wave train, the anisotropy could be due to an excess flux from the antigarden hose direction. The establishment of such a positive density gradient at low energies ($\sim$10–50 MeV) during late times in the decay of flare events (McCracken *et al.*, 1971; Rao *et al.*, 1971a) adds strength to the basic concept proposed.

The ideas on the role of convection and field aligned diffusion which have been very successful in explaining the equilibrium anisotropies observed in the decay of flare particle events (McCracken *et al.*, 1971 and Rao *et al.*, 1971a) have recently been extended to diurnal variation by Forman and Gleeson (1970), Rao *et al.* (1971b) and Hashim *et al.* (1971) to provide a satisfactory unified model to explain both the average and day to day characteristics of diurnal variation. Figure 37a depicts such a model. Referring to flare particle anisotropy, it is seen that at early times in a flare event, the diffusive current driven by a negative cosmic ray density gradient due to solar produced particles dominates over the small convective vector resulting in a predominantly field aligned anisotropic flux. At late times, the solar cosmic ray flow is in equilibrium and is consistent with it being simply convected out by the solar wind. At very late times, the positive density gradient created by the earlier convection provides a diffusive current which when superposed upon the convective vector results in an easterly anisotropy.

In the case of diurnal anisotropy, at relativistic energies and under equilibrium conditions, when there is no net flow of cosmic radiation either into or from the solar

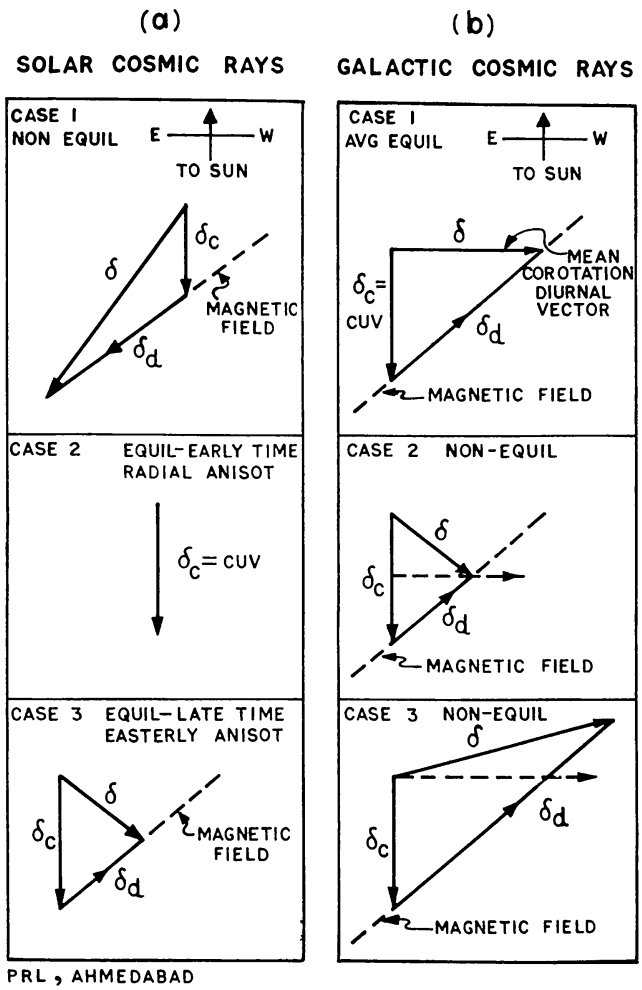

Fig. 37a. Unified model to explain the cosmic ray diurnal as well as flare anisotropy in terms of convective and diffusive flows (after Rao *et al.*, 1971b).

system, the radial convection current $S_c = \text{CUV}$ is exactly balanced by inward diffusion $K_{\|}(\partial u/\partial r)_{\|}$ resulting in an average corotational anisotropy of $\sim 0.35\%$ along the 1800 h direction. On a day to day basis, the diffusion vector need not exactly balance the convective vector. In the case when the diffusion vector is smaller, the resulting observed anisotropy would show a maximum earlier to 1800 h and in the case of enhanced diurnal variation when diffusive vector is very much greater than the convective vector, the time of maximum of the resulting diurnal variation will shift towards ~ 2100 h, the mean direction of the interplanetary magnetic field. The diffusive vector, in all cases, is aligned parallel or anti-parallel to the magnetic field.

Representing the observed diurnal vector (δ) as a summation of convective (δ_c) and diffusive anisotropy (δ_d)

$$\delta = \delta_c + \delta_d \tag{4.7}$$

Rao *et al.* (1971b) and Hashim *et al.* (1971) have shown that the diffusive anisotropy at all times, both during quiet and disturbed periods, is field aligned. Figure 37b shows the excellent alignment between the interplanetary field vector and the diffusive vector

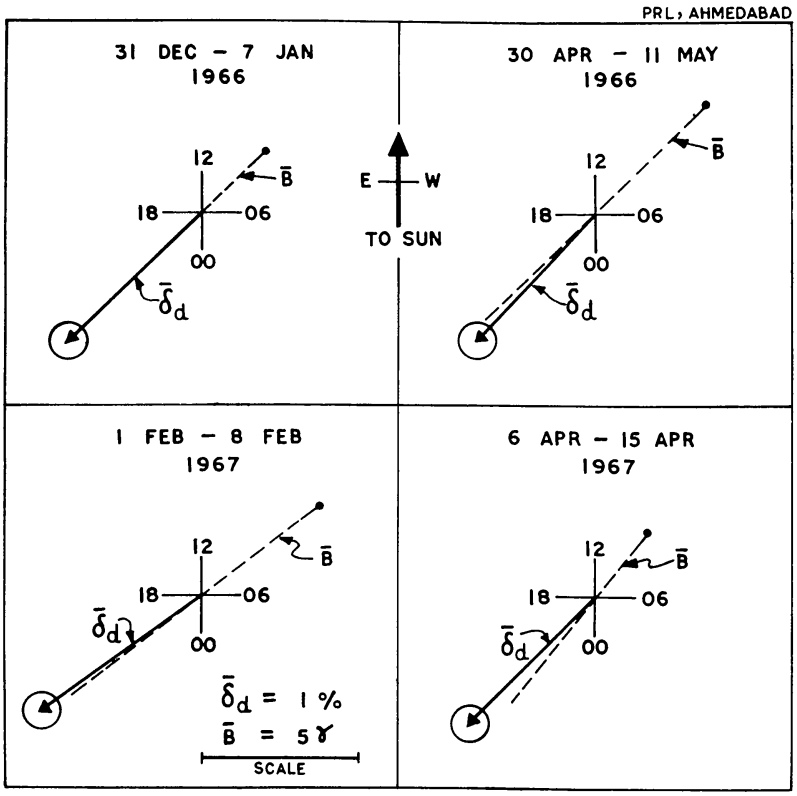

Fig. 37b. Showing the field aligned characteristic of the average diffusive anisotropy vector during four enhanced diurnal variation events (after Rao *et al.*, 1971b).

for four enhanced diurnal variation events, the interplanetary field values being obtained from Explorer 33 and 35 measurements. On an annual average basis, Rao *et al.* (1971b) have shown that the phase difference between the interplanetary field vector and the diffusive vector is only $3° \pm 2°$, indicating that $K_\perp/K_\parallel$ on an average <0.05. The observed annual average field aligned diffusive vector is consistent (Rao *et al.*, 1971b) with the observed radial density gradients of $\sim 8\%$/AU at these energies.

Even though $K_\perp \ll K_\parallel$, on an average basis, there are some days when it can become significant resulting in a reduction in anisotropy. For example, the observed small reduction in diurnal amplitude in 1965 is explainable as due to an increase in $K_\perp/K_\parallel \approx 0.2$. We believe that this new concept which attempts to explain both the average and day to day diurnal variation in terms of simple convection and diffusion is particularly attractive since the same concept has also been successful in explaining the observed low energy flare anisotropies.

5. Short Term Variations of Cosmic Ray Intensity

5.1. Introduction

In contrast to the eleven year variation of cosmic ray intensity which is well understood both theoretically and from the experimental point of view, not much progress has been made in our understanding of the short term fluctuations of cosmic ray

intensity. The short term fluctuations include 27 day variations, Forbush decreases and short period fluctuations (Periodicity of a few cycles per hour), of which the most prominent variation is undoubtedly the Forbush decrease.

Theoretically the Forbush decrease is explained as being caused by convection by the solar wind and deceleration in the expanding cloud containing disordered magnetic fields. The difference between the Forbush decreases and the eleven year cycle variation is essentially attributed to the scale size of the phenomenon. Whereas the Forbush decrease is a transient and a highly asymmetric phenomenon, the eleven year cycle is a large scale phenomenon which extends symmetrically to quite large distances (10–15 AU) from the Sun. Essentially two models for the magnetic field regime have been proposed to explain the transient decreases. Both the 'Magnetic tongue' model that has been developed by Dorman (1957) and Gold (1959) in which the magnetic field in the expanding cloud is stretched in the form of an ordered loop structure at the Earth and the 'Blast wave model' proposed by Parker (1961) in which the shock wave ahead of the plasma cloud plays a dominant role in producing transient decreases at the earth can qualitatively explain the Forbush decrease effects. Figure 38 shows the artistic sketch of the two models for the interplanetary magnetic field clouds proposed by Gold and Parker. Even though considerable amount of experi-

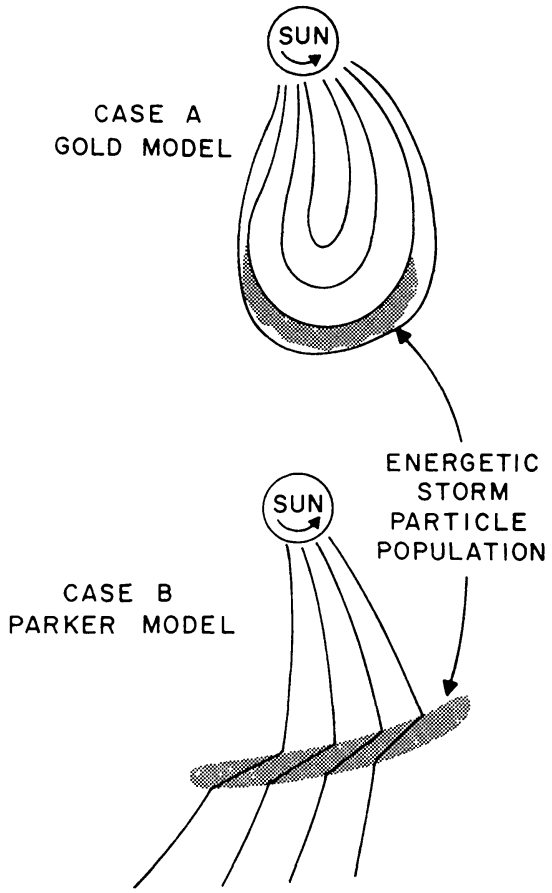

Fig. 38. Artistic sketch showing the 'Blast-wave' and 'magnetic tongue' models for the interplanetary field (after Rao *et al.*, 1967b).

mental data have been accumulated in the recent times on the existence of anisotropies and on the energy spectrum, the theoretical formulation of the problem, has progressed very little beyond what is in the original discussion by Parker (1963) which has been recently reviewed by Quenby (1967). In this article, we will only summarize the recent experimental results on the Forbush decreases and on short period variations and discuss these in terms of the known properties of the interplanetary medium.

5.2. Forbush decreases

5.2.1. *Anisotropies During Forbush Decreases*

The differences in the onset times of Forbush decreases as observed at different stations has been studied by a number of workers (Fenton *et al.*, 1959, Lockwood and Razdan, 1963; Mercer and Wilson, 1968; Ables *et al.*, 1967). All these studies have clearly indicated the existence of an initial anisotropy in the onset of the Forbush decrease aligned along a direction 30–50° W of the Earth-Sun line. On some occasions, depressed cosmic ray intensity has been observed from the garden hose direction even before the onset of the sudden commencement (Fenton *et al.*, 1959; Mathews *et al.*, 1968) magnetic storms indicating that the ground based cosmic ray instruments detected depressed intensity long before the engulfment of the Earth by the solar plasma. Figure 39 shows the plot of intensity contours as a function of both space and time, derived from various ground based monitors. As the Earth spins, each monitor traces a diagonal line on the time-direction map. The large depressions are shown by dark squares in the diagram. In all the events considered, the cosmic ray intensity depression is found to be initially limited to directions around 60° W after which the depression becomes isotropic.

The observed initial anisotropy in the Forbush decrease events has been explained (McCracken, 1962) as due to the sampling of the inner regions of the plasma cloud emitted from the Sun containing depressed cosmic ray intensity which become accessible to detectors looking along this direction. The anisotropic depression from West ceases when the detector is completely engulfed by the plasma cloud resulting in an isotropic decrease of cosmic ray intensity at the detector. The model clearly suggests that the occurrence of pre-event decreases and their direction of anisotropy will depend on the location of the parent flare, the maximum effect being observed for flares occurring on the western disk of the Sun.

The original method of displaying intensity as a function of space and time in a three dimensional diagram has been greatly improved recently by Ables *et al.* (1967) and Mercer and Wilson (1968). Figure 40 shows one such intensity contour map for the Forbush event of 17–22 January, 1966. The Forbush event when it was detected at around 2000 UT on January 19, was observed to be present only over a limited set of directions around 65° W of the Earth-Sun line which persisted upto 0900 UT on January 20. At about 1000 UT on January 20 a general decrease is observed in all directions excepting around 65–90° W of the Earth-Sun line. The anisotropic excess flux seen from a mean direction of 84° W of the Earth-Sun line for nearly 16 hr after

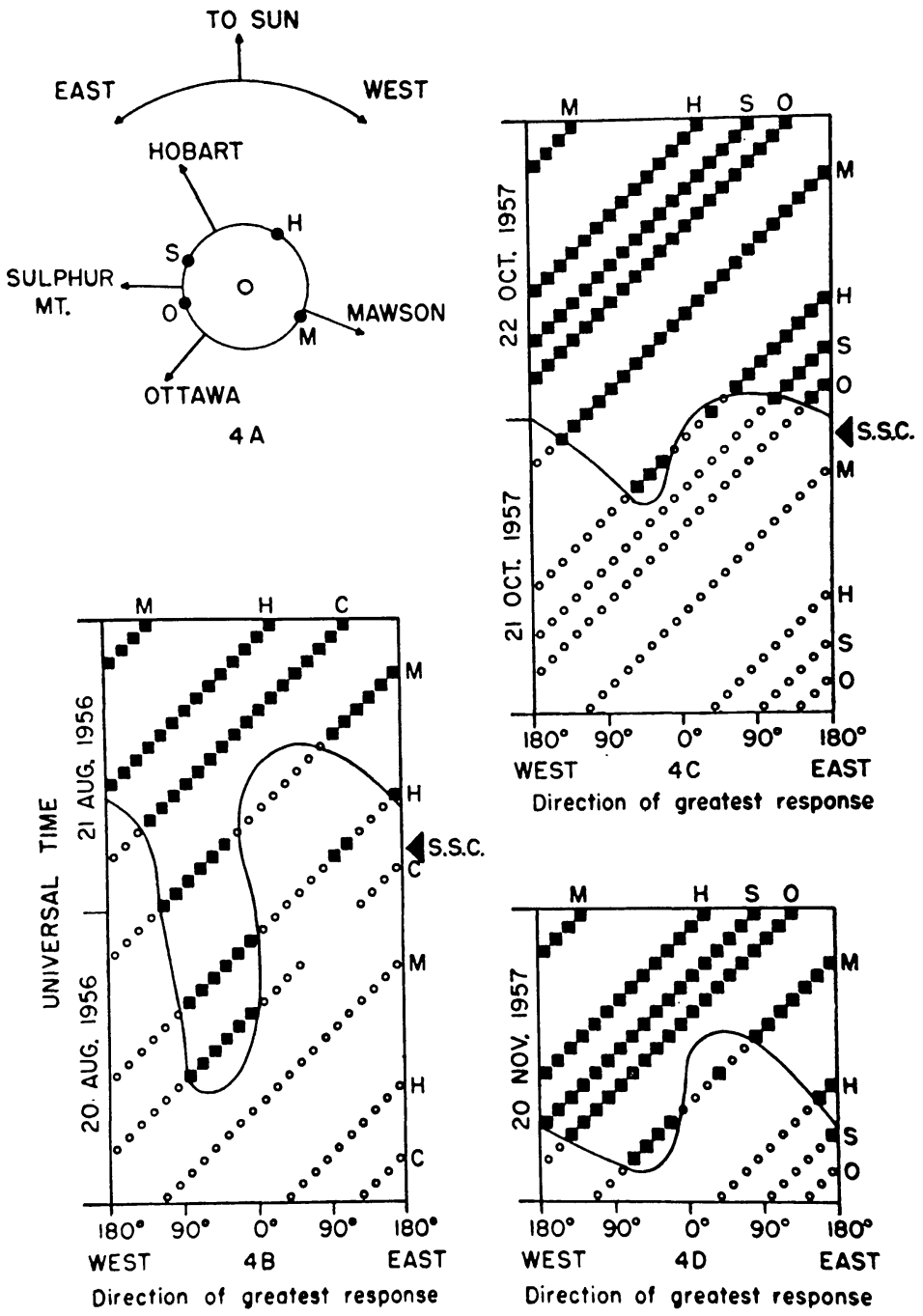

Fig. 39. Space time contours of cosmic ray intensity during some Forbush decreases. The letters H, M, S, O and C stand for neutron intensities measured at Hobart, Mawson, Sulphur Mountain, Ottawa and Climax respectively. The dark solid diamonds indicate the direction of maximum depression (after Fenton *et al.*, 1959).

its onset, coincides with the onset of an energetic storm particle event (ESP) observed on Pioneer 6 by Rao *et al.* (1967b). The close agreement between the direction of the anisotropic flux observed by neutron monitors and the direction of anisotropy in the energetic particle enhancement suggests that the excess flux seen by neutron monitors may be the high energy tail of the ESP event. The Forbush decrease becomes com-

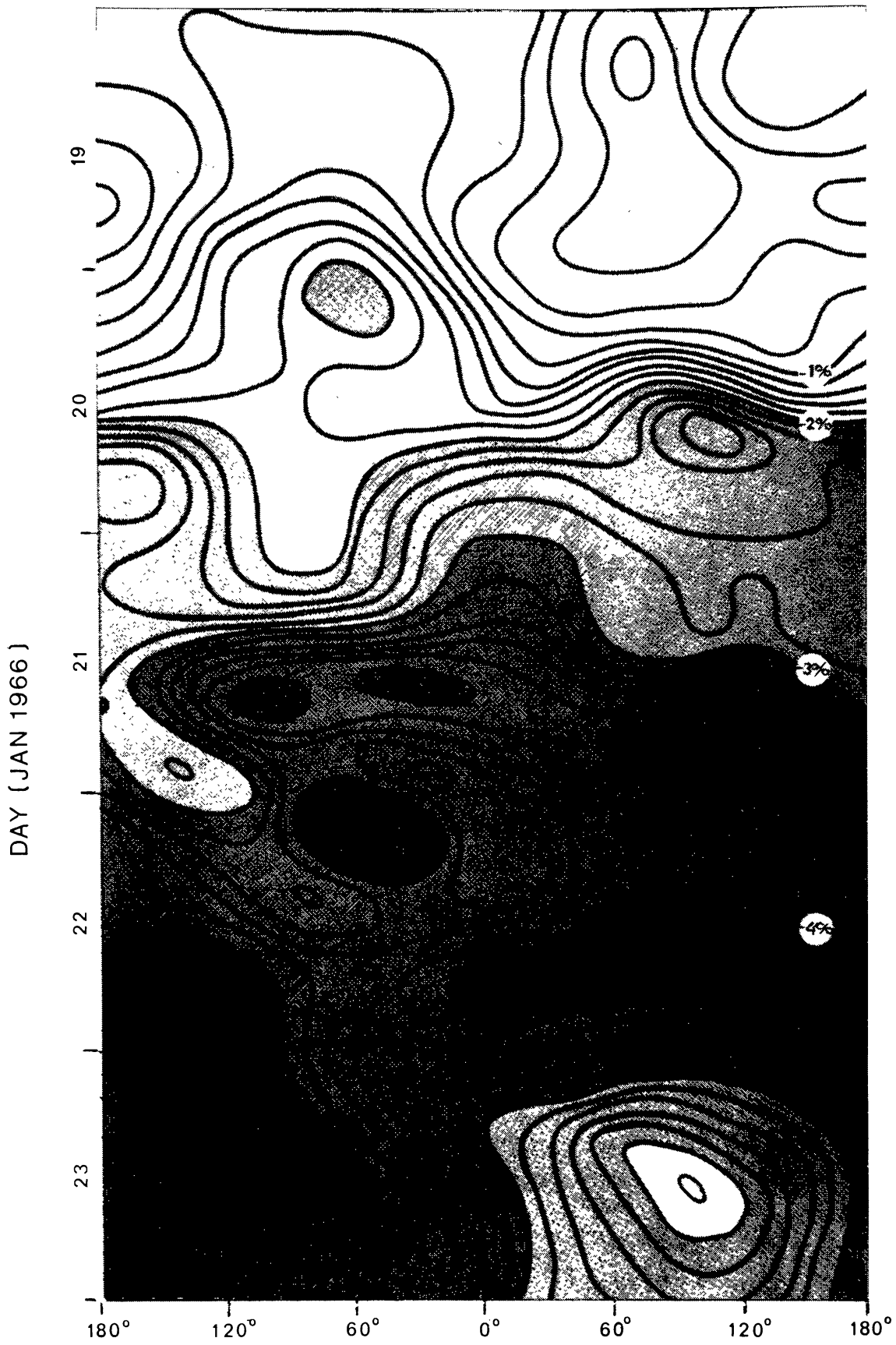

Fig. 40. High energy cosmic ray flux in space ($\gtrsim$ 1 GeV) during the Forbush event of 17–22 January, 1966 plotted as a function of direction. Equal intensity contours at 0.2% interval are drawn in the figure. The heavier the shading, the larger is the depression (after Ables *et al.*, 1967).

pletely isotropic at 1000 UT on January 21. The westerly shift in the direction of anisotropic flux to 84° W is in agreement with the expected direction of field lines in the shock front.

Besides the generally observed westerly anisotropy, Mercer and Wilson (1968) have also reported an anisotropy developing from 90° E during the onset of the Forbush event of 23 March, 1966 which is not easily explainable. Study of anisotropies during the main phase of Forbush decreases have shown (Lockwood and Razdan, 1963) that the intensity increases or decreases which are often observed to be super-imposed on the general time profile of the Forbush decrease also exhibit strong anisotropies, the decreases being predominantly observed from west of the Sun and increases from east of the Sun.

It is obvious that with the availability of high counting rate data from superneutron monitors at different locations, we can persue the study of small anisotropies in a great detail and in conjunction with the low energy cosmic ray data from spacecrafts, we can now obtain a great insight into the time profile of different anisotropies and the mechanism responsible for the same. The limiting factor, at present, is the presence of two major gaps in the worldwide coverage of neutron monitoring stations caused by the dearth of observing stations in the Atlantic and Asiatic-Pacific regions on the Earth.

5.2.2. *Ring Current Effects on Cosmic Rays*

Transient increases in cosmic radiation during the main phase of the Forbush decreases have often been attributed to the change in the cut off rigidities which may be caused by the establishment of a strong ring current (Yoshida and Wada, 1959; Kondo, 1961; Lockwood, 1960). Such a ring current, in general, tends to decrease the Earth's magnetic field thereby reducing the cut off rigidity and causing an increase in intensity. Since the storm time increase is superposed on the Forbush decrease main phase which has a large magnitude, the separation of the increase from the general decrease is often quite difficult. An important consideration to attribute transient increases to ring currents will be to show that such increases are quite insignificant at polar latitudes where the ring current will have negligible effect on the cosmic ray intensity measured at the Earth, the lower limit of rigidities for the entry of cosmic radiation at these latitudes being determined by the atmospheric cut off rather than the geomagnetic condition. Besides affecting the cut off rigidity, a strong ring current can also introduce significant changes in the asymptotic cones of acceptance of the detectors. Using the available trajectory tracing programmes (McCracken *et al.*, 1962, 1965). Yoshida *et al.* (1968) have theoretically estimated the effects of ring currents on the trajectories and on the cut off rigidities for a few typical ring current models (Akasofu *et al.*, 1962; Chapman *et al.*, 1968). They have been able to explain the often observed larger frequency of the storm time increase in the late morning and noon sectors invoking an asymmetric ring current model in conjunction with the distortion of the magnetosphere.

The difficulty in making an exact estimation of storm time increases which are

superposed on large decreases coupled with our inadequate knowledge of the ring current systems renders quantitative comparison of the theoretical model with observations difficult. However, since even a reduction in cut off rigidity from 3.0 GV to 2.0 GV can produce an increase in the cosmic ray flux by about 5% at a station like Deep River, the explanation of storm time increases invoking ring currents seems to be a reasonable hypothesis.

5.3. Energetic storm particle events

Enhancement of very low energy particles $\lesssim 10$ MeV closely associated with large Forbush decreases at the Earth have been reported by Rao *et al.* (1967b, 1968) and Bryant *et al.* (1965). These events which have been called as 'Energetic Storm Particle Events' (ESP) are characterised by a rapid rise to maximum and a fast decay with a characteristic time scale of ~ 6 hr. Figure 41 shows the energetic storm particle event associated with Forbush decrease event of 23 September 1966. From a close examination of the time profile of the ESP event, and the Forbush decrease, Rao *et al.* concluded that the onset of ESP enhancement occurred after the onset, but coinciding with the isotropic phase of the Forbush decrease. Even though a detailed discussion of the ESP event which has recently been reviewed by McCracken and Rao (1970), is beyond the purview of this review, it is interesting to note that from the steep energy spectrum and flux considerations, Rao *et al.* concluded that these particles must have

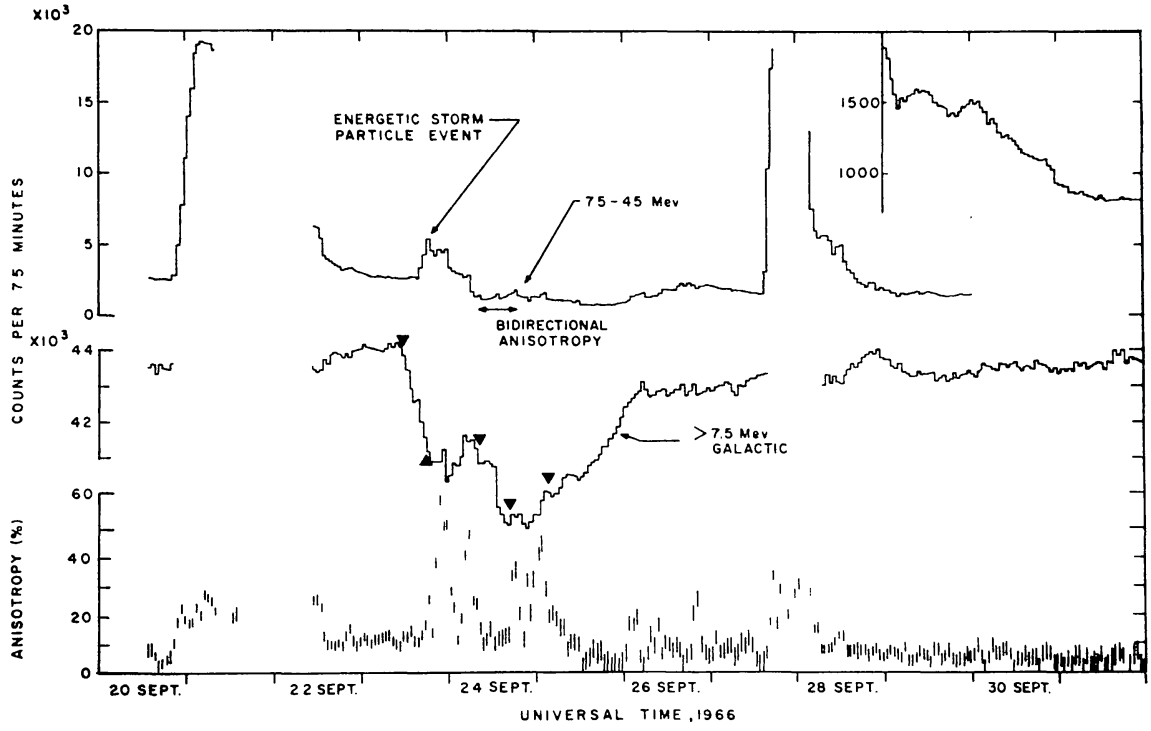

Fig. 41. The temporal variation of the cosmic ray counting rates and cosmic ray anisotropy during the interval September 20–October 1, 1966, as observed on Pioneer 7 spacecraft. The time coincidence between the energetic storm particle event and the onset of the Forbush decrease is clearly shown in the figure (after Rao *et al.*, 1967b).

been accelerated in the shock fronts associated with the blast wave that is responsible for the occurrence of Forbush decrease at Earth.

5.3.1. *Discussion of Two Field Models*

Since both magnetic tongue and the blast wave models predict similar cosmic ray effects, it has been usually found difficult to unambiguously distinguish between the two models with the available experimental data. The detailed analysis of the anisotropic conditions during a Forbush decrease of 17–22 January, 1966 (Figure 40) shows clearly that even though the initial anisotropic pre-event decrease was from a direction 65° W of the Earth-Sun line, the incidence of anisotropic flux a little later in the event was from a direction 84° W of the Earth-Sun line, characteristic of the field configuration in the shock. The ratios of cosines of the field angles across the shock front is found to be approximately 4 in agreement with the theoretical expectations from Parker's blast wave model.

Rao *et al.* (1967b, 1968) have utilised the anisotropy characteristics observed during the ESP event of 23 March, 1966, to demonstrate the validity of Parker's model. In all the ESP events observed by these authors, no evidence for the existence of bidirectional anisotropy was seen during the ESP event. Following the cessation of the ESP events, however, bidirectional anisotropies were commonly observed. If the existence of such bidirectional anisotropy is taken as indicative of the existence of the tongue (the bidirectional anisotropy being produced by the particles mirroring within the quasi-trapped region of the tongue), then a subsequent injection of particles at the Sun must immediately yield a bidirectional cosmic ray flux at the instrument, the bidirectionality becoming evident after a time comparable to the 'bounce time' for a cosmic ray particle in the magnetic field structure of the tongue.

Figure 42 shows the observed anisotropy characteristics during the complex flare event of 23–25 March, 1966. After the cessation of the ESP event, strong bidirectional anisotropy was observed from around 1100 UT on 23 March to 2200 UT implying that scattering in inhomogeneities in the interplanetary magnetic field was insufficient to destroy the anisotropy. In other words, if there were to be subsequently an injection of fresh particles from the Sun, one would expect to observe strong bidirectional anisotropies in the Gold model. Such an injection was provided by a solar flare which occurred at 2250 UT on 23 March. Figure 42 shows that not only bidirectional anisotropy was not observed during this flare, but the cosmic ray flux exhibited a strong single flux maximum from the direction of Sun for in excess of 48 hr subsequent to this flare, an observation strongly contradicting Gold's model, but quite consistent with Parker's blast wave model.

5.4. Corotating Forbush Decreases

Besides the flare associated Forbush decreases, McCracken *et al.* (1966) have recently reported the existence of recurrent corotating Forbush decreases in the low energy cosmic radiation which are related to M region magnetic storms. Figure 43 shows the time profile of cosmic ray intensity ($E \gtrsim 7.5$ MeV) observed in space in which a pro-

nounced tendency for counting rate depression to recur after 27 days is clearly seen. Practically all the recurrent Forbush decreases reported by McCracken *et al.* were associated with recurrent geomagnetic disturbances (M region geomagnetic storms) and were not associated with major solar flares on the Sun. Comparing the time profile of the same corotating Forbush decrease event which was observed during

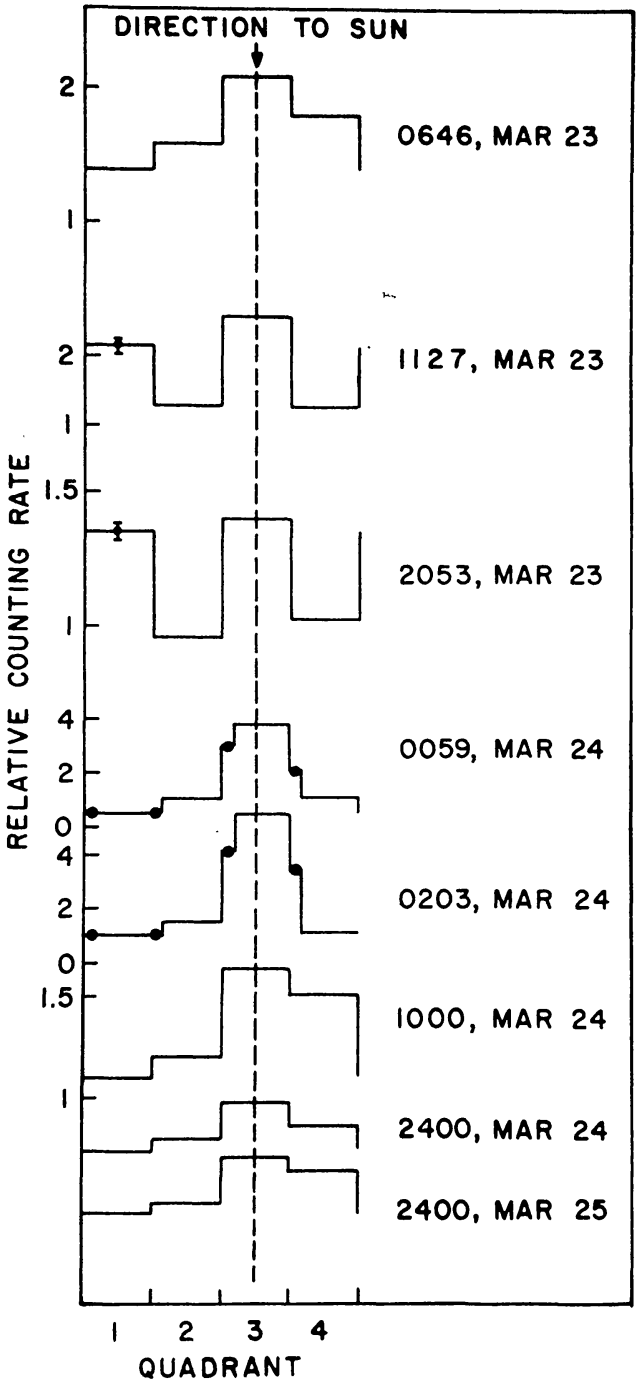

Fig. 42. Anisotropy snapshots demonstrating a bidirectional anisotropy after the cessation of the ESP event. Immediately following this, there was a fresh injection of cosmic ray particles from another flare which evidently exhibited a strong unidirectional anisotropy (after Rao *et al.*, 1967b).

20–26 August, 1966, on two spacecrafts Pioneer 6 and 7 separated in solar longitude by nearly 50°, Bukata *et al.* (1968) conclusively showed that the time delay in the onset of the event at the two spacecrafts was consistent with the expected corotation time delay of 89 hr and the onset time profile was similar at both spacecrafts indicating that the detailed structure of the standing shock was essentially invariant over the 4 day period. Both corotating and flare initiated Forbush decreases seem to exhibit similar spectral behaviour, the main difference between the two types being in onset

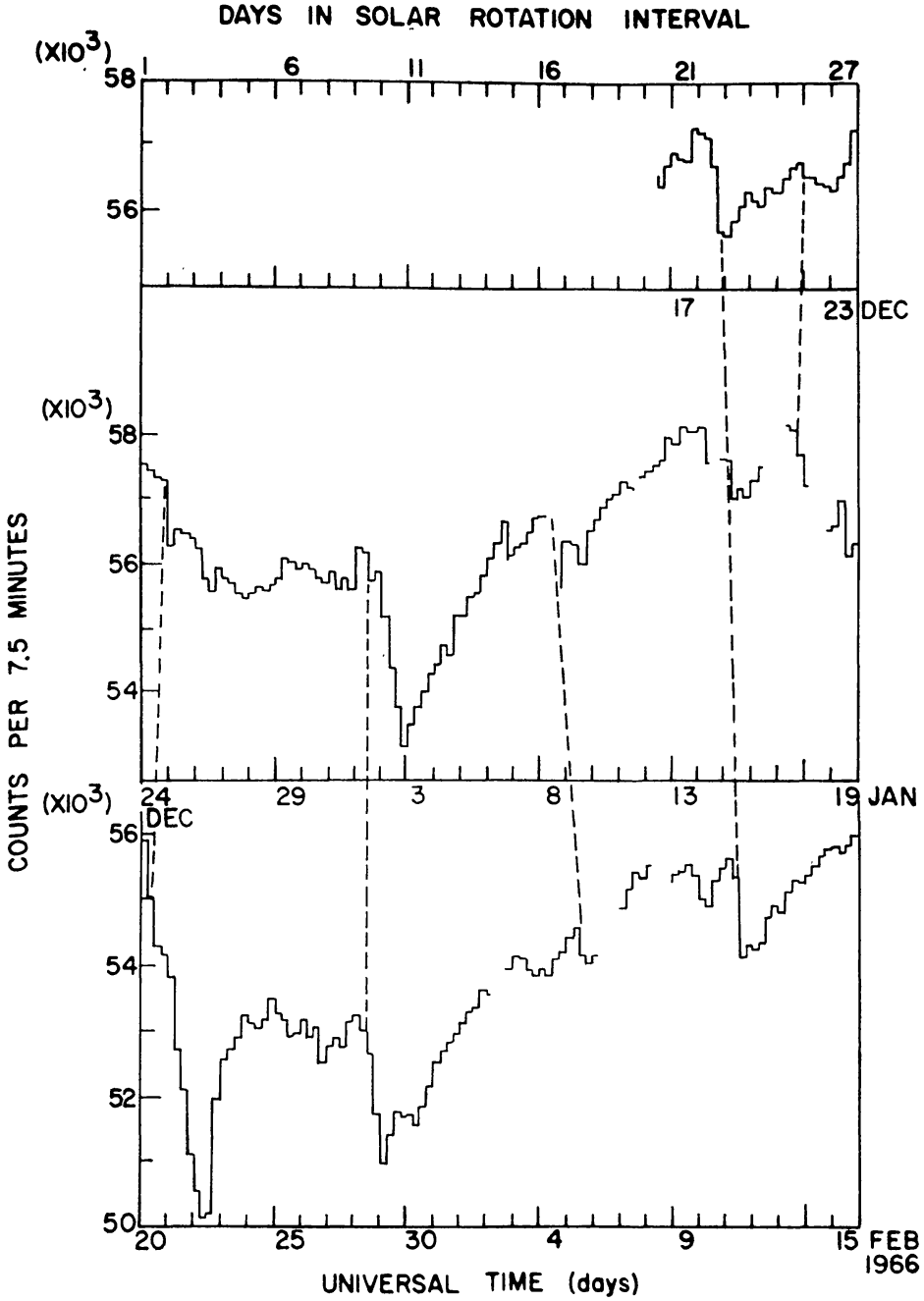

Fig. 43. The six hourly mean cosmic radiation intensity ($E \gtrsim 7.5$ MeV) as a function of time during 16 December, 1965 to 15 February, 1966 plotted on a 27 day scale. The corotating Forbush decreases are clearly marked with dotted lines (after McCracken *et al.*, 1966).

time characteristics and the azimuthal dependence of amplitude. Table VII illustrates the difference between flare-initiated and corotating Forbush decreases.

McCracken *et al.* (1966) have explained the corotating recurrent Forbush decreases as due to the exclusion of galactic cosmic ray particles by the corotating shock fronts. As Sarabhai (1963) pointed out, a standing shock wave will be created at the interface where the fast moving plasma from a 'hot spot' on the corona overtakes the

TABLE VII

Comparison of the properties of corotating and flare initiated Forbush decreases (after Bukata *et al.*, 1968).

Corotating Forbush Decrease	Flare initiated Forbush Decrease
(1) Not accompanied by solar generated cosmic rays.	Accompanied by solar cosmic rays and an energetic storm particle event (see Rao *et al.* 1967).
(2) Onset time difference at different longitudes equal to corotation time.	Simultaneous onset upto 100° off the axis of Forbush decrease.
(3) No amplitude dependence over ~ 60° of solar azimuth.	Amplitude varies by a factor of ~ 4.0 over 60° of solar azimuth.
(4) The energy dependence of both classes of event is essentially the same.	

slow moving plasma ahead of it. Figure 44 illustrates such a situation where the enhanced plasma density in the shock will cause enhanced geomagnetic activity while the enhanced magnetic field strength at the shock would inhibit the galactic cosmic ray diffusion across the magnetic lines of force. The observation of enhancement of the magnetic field by almost a factor of 4 (McCracken *et al.*, 1966) during the onset of such corotating Forbush decreases further substantiates the theoretical model proposed. With the passage of time, diffusion along the lines of force would cause the cosmic ray density at a fixed point relative to the shock to increase in a monotonic fashion. Consequently, an observer crossing from outside to inside the shock will observe a steadily decreasing cosmic ray intensity while passing through the shock and once inside the shock would observe a steadily increasing intensity with time due to longitudinal diffusion. One characteristic of this model is that the decreasing phase of the Forbush decrease is associated with the inhibition of diffusion by the stronger magnetic fields within the shock; consequently, the model predicts that the decreasing intensity phase terminates once the interplanetary magnetic field strength returns to its normal value which has also been experimentally verified by McCracken *et al.* (1966). Since a shock due to a persistent 'hot spot' on the corona would remain stationary relative to a point on the rotating Sun, an observer near Earth would observe the shock once every 27 days. In other words, each 'hot spot' on the corona would have a standing shock of its own.

The continual presence of a number of such quasi-permanent standing shock waves corotating with the Sun would, in fact, act as the vanes of a centrifugal pump thereby

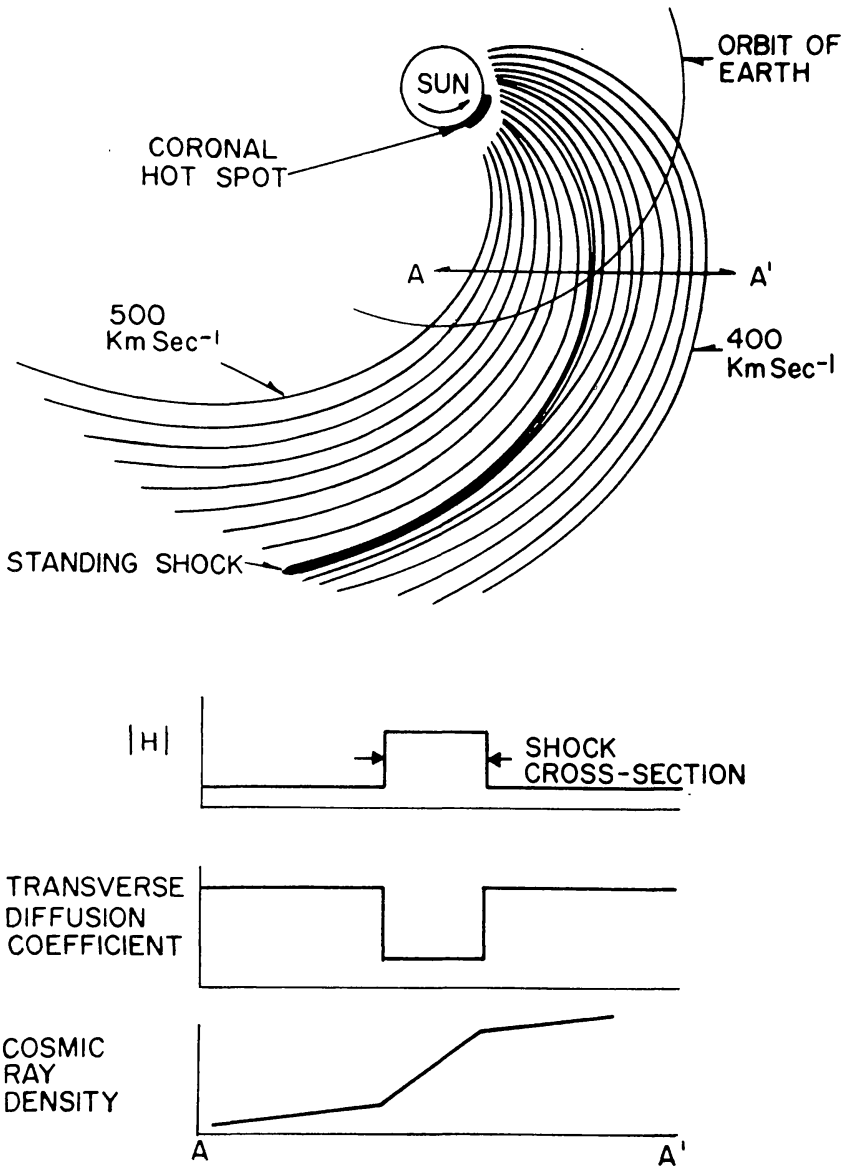

Fig. 44. A plausible model of the standing shock wave generated by a typical coronal hot-spot (after McCracken *et al.*, 1966).

establishing a radial cosmic ray density gradient. The change in frequency and intensity of such 'vanes' with the solar cycle would also contribute to the 11 yr modulation of cosmic radiation in the solar system.

Recurrent Forbush decreases observed at low energies are not often observed at high energies recorded by ground based neutron monitoring stations. The amplitude of corotating Forbush decreases, in general, being about $\sim 5\%$, the corresponding intensity changes in the high latitude neutron monitor of $\sim 1.5\%$ would be normally observed as enhanced diurnal variation. Recurrent Forbush decreases lasting for several days can also cause the so-called 27 day intensity variations observed by ground monitors.

The enhanced magnetic fields in the shock fronts associated with recurrent Forbush

decreases can, in principle, cause acceleration of very low energy particles resulting in recurrent energetic storm particle events. Recurrent proton events, persisting for several solar rotations, have been reported by a number of authors (Bryant *et al.*, 1965; Fan *et al.*, 1966a; O'Gallagher and Simpson, 1966; Krimigis and Van Allen, 1966; McDonald and Desai, 1971). Further, Rao *et al.* (1967b) have presented reasonable evidence to demonstrate the correlation between the recurrent Forbush decreases observed by them at energies $\gtrsim 7.5$ MeV and the recurrent proton events at ~ 1 MeV observed by O'Gallagher and Simpson.

5.5. Propagation of shock waves through the interplanetary medium

It has been known for some time (Gosling *et al.*, 1968) that the velocity of shock wave propagation derived from the transit time measurements are significantly higher than the actual experimental observations of plasma velocity. Thus, for example, Hundhausen (1970), from an analysis of a large amount of data finds that whereas the mean velocity of a number of shock waves calculated from the transit time between the occurrence of the flare on the Sun to the onset of the sudden commencement geomagnetic storm is about 700 km/s, the observed mean velocity from solar plasma measurements is only about 500 km/s. Vernov *et al.* (1970a) have examined a large number of Forbush decreases to investigate this problem. Considering the onset of Forbush decreases measured at different heliodistances using different spacecrafts, they have been able to convincingly demonstrate the deceleration of shock waves both with time and distance. Typically the deceleration is found to increase from about 1.5 to 40 m s^{-2} between the orbit of the Earth and that of Mars, the initial deceleration being dependent on the square of the initial velocity of plasma ejection from the Sun. Such a deceleration of the shock front will result in a gradual decrease in the Forbush decrease effect with distance.

It must be remembered that due to the fact that the onset of the Forbush decrease has been known to occur occasionally much before the onset of the sudden commencement geomagnetic storm, the velocities derived from the transit times between the onset of Forbush decrease and the flare occurrence on the Sun is not always reliable. Besides, it is also known that where successive flares occur, the velocities of subsequent shock fronts derived from transit times are significantly greater than the velocity of the first shock suggesting that the higher velocity inferred for subsequent shocks may be due to their propagation in a vacuum (rarefied medium). It is obvious that a better theoretical understanding of shock wave propagation is essential before we can claim a complete understanding of the Forbush decrease phenomena. Nevertheless, the observations of Vernov *et al.* (1970b) clearly show that the solar wind, as it propagates to large distances from the Sun, suffers severe deceleration.

5.6. Rigidity dependence of Forbush decreases and their relationship with 11 year variation

Since both the Forbush decrease and the 11 yr variation are essentially a result of the modulation of cosmic radiation in the disordered fields in the interplanetary medium,

many efforts have been directed at comparison of the rigidity dependence of Forbush decreases and 11 yr variation. If, as Singer (1958) first suggested, the 11 yr variation is only a result of the cumulative effect of many Forbush decreases, one would expect to observe the same rigidity dependence for both these effects. The analysis of the experimental observations, however, have yielded conflicting results. Whereas McDonald and Webber (1960), Webber (1962) and more recently Balasubrahmanyan and Venkatesan (1970), and Mathews *et al.* (1971) believe that the Forbush decreases and the long-term variation have essentially same rigidity dependence, McCracken (1960), Kane (1966), Bukata *et al.* (1968), Kane and Winkler (1969) and Lockwood *et al.* (1970) have concluded that the rigidity dependence of Forbush decrease is substantially different from the rigidity dependence of the 11 yr variation.

Even though, in principle, extension of analysis to lower energies utilising the spacecraft data, should yield unambiguous results, the uncertainty in the background contribution to the low energy cosmic rays from local secondaries produced in the spacecraft and the difficulty in the exact determination of the solar contribution to the low energy cosmic radiation renders the interpretation derived from using the low energy cosmic radiation difficult. From a careful analysis of data on the low energy cosmic ray observations made on Pioneer spacecraft and the data from the ground neutron monitors, Bukata *et al.* (1968) and Lockwood *et al.* (1970) have concluded that the rigidity dependence of Forbush decreases is much flatter than the rigidity dependence of 11 yr variation. The conclusion derived from an analysis of the data from different ground based monitors alone, after making adequate corrections for the long-term drifts in the monitors, are also consistent with this picture and show that whereas the 11 yr variation shows a dependence of $\sim E^{-1}$, the Forbush decreases generally show a dependence of $E^{-0.7} \sim E^{-0.8}$. We believe that the smaller scale size associated with the Forbush decrease is responsible for the difference in the rigidity dependence of the Forbush decreases and 11 yr variations of cosmic ray intensity.

A consequence of the applicability of different rigidity responses for short-term Forbush decreases is to add a considerable ambiguity in our determination of radial density gradients, which are customarily derived by comparing the spacecraft observations at different heliodistances with the normalized cosmic ray flux observed by ground based detectors. Adequate correction factors have to be applied to take into account the different rigidity response of short time modulating effects to evaluate the radial density gradients accurately.

5.7. Short period fluctuations

Subjecting the high counting rate muon data recorded at Chacaltaya, Bolivia to power spectral analysis, Dhanju and Sarabhai (1967, 1970) observed significant short period fluctuations of amplitude $\sim 0.04\%$ at about 18 and 25 cph. The observed amplitudes of these spectral peaks are not explainable in terms of changes in the cut off energy caused by corresponding changes in the geomagnetic field. The observation of similar spectral peaks in the magnetosheath magnetic field by Ness *et al.* (1966) on Pioneer 6 suggests the cause of these fluctuations to be of interplanetary origin. Even though the

average power is slightly lesser during disturbed periods, as compared to the power during quiet Sun periods, the amplitude of the spectral peak during disturbed periods is considerably enhanced. Dhanju and Sarabhai have tried to qualitatively relate the origin if these small period fluctuations to the small scale magnetic irregularities of the size 0.5×10^{-3} AU observed in the interplanetary space which themselves may be related to the granular activity on the Sun.

Even though recent attempts using both ground based monitors (Ruthberg *et al.*, 1970) and balloon borne instrumentation (Ageshin *et al.*, 1970) have confirmed the presence of systematic short period fluctuations of various periodicities of the order of a few minutes, detailed study correlating these periodicities with other solar terrestrial parameters with improved statistical accuracy are needed to understand the exact origin of these fluctuations.

Acknowledgements

The author wishes to express his grateful thanks to Dr T. Mathews and to Dr L. J. Gleeson for helpful comments and suggestions and to Mr S. P. Agrawal and Mr A. G. Ananth for their help in preparing the manuscript. The research was supported by the funds from the Department of Atomic Energy, Government of India, and funds from the grant number No. 17, Day Fund from the National Academy of Sciences, U.S.A.

References

Ables, J. G., Barouch, E., and McCracken, K. G.: 1967, *Planetary Space Sci.* **15**, 547.
Ables, J. G., McCracken, K. G., and Rao, U. R.: 1965, *Proc. Intern. Conf. on Cosmic Rays, London*, p. 208.
Ageshin, P. N., Zatsepin, V. I., Krasotkin, A. F., Rubtsov, V. I., and Charakhchayan, A. N.: 1970, *Acta. Phys. Hung.*, Sup. 29/2, 247.
Agrawal, S. P. and Rao, U. R.: 1969, *Proc. 11th Symposium on Cosmic Rays, Astrophysics, Geophysics and Elementary Particle Physics*, Delhi, India, Vol. **II**, 332.
Agrawal, S. P., Ananth, A. G., and Rao, U. R.: 1971, *Can. J. Phys.* (to be published).
Ahluwalia, H. S. and Dessler, A. J.: 1962, *Planetary Space Sci.* **9**, 195.
Ahluwalia, H. S. and Ericksen, J. H.: 1970, *Acta. Phys. Hung.*, Sup. 29/2, 139.
Ahluwalia, H. S. and McCracken, K. G.: 1966, *Space Res.* **6**, 872.
Akasofu, S. I., Cain, J. C., and Chapman, S.: 1962, *J. Geophys. Res.* **67**, 2645.
Alfvén, H.: 1949, *Phys. Rev.* **75**, 1732.
Anderson, H. R.: 1965, *Space Res.* **5**, 521.
Anderson, H. R.: 1968, *J. Geophys. Res.* **73**, 2897.
Axford, W. I.: 1965, *Planetary Space Sci*, **13**, 115.
Axford, W. I.: 1968, *Space Sci. Rev.* **8**, 331.
Badhwar, G. D., Deney, C. L., Dennis, B. R., and Kaplon, M. F.: 1968, *Can. J. Phys.* **46**, 900.
Balasubrahmanyan, V. K. and Venkatesan, D.: 1970, *Acta. Phys. Hung.*, Sup. 29/2, 327.
Balasubrahmanyan, V. K., Hagge, D. E., Ludwig, G. H., and McDonald, F. B.: 1965, *Proc. 9th Intern. Conf. on Cosmic Rays, London*, **1**, 427.
Balasubrahmanyan, V. K., Hagge, D. E., and McDonald, F. B.: 1968, *Can. J. Phys.* **46**, 887.
Bartley, W. C., Bukata, R. P., McCracken, K. G., and Rao, U. R.: 1966, *J. Geophys. Res.* **71**, 3297.
Belcher, J. W. and Davis, Jr. L.: 1971, *J. Geophys. Res.* **76**, 3534.
Belcher, J. W., Coleman, P. J. Jr., Davis, L., Jr. Jones, D. E., and Smith, E. J.: 1971, *J. Geophys. Res.* (in press).

Bercovitch, M.: 1967, *Proc. Intern. Conf. on Cosmic Rays, Calgary*, Part A, p. 269.
Bercovitch, M.: 1971, *Proc. Intern. Conf. on Cosmic Rays*, Hobart, Vol. **2**, p. 579.
Beuermann, K. C., Rice, C. J., Stone, E. C., and Vogt, R. E.: 1969, *Phys. Rev. Letters* **22**, 412.
Biswas, S., Ramadurai, S., and Sreenivasan, N.: 1966, *Phys. Rev.* **149**, 1037.
Biswas, S., Ramadurai, S., and Sreenivasan, N.: 1967, *Phys. Rev.* **150**, 1963.
Bleeker, J. A. M., Burger, J. J., Deerenberg, A. J. M., Scheepmaker, A., Swanenburg, B. N., and Tanaka, Y.: 1968, *Can. J. Phys.* **46**, 911.
Bleeker, J. A. M., Burger, J. J., Deerenberg, A. J. M., Hulst, H. C., Van de, Scheepmaker, A., Swanenburg, B. N., and Tanaka, Y.: 1969, *Acta. Phys. Hung.*, Sup. 29/1, 209.
Brandt, J. C.: 1967, *Astrophys. J.* **147**, 201.
Brunberg, E. A. and Dattner, A.: 1953, *Tellus* **5**, 135, 269.
Brunberg, E. A.: 1958, *Arkiv Fysik* **14**, 195.
Bryant, D. A., Cline, T. L., Desai, U. D., and McDonald, E. B.: 1965, *Astrophys. J.* **141**, 478.
Bukata, R. P., McCracken, K. G., and Rao, U. R.: 1968, *Can. J. Phys.* **46**, 994.
Burger, J. J. and Tanaka, Y.: 1970, *Astrophys. J.* **162**, 305.
Burlaga, L. F.: 1968, *Solar Phys.* **4**, 67.
Burlaga, L. F.: 1969, *Solar Phys.* **7**, 54.
Burlaga, L. F. and Ness, N. F.: 1968, *Can. J. Phys.* **46**, 5962.
Castagnoti, G. C. and Dodero, M. A.: 1969, *J. Geophys. Res.* **74**, 2414.
Chapman, S., Kendall, P. C., Swatztrauber, P. N., and Winde, D. W.: 1968, *Geophys. J.* **15**, 317.
Coleman, P. J., Jr.: 1966, *J. Geophys. Res.* **71**, 5509.
Coleman, P. J., Jr., Davis, L., Jr., Smith, E. J., and Jones, O. E.: 1966, *J. Geophys. Res.* **71**, 2831.
Coon, J. H.: 1968, *Earth's Particles and Fields* (ed. by B. M. McCormac), Reinhold, New York.
Dhanju, M. S. and Sarabhai, V. A.: 1967, *Phys. Rev. Letters* **19**, 252.
Dhanju, M. S. and Sarabhai, V. A.: 1970, *J. Geophys. Res.* **75**, 1795.
Dolginov, A. Z. and Toptygin, I. N.: 1966, 'Book of Abstracts', *Symposium on Solar Terrestrial Physics (Belgrade)*.
Dorman, L. I.: 1957, *Cosmic Ray Variations*, State Publ. House, Moscow.
Dorman, L. I.: 1963, *Progress in Elementary Particles and Cosmic Rays Physics*, North-Holland Publ. Co., Amsterdam.
Duggal, S. P., Forbush, S. E., and Pomerantz, M. A.: 1970, *J. Geophys. Res.* **75**, 1150.
Duggal, S. P., Nagashima, K., and Pomerantz, M. A.: 1961, *J. Geophys. Res.* **66**, 1970.
Duggal, S. P., Pomerantz, M. A., and Forbush, S. E.: 1967, *Nature* **214**, 154.
Ehmert, A.: 1960, *Proc. 6th Intern. Cosmic Rays Conf. Moscov* **3**, 142.
Elliot, H. and Dolbear, D. W. N.: 1951, *J. Atmospheric Terrest. Phys.* **1**, 215.
Fan, C. Y., Gloeckler, G., and Simpson, J. A.: 1966a, *Phys. Rev. Letters* **17**, 329.
Fan, C. Y., Gloeckler, G., and Simpson, J. A.: 1966b, *Proc. Conf. Cosmic Rays, London*, 109.
Fan, C. Y., Gloeckler, G., McKibben, B., Pyle, K. B., and Simpson, J. A.: 1968, *Can. J. Phys.* **46**, 498.
Fan, C. Y., Gloeckler, G., McKibben, R. B., and Simpson, J. A.: 1970, *Acta Phys. Hung.*, Sup. 29/2, 261.
Fenton, A. G., McCracken, K. G., Rose, D. C., and Wilson, B. G.: 1959, *Can. J. Phys.* **37**, 970.
Fisk, L. A.: 1970, Preprint, G.S.F.C., Maryland.
Fisk, L. A.: 1971, *J. Geophys. Res.* **76**, 221.
Fisk, L. A. and Axford, W. I.: 1968, *J. Geophys. Res.* **73**, 4396.
Fisk, L. A. and Axford, W. I.: 1969, *J. Geophys. Res.* **74**, 4973.
Fisk, L. A. and Axford, W. I.: 1970, *Solar Phys.* **12**, 304.
Fisk, L. A., Gleeson, L., and Axford, W. I.: 1970, *Acta Phys. Hung.*, Sup. 29/2, 105.
Forbush, S. E.: 1958, *J. Geophys. Res.* **63**, 651.
Forbush, S. E.: 1969, *J. Geophys. Res.* **74**, 3451.
Forman, M. A.: 1970a, *Planetary Space Sci.* **18**, 25.
Forman, M. A.: 1970b, *J. Geophys. Res.* **75**, 3147.
Forman, M. A.: 1971, *Proc. Intern. Conf. on Cosmic Rays*, Hobart, Vol. **2**, p. 575.
Forman, M. A. and Gleeson, L. J.: 1970, Preprint, Monash Univ.
Frier, P. S. and Waddington, C. J.: 1965, *Space Sci. Rev.* **4**, 313.
Fujii, Z., Fujimoto, K., Ueno, H., Kondo, I., and Nagashima, K.: 1970, *Acta. Phys. Hung.*, Sup. 29/2, 83.
Gall, R.: 1968, *J. Geophys. Res.* **73**, 4400.

Gleeson, L. J.: 1969, *Planetary Space Sci.* **17**, 31.
Gleeson, L. J.: 1971, *Astrophys. Space Sci.* **10**, 471.
Gleeson, L. J. and Axford, W. I.: 1967, *Astrophys. J.* **149**, L 115.
Gleeson, L. J. and Axford, W. I.: 1968a, *Can. J. Phys.* **46**, 937.
Gleeson, L. J. and Axford, W. I.: 1968b, *Astrophys. J.* **151**, 1011.
Gleeson, L. J., Krimigis, S. M., and Axford, W. I.: 1970, Preprint, Johns Hopkins Univ.
Gleeson, L. J. and Urch, I. H.: 1971, *Astrophys. Space Sci.* **11**, 288.
Gloeckler, G. and Jokipii, J. R.: 1966, *Phys. Rev. Letters* **17**, 203.
Gloeckler, G. and Jokipii, J. R.: 1967, *Astrophys. J.* **148**, L41.
Gold, T.: 1959, *J. Geophys. Res.* **64**, 1665.
Goldstein, M. L., Fisk, L. A., and Ramaty, R.: 1970, *Phys. Rev. Letters* **25**, 832.
Gosling, J. T., Asbridge, T. R., Bame, S. J., Hundhausen, A. J., and Strong, I. B.: 1968, *J. Geophys. Res.* **73**, 43.
Gosling, J. T., Hansen, R. T., and Bame, S. J.: 1971, *J. Geophys. Res.* **76**, 1811.
Gringauz, K. I., Kurt, V. G., Moroz, V. I., and Shklovsky, I. S.: 1960, *Dokl. Akad. Nauk S.S.S.R.* **132**, 1062.
Hashim, A., Peacock, D. S., Quenby, J. J., and Thambyahpillai, T.: 1969, *Planetary Space Sci.* **17**, 1749.
Hashim, A. and Thambyahpillai, T.: 1969, *Planetary Space Sci.* **17**, 1879.
Hashim, A., Bercovitch, M., and Steljes, J. F.: 1971, *Solar Phys.* (in press).
Hatton, C. J., Marsden, P. L., and Willets, A.: 1963, *Proc. Intern. Conf. on Cosmic Rays, Jaipur* **2**, 381.
Hatton, C. J., Marsden, P. L., and Willets, A.: 1966, *J. Geophys. Res.* **71**, 1481.
Holzer, R. E., McLeod, M., and Smith, E. J.: 1966, *J. Geophys. Res.* **71**, 1481.
Hsieh, K. C.: 1969, Rep. EFI-69-26, Univ. of Chicago.
Hsieh, K. C.: 1970, *Astrophys. J.* **159**, 61.
Hundhausen, A. J.: 1970, *Rev. Geophys.* **8**, 729.
Jacklyn, R. M.: 1965, *Nuovo Cimento* **36**, 1135.
Jacklyn, R. M. and Humble, J. E.: 1965, *Australian J. Phys.* **18**, 451.
Jacklyn, R. M. and Vrana, A.: 1969, *Proc. Astron. Soc. Australia* **1**, 1.
Jacklyn, R. M., Duggal, S. P., and Pomerantz, M. A.: 1970, *Acta Phys. Hung.*, Sup. 29/2, 47.
Jokipii, J. R.: 1971, *Rev. Geophys. Space Phys.* **9**, 27.
Jokipii, J. R.: 1966, *Astrophys. J.* **146**, 480.
Jokipii, J. R.: 1967, *Astrophys. J.* **149**, 405.
Jokipii, J. R.: 1968, *Astrophys. J.* **152**, 671.
Jokipii, J. R.: 1971, *Rev. Geophys. Space Phys.* **9**, 27.
Jokipii, J. R. and Coleman, Jr. ,P. J.: 1968, *J. Geophys. Res.* **73**, 5495.
Jokipii, J. R. and Parker, E. N.: 1967, *Planetary Space Sci.* **15**, 1375.
Jokipii, J. R. and Parker, E. N.: 1968a, *Phys. Rev. Letters* **21**, 44.
Jokipii, J. R. and Parker, E. N.: 1968b, *J. Geophys. Res.* **73**, 3367.
Jokipii, J. R. and Parker, E. N.: 1969, *Astrophys. J.* **155**, 777.
Jokipii, J. R. and Parker, E. N.: 1970, *Astrophys. J.* **160**, 735.
Kane, R. P.: 1966, *Nuovo Cimento* **45**, 132.
Kane, R. P.: 1970, *J. Geophys. Res.* **75**, 4350.
Kane, S. R. and Winckler, J. R.: 1969, *J. Geophys. Res.* **74**, 6247.
Katzman, J. and Venkatesan, D.: 1960, *Can. J. Phys.* **38**, 1011.
Kinsey, J. H.: 1970, *Phys. Rev. Letters* **24**, 246.
Kondo, I.: 1961, *Rept. Ionosphere Res. Japan* **15**, 319.
Krimigis, S. M.: 1968, *Can. J. Phys.* **46**, S976.
Krimigis, S. M.: 1970, *Acta. Phys. Hung.*, 29/2, 125.
Krimigis, S. M. and Van Allen, J. A.: 1966, *Phys. Rev. Letters* **15**, 419.
Krimigis, S. M. and Venkatesan, D.: 1969, *J. Geophys. Res.* **74**, 4129.
Lezniak, J. A. and Webber, W. R.: 1969, *Proc. Midwest Conf. Baton Rouge.*
Lezniak, J. A. and Webber, W. R.: 1970, *Acta. Phys. Hung.*, Sup. 29/2, 111.
Lezniak, J. A. and Webber, W. R.: 1971, *J. Geophys. Res.* **76**, 1605.
L'Heureux, J. and Meyer, P.: 1968, *Can. J. Phys.* **46**, 892.
L'Heureux, J., Meyer, P., Verma, S. D., and Vogt, R.: 1968, *Can. J. Phys.* **46**, 896.
Lietti, B. and Quenby, J. J.: 1968, *Can. J. Phys.* **46**, 942.
Lockwood, J. A.: 1960, *J. Geophys. Res.* **65**, 27.

Lockwood, J. A. and Razdan, H.: 1963, *J. Geophys. Res.* **68**, 1593.
Lockwood, J. A., Lezniak, J., Singh, P., and Webber, W. R.: 1970, *J. Geophys. Res.* **75**, 6885.
Mathews, T., Mercer, J. B., and Venkatesan, D.: 1968, *Can. J. Phys.* **46**, 854.
Mathews, T., Stoker, P. H., and Wilson, B. G.: 1971, *Planetary Space Sci.* (in press).
Mathews, T., Venkatesan, D., and Wilson, B. G.: 1969, *J. Geophys. Res.* **74**, 1218.
Mathews, T., Quenby, J., and Sean, J.: 1971, *Nature* **229**, 246.
McCracken, K. G.: 1960, *Phys. Rev. Letters* **117**, 1570.
McCracken, K. G.: 1962, *J. Geophys. Res.* **67**, 447.
McCracken, K. G. and Ness, N. F.; 1966, *J. Geophys. Res.* **71**, 3315.
McCracken, K. G. and Rao, U. R.: 1965, *Proc. Intern. Conf. on Cosmic Rays, London* **1**, 213.
McCracken, K. G. and Rao, U. R.: 1966, *Planetary Space Sci.* **14**, 649.
McCracken, K. G. and Rao, U. R.: 1970, *Space Sci. Rev.* **11**, 155.
McCracken, K. G., Rao, U. R., and Bukata, R. P.: 1966, *Phys. Rev. Letters* **17**, 928.
McCracken, K. G., Rao, U. R., and Bukata, R. P.: 1967, *J. Geophys. Res.* **72**, 4293.
McCracken, K. G., Rao, U. R., Bukata, R. P., and Keath, E.: 1971, *Solar Phys.* **18**, 100.
McCracken, K. G., Rao, U. R., Fowler, B. C., Shea, M. A., 1962, Tech. Report 77, Mass. Inst. Technology.
McCracken, K. G., Rao, U. R., Fowler, B. C., Shea, M. A., and Smart, D. C., 1965, IQSY Instruction Manual No. 10.
McDonald, F. B. and Desai, U. D.: 1971, *J. Geophys. Res.* **76**, 808.
McDonald, F. B. and Webber, W. R.: 1960, *J. Geophys. Res.* **65**, 767.
Mercer, J. B. and Wilson, B. C.: 1968, *Can. J. Phys.* **46**, 849.
Mercer, J. B., Barker, D. N. H., Griffiths, W. K., and Hatton, C. J.: 1971, *Proc. Intern. Conf. on Cosmic Rays*, Hobart, Vol. 2, p. 717.
Michel, F. C.: 1965, *Planetary Space Sci.* **13**, 753.
Michel, F. C.: 1967, *J. Geophys. Res.* **72**, 1917.
Mori, S.: 1968, *Nuovo Cimento* **58**, 1.
Morrison, P.: 1956, Phys. Rev. 101, 1397.
Nagashima, K.: 1951, *J. Geomagn. Geoelect* **3**, 100.
Nagashima, K., Duggal, S. P., and Pomerantz, M. A.: 1966, *Planetary Space Sci.* **14**, 177.
Neher, H. V.: 1967, *J. Geophys. Res.* **72**, 1527.
Neher, H. V. and Anderson, H. B.: 1964, *J. Geophys. Res.* **69**, 1911.
Ness, N. F. and Wilcox, J. M.: 1966, *Astrophys. J.* **143**, 13.
Ness, N. F., Scearce, C. S., and Cantarano, S.: 1966, *J. Geophys. Res.* **71**, 3305.
Ness, N. F., Scearce, C. S., and Seek, J. B.: 1964, *J. Geophys. Res.* **69**, 3531.
Neugebauer, M. and Snyder, C. W.: 1966, *J. Geophys. Res.* **71**, 4469.
O'Gallagher, J. J.: 1967, *Astrophys. J.* **150**, 675.
O'Gallagher, J. J.: 1968, *Can. J. Phys.* **46**, 946.
O'Gallagher, J. J.: 1969, *J. Geophys. Res.* **74**, 43.
O'Gallagher, J. J. and Simpson, J. A.: 1966, *Phys. Rev. Letters* **16**, 1212.
O'Gallagher, J. J. and Simpson, J. A.: 1967, *Astrophys. J.* **147**, 819.
Ormes, J. F. and Webber, W. R.: 1968, *J. Geophys. Res.* **73**, 4231.
Pai, L. G., Bridge, H. S., Lynn, E. F., and Egidi, A.: 1967, *Trans. Am. Geophys. Union* **48**, 176.
Parker, E. N.: 1958, *Phys. Rev.* **110**, 1445.
Parker, E. N.: 1961, *Astrophys. J.* **133**, 1014.
Parker, E. N.: 1963, *Interplanetary Dynamical Processes*, Interscience, New York.
Parker, E. N.: 1964, *Planetary Space Sci.* **12**, 735.
Parker, E. N.: 1965, *Planetary Space Sci.* **13**, 9.
Parker, E. N.: 1966, *Planetary Space Sci.* **14**, 371.
Parker, E. N.: 1967, *Planetary Space Sci.* **15**, 1723.
Parker, E. N.: 1969, *Space Sci. Rev.* **9**, 325.
Patel, D., Sarabhai, V., and Subramanian, G.: 1968, *Planetary Space Sci.* **16**, 1131.
Pathak, P. N. and Sarabhai, V.: 1970, *Planetary Space Sci.* **18**, 81.
Peacock, D. S.: 1970, *Acta. Phys. Hung.*, Sup. 29/2, 189.
Pomerantz, M. A. and Duggal, S. P.: 1971, *Space Sci. Rev.* **12**, 75.
Price, P. B., Fleischer, R. L., Peterson, D. D., O'Cealleigh, G., O'Sullivan, D., and Thompson, A.: 1968, *Phys. Rev. Letters* **21**, 630.

Quenby, J. J.: 1965, *Proc. 9th Intern. Conf, on Kosmic Rays* **1**, 3.
Quenby, J. J.: 1967, *Handbuch der Physik* (ed. by K. Sitte), p. 310.
Quenby, J. J. and Lietti, B.: 1968, *Planetary Space Sci.* **16**, 1209.
Ramadurai, S.: 1970, Ph. D. Thesis, submitted to Bombay Univ.
Ramaty, R. and Lingenfelter, R. E.: 1968, *Can. J. Phys.* **46**, 627.
Rao, U. R. and Agrawal, S. P.: 1970, *J. Geophys. Res.* **75**, 2391.
Rao, U. R. and Sarabhai, V.: 1961, *Proc. Roy. Soc. (London)* **263A**, 118.
Rao, U. R. and Sarabhai, V.: 1964, *Planetary Space Sci.* **12**, 1055.
Rao, U. R., McCracken, K. G., Allum, F. R., Palmeira, R. A. R., and Palmer, I.: 1971a; *Solar Phys.* (in press).
Rao, U. R., Agrawal, S. P., and Ananth, A. G.: 1971b, *Solar Phys.* (in press).
Rao, U. R., McCracken, K. G., and Bartley, W. C.: 1967a, *J. Geophys. Res.* **72**, 4343.
Rao, U. R., McCracken, K. G., and Bukata, R. P.: 1967b, *J. Geophys. Res.* **72**, 4325.
Rao, U. R., McCracken, K. G., and Bukata, R. P.: 1968, *Can. J. Phys.* **46**, 844.
Rao, U. R., McCracken, K. G., and Venkatesan, D.: 1963, *J. Geophys. Res.* **68**, 345.
Reid, G. C. and Sauer, H. H.: 1967, *J. Geophys. Res.* **72**, 197.
Rockstroh, J. and Webber, W. R.: 1969, Res. Rept. CR 126, Univ. of Minnesota.
Roeloff, E. C.: 1965, Ph.D. Thesis, Univ. of Calif., Berkeley.
Rossi, B. and Olbert, S.: 1970, *Introduction to Physics of Space*, McGraw Hill.
Ruthberg, S., Dyring, E., Lindgren, S., Sporee, B., Ostman, B., and Tanskanen, P.: 1970, *Acta Phys. Hung.* 29/2, 241.
Sarabhai, V.: 1963, *J. Geophys. Res.* **68**, 1555.
Sarabhai, V. and Subramanian, G.: 1965, *Proc. Intern. Conf. on Cosmic Rays, London* **1**, 170.
Sarabhai, V and Subramanian, G.: 1966, *Astrophys. J.* **14**, 206.
Sarabhai, V., Desai, U. D., and Venkatesan, D.: 1954, *Phys. Rev.* **96**, 2213.
Sarabhai, V., Pai, G. L., and Wada, M.: 1965, *Nature* **206**, 703.
Sari, J. W. and Ness, N. F.: 1969, *Solar Phys.* **8**, 155.
Severny, A., Wilcox, J. M., Scherrer, P. H., and Colburn, D. S.: 1971, *Solar Phys.* (in press).
Shea, M. A., Smart, D. F., McCracken, K. G., and Rao, U. R.: 1968, AFRL Special Report No. 71.
Simnett, G. M. and McDonald, F. B.: 1968, *Bull. Acad. Polon. Sci.* **13**, 1460.
Simpson, J. A.: 1963, *Proc. Intern. Conf. on Cosmic Rays, Jaipur* **2**, 155.
Simpson, J. A. and Wang, J. R.: 1967, *Astrophys. J. Letters* **149**, 73.
Simpson, J. A. and Wang, J. R., 1970, *Astrophys. J.* **161**, 265.
Simpson, J. A., Fan, C. Y., and Meyer, P.: 1962, *J. Phys. Soc. Japan* **17**, Suppl. A-II, 505.
Singer, S. F.: 1958, *Nuovo Cimento Suppl. Ser. X* **8**, 1961.
Singer, S. F., Laster, H., and Lencheck, A. M.: 1962, *J. Phys. Soc. Japan* **17**, Suppl. A-II, 583.
Siscoe, G. L., Davis, Jr., L., Coleman, Jr., P. J., Smith, E. J., and Jones, D. E.: 1968, *J. Geophys. Res.* **73**, 61.
Skadron, G.: 1967, Tech. Report No. 678, Univ. of Maryland.
Snyder, C. W., Neugebauer, M., and Rao, U. R.: 1963, *J. Geophys. Res.* **68**, 6361.
Stern, D.: 1964, *Planetary Space Sci.* **12**, 973.
Stozhkov, Yu. I. and Charakh Chyan, T. N.: 1970, *Acta Phys. Hung.*, Sup. 29/2, 301.
Strong, I. B., Asbridge, J. R., Barne, S. J., and Hundhausen, A. J.: 1967, 'Zodiacal Light and the Interplanetary Medium', NASA SP-150 (ed. by J. Weinberg).
Subramanian, G.: 1971a, *J. Geophys. Res.* **76**. 1093.
Subramanian, G.: 1971b, *Can. J. Phys.* **49**, 34.
Subramanian, G. and Sarabhai, V.: 1967, *Astrophys. J.* **149**, 417.
Summer, D. J. and Thompson, D.: 1970, *Acta. Phys. Hung.*, Sup. 29/2, 69.
Thambyahpillai, T. and Elliot, H.: 1953, *Nature* **171**, 918.
Vernov, S. N., Chudakov, A. Ye, Vakulov, P. V., Gordakov, Ye, V., Logatchev, Yu. I., Lyubimov, G. P., and Nipoloyev, A. G., 1964, *Kosmich. Issled.* **2**, 633.
Vernov, S. N., Chudakov, A. Ye., Vakulov, P. V., Logatchev, Yu, I., Lyubimov, G. P., and Pereslegina, N. V.: 1966, *Intern. Union Symp. on Solar Terr. Phys., Belgrade.*
Vernov, S. N., Gortchakov, E. V., Logatchov, Yu. I., Lyubimov, G. P., Pereslegina, N. V., Tverskoy, B. A., and Chudakov, A. E.: 1968, *Can. J. Phys.* **46**, 812.
Vernov, S. N., Chudakov, A. E., Vakulov, P. V., Gortchakov, E. V., Kontar, N. N., Logachev, Yu. I., Lyubimov, G. P., Pereslegina, N. V., Timofeev, G. A.: *Acta. Phys. Hung.*, Sup. 29/2, 459.

Vernov, S. N., Chudakov, A. E., Vakulov, P. V., Gorehakov, E. V., Kontor, N. N., Logachev, Yu. I., Lyubimov, G. P., Pereslegina, N. V., and Timofeev, G. A.: 1970b, *Proc. Third ESLAB/ESRIN Symposium, Noordwijk*, p. 53.
Wang, J. R.: 1970, *Astrophys. J.* **160**, 261.
Webber, W. R.,: 1962, *Progress in Elementary Part and Cosmic Ray Physics* **6**, 224.
Webber, W. R.,: 1967, *J. Geophys. Res.* **72**, 5949.
Webber, W. R.: 1969, *Proc. Leningrad Conf.*, p. 188.
Webber, W. R. and Quenby, J. J.: 1959, *Phil. Mag.* **4**, 654.
Wilcox, J. M. and Colburn, D. S.: 1969, *J. Geophys. Res.* **74**, 2388.
Wilcox, J. M. and Colburn, D. S.: 1970, *J. Geophys. Res.* **75**, 6366.
Wilcox, J. M. and Ness, N. F.: 1965, *J. Geophys. Res.* **70**, 5793.
Wilcox, J. M. and Ness, N. F.: 1967, *Solar Phys.* **1**, 437.
Wolfe, J. H., Silva, R. W., McKibbin, D. D., and Mason, R. H.: 1966, *J. Geophys. Res.* **71**, 3329.
Yoshida, S. and Wada, M.: 1959, *Nature* **183**, 381.
Yoshida, S., Akasofu, S. I., and Kendall, P. C.: 1968, *J. Geophys. Res.* **73**, 3377.